1970

A theoretical and experimental study of three jet interaction.

Hiriart Le-Bert, Gerardo

Monterey, California ; Naval Postgraduate School

A THEORETICAL AND EXPERIMENTAL STUDY OF THE THREE JET INTERACTION

Gerardo Hiriart Le-Bert

United States
Naval Postgraduate School

THESIS

A THEORETICAL AND EXPERIMENTAL STUDY

OF THE THREE JET INTERACTION

by

Gerardo Hiriart Le-Bert

April 1970

This document has been approved for public release and sale; its distribution is unlimited.

A Theoretical and Experimental Study of the Three Jet Interaction

by

Gerardo Hiriart Le-Berr
Teniente 1°, Chilean Navy

Submitted in partial fulfillment of the
requirements for the degrees of

MECHANICAL ENGINEER

and

MASTER OF SCIENCE IN MECHANICAL ENGINEERING

from the

NAVAL POSTGRADUATE SCHOOL
April 1970

ABSTRACT

The interaction of three jets is studied both theoretically and experimentally. The angle of deflection and the velocity and turbulence distributions were determined through the use of a hot-wire anemometer. The free-streamline theory has been applied to the determination of the jet deflection and the results so obtained were found to be in good agreement with those obtained experimentally. The study is a convincing evidence of the fact that a proper combination of inviscid flow analysis together with experimental results can provide the necessary guidance for the design of proportional amplifiers.

TABLE OF CONTENTS

LIST OF ILLUSTRATIONS

LIST OF SYMBOLS

a	Power nozzle width
b	Control nozzles width
CF(P)	Pressure correction factor for rotameter
d	Resultant jet's width at vena contracta
$\mathcal{J}$	Imaginary part of the expression
i	$\sqrt{-1}$
PA	Power jet, stagnation pressure
PC,PG	Control jets, stagnation pressure
q	Magnitude of local velocity
$\mathcal{R}$	Real part of the expression
r	Distance from pivoting point
Re	Reynolds number
s	Setback of control nozzles
t	Coordinate in t-plane
U	Instantaneous velocity
U	Local mean velocity
$\sqrt{\overline{u^2}}$	R.M.S. value of the fluctuating component of velocity
VA	Power jet velocity
VC	Left control jet velocity
VG	Right control jet velocity
VRO	Reference velocity VRO = 0.3 VA
VRI	Reference velocity VR1 = 0.4 VA
Vj	Resultant jet velocity

β	Complement of the deflection angle
δ	Deflection angle of resultant jet
Ω	Coordinate in the Ω -plane

ACKNOWLEDGEMENT

The work described herein was made possible through the sponsorship of the U. S. Army Research Office in Durham, North Carolina. I wish to express my appreciation to Dr. T. Sarpkaya for his inspired guidance and advice during the course of this investigation. A special note of appreciation is also extended to my wife for her patient encouragement during this work.

I. INTRODUCTION

The interaction of compressible or incompressible jets has been subject to study for at least the past fifty years for the purpose of predicting the velocity and turbulence distributions in the combined jets and in general for the purpose of predicting the performance characteristics of all sorts of machinery where such jet interaction plays a significant role. Most of the theoretical analyses have been restricted to the study of the interaction of jets of an inviscid fluid, and the complex effects of viscosity and the effects of the bounding walls have been largely ignored.

The advance of the fluidics technology and the discovery, among others, of proportional amplifiers have renewed a strong interest in both the theoretical and experimental investigation of jet interaction. Proportional amplifiers were designed and operated either through the use of the "pressure control" concept or through the use of "momentum control" concept. In either case, both the single-sided and double-sided devices were considered. The pressure controlled device is operated on the basis of the differential pressure between the two cavities placed on the two sides of the resultant jet. The vents are not open to the atmosphere. The momentum controlled proportional amplifier operates, as its name implies, on the momentum balance of the combining jets. Thus, it is apparent that, whereas the pressure-controlled amplifier depends primarily on pressure to deflect the jet, the momentum-controlled amplifier depends primarily on momentum. For certain configurations where the venting of the side cavities is not complete or where the entrainment from the two sides of the jet is not completely

attainable, then it is necessary to take both pressure and momentum effects into account in attempting to design amplifiers optimized for particular conditions. It should, in passing, be noted that the use of both control mechanisms tends to produce devices whose band-widths are relatively small, even though they may have significantly higher pressure gains. We shall confine our attention here to a thorough study of the momentum-controlled devices or beam-deflection amplifiers, both for the purpose of understanding their fluid mechanics and for the purpose of contributing to a predictable design of proportional amplifiers.

The literature concerning the fundamental behavior of beam-deflection devices is still relatively limited but is growing rapidly with the increasing realization of the design limitations of current fluidics technology.

The prediction of the performance of such devices depends on a knowledge of the exact mode of interaction of the jets. There are, obviously, many possible geometric and kinematic variables for the interaction process and it is not economically feasible to experimentally investigate the characteristics of the mode of operation of each and every possible combination. This realization necessarily led, in the first decade of fluidics, to the evolution of several flow models with varying degrees of approximations and complexities. There are, to be sure, essential differences, as well as similarities, among these models, and all must be carefully assessed before a design choice is made.

Dexter [Ref. 1] employed the "submerged jet" model, assuming that viscous mixing with the surrounding fluid has reached the stage where the velocity profile of the deflected jet is of Gaussian form. Moynihan and Reilly [Ref. 2] employed the "self preservation" model in which each jet is assumed to have retained its identity during interaction and is

not subjected to any viscous effects as it proceeds downstream. Douglas and Neve [Ref. 3] extended the works in the references just cited by applying the two models to the appropriate regions of the resultant jet.

The present work presents the theoretical results obtained through the use of the free-streamline theory for symmetric control-jet configurations and the experimental results obtained with a hot-wire anemometer.

II. THEORETICAL CONSIDERATIONS

As in all applications of the free-streamline theory, the pressure and magnitude of velocity along the free-stream lines are assumed constant. It is further assumed that both the pressure and velocity are continuous along the separation lines between the power jet and the control jets.

Experiments show that each control jet retains a large measure of its integrity, and the power jet undergoes an acceleration or a "vena contracta" effect during the initial face of the interaction. The combined jet attains a Gaussian profile only after a distance of two to six nozzle widths from the pivoting point, depending on the flow ratio and the geometry of the system.

It is apparent from the foregoing that the flow in the region in which the momentum-exchange and the turbulent mixing take place does not, strictly speaking, follow the assumptions made in the free-streamline theory. The complicated interaction between the jets, and the pressure of turbulent mixing, make the analytical predictions of three-dimensional flow field extremely difficult. To obtain analytical solutions, a simplified incompressible flow model, which retains some of the major features of the actual flow field, must be employed. Although the probable error introduced through the use of such a model is very difficult to estimate, previous analyses place a reasonable degree of confidence in the applicability of the model to certain features of the jet interaction phenomenon.

A. TRANSFORMATION PLANES

A schematic drawing of the flow configuration, together with the

resultant jet, is shown in Fig. 1a. This configuration may be transformed to an Ω-plane through the use of the Planck's transformation with the usual assumptions of the free-streamline theory. Thus, writing

$$\Omega = \ln \frac{v_j}{q} + i\theta \tag{1}$$

and carrying out the necessary manipulations, one obtains Fig. 1b.

It is a well-known fact that any polygon, such as the one shown in Fig. 1b, may be transformed to the upper or the lower half of a real plane through the use of Schwartz-Christoffel transformation given by

$$\Omega = \int \frac{M\,dt}{(t-z_1)^{\alpha_1/\pi}(t-z_2)^{\alpha_2/\pi}(t-z_3)^{\alpha_3/\pi}(t-z_4)^{\alpha_4/\pi}(t-z_5)^{\alpha_5/\pi}} + N \tag{2}$$

where M and N are constants to be determined and z_i and α_i are given by

$$z_1 = 0 \qquad z_2 = 1 \qquad z_3 = -1 \qquad z_4 = k \qquad z_5 = -k$$

$$\alpha_1 = -\pi \qquad \alpha_2 = \frac{\pi}{2} \qquad \alpha_3 = \frac{\pi}{2} \qquad \alpha_4 = \pi \qquad \alpha_5 = \pi$$

Then one has

$$\Omega = \int \frac{M\,t\,dt}{(t^2-k^2)\sqrt{t^2-1}} + N \tag{3}$$

The evaluation of this integral is shown in detail in Appendix I. The result is that

$$\Omega = \ln\left(\frac{\sqrt{1-k^2}+\sqrt{1-t^2}}{\sqrt{t^2-k^2}}\right) \quad \text{for} \quad t \le -k \tag{4}$$

$$\Omega = \ln\left(\frac{\sqrt{1-k^2}+\sqrt{1-t^2}}{-\sqrt{t^2-k^2}}\right) \quad \text{for} \quad -k \le t \le 1 \tag{5}$$

$$\Omega = \ln\left(\frac{-\sqrt{1-k^2}+\sqrt{1-t^2}}{\sqrt{t^2-k^2}}\right) \quad \text{for} \quad t \ge 1 \tag{6}$$

Table I gives the corresponding values between the points in the Ω -plane and the t-plane shown in Fig. 1c.

The relationships between the parameters shown in the t-plane and various velocity ratios are obtained as follows:

Through the use of the conditions at point A

$$-\ln \frac{V_A}{V_j} + i\frac{\pi}{2} = \ln\left(\frac{\sqrt{1-k^2}+1}{-\sqrt{-k^2}}\right)$$

one has

$$\eta = \frac{V_A}{V_j} = \frac{k}{1+\sqrt{1-k^2}} \tag{7}$$

Through the use of the conditions at point C

one has

$$-\ln \frac{V_C}{V_j} + i0 = \ln\left(\frac{\sqrt{1-k^2}+\sqrt{1-c^2}}{\sqrt{c^2-k^2}}\right)$$

$$\alpha = \frac{V_C}{V_j} = \frac{\sqrt{c^2-k^2}}{\sqrt{1-k^2}+\sqrt{1-c^2}} \tag{8}$$

Through the use of the conditions at point G

one has

$$-\ln \frac{V_G}{V_j} + i\pi = \ln\left(\frac{\sqrt{1-k^2}+\sqrt{1-g^2}}{-\sqrt{g^2-k^2}}\right)$$

$$\gamma = \frac{V_G}{V_j} = \frac{\sqrt{g^2-k^2}}{\sqrt{1-k^2}+\sqrt{1-g^2}} \tag{9}$$

Through the use of the conditions at point E

one has

$$i\beta = \ln\left(\frac{\sqrt{1-k^2}+\sqrt{1-f^2}}{\sqrt{f^2-k^2}}\right)$$

$$\sin\beta = \sqrt{\frac{f^2-1}{f^2-k^2}} \quad \text{and} \quad \cos\beta = \sqrt{\frac{1-k^2}{f^2-k^2}} \tag{10}$$

Finally, through the use of the conditions on the free streamline, we obtain

$$\Omega = i\theta = \ln\left(\frac{\pm\sqrt{1-k^2}+\sqrt{1-t^2}}{\sqrt{t^2-k^2}}\right)$$

or

$$e^{i\theta} = \pm\sqrt{\frac{1-k^2}{t^2-k^2}} + i\sqrt{\frac{t^2-1}{t^2-k^2}}$$

$$e^{\Omega} = \cos\theta + i\sin\theta \tag{11}$$

It should be noted that the conservation of mass yields

$$d = (\alpha+\gamma)b + \eta a$$

The t-plane is comprised of three sources and one sink. Thus, the complex potential for the flow in the upper half of the t-plane may be written in terms of the known potentials of sources and sinks as:

$$w = \frac{V_j d}{\pi}\ln(t+f) - \frac{V_A a}{\pi}\ln t - \frac{V_C b}{\pi}\ln(t+c) - \frac{V_G b}{\pi}\ln(t-g) \tag{12}$$

where $w = \phi + i\psi$ and ϕ is the complex potential and ψ the stream function.

Taking the derivative of w with respect to t, making use of Eqs. (7), (8), and (9), and the conservation of mass relationship, one has

$$\frac{dw}{dt} = -\frac{V_j}{\pi}\left[-\frac{d}{t+f} + \frac{\eta a}{t} + \frac{\alpha b}{t+c} + \frac{\gamma b}{t-g}\right] \tag{13}$$

The distances between various points in the z-plane, the contraction coefficient, and the angle of deflection may be evaluated as follows:

$$\overline{DF} = \mathcal{R}\left[\int dz\right] \tag{14}$$

and noting that $\overline{DF} = a + 2s$, one has

$$a + 2s = \mathcal{R}\left[\int_{-1}^{+1} e^{-\Omega} \left(-\frac{1}{v_j} \frac{dw}{dt} \right) dt \right]$$

Replacing $\frac{dw}{dt}$ from Eq. (13) and Ω from Eqs. (4) and (6), and taking the Cauchy principal value of the integral to account for the discontinuity at t = -f, we finally have,

$$a + 2s = d \sin\beta + \lim_{\varepsilon \to 0} \left[\frac{\sqrt{1-k^2}}{\pi} \int_{-1}^{-f+\varepsilon} \left(\eta \frac{a}{t} + \frac{\alpha b}{t+c} + \frac{\delta b}{t-g} - \frac{d}{t+f} \right) \frac{dt}{\sqrt{t^2-1}} \right]$$

$$+ \lim_{\substack{\varepsilon \to 0 \\ Q \to \infty}} \left[\frac{\sqrt{1-k^2}}{\pi} \int_{-f-\varepsilon}^{-Q} \left(\eta \frac{a}{t} + \frac{\alpha b}{t+c} + \frac{\delta b}{t-g} - \frac{d}{t+f} \right) \frac{dt}{\sqrt{t^2-1}} \right] \qquad (15)$$

$$- \lim_{Q \to \infty} \left[\frac{\sqrt{1-k^2}}{\pi} \int_{Q}^{+1} \left(\eta \frac{a}{t} + \frac{\alpha b}{t+c} + \frac{\delta b}{t-g} - \frac{d}{t+f} \right) \frac{dt}{\sqrt{t^2-1}} \right]$$

The details of the integration are shown in Appendix II. The results may be expressed as:

$$\frac{a+2s}{b} = \frac{d}{b} \sin\beta + 2\frac{\sqrt{1-k^2}}{\pi} \left[\frac{\eta}{k} \frac{a}{b} \sin^{-1} k - \frac{\alpha}{\sqrt{c^2-k^2}} \ln \frac{\sqrt{1-c^2}}{\sqrt{1-k^2}+\sqrt{c^2-k^2}} \right. \qquad (16)$$

$$\left. - \frac{\delta}{\sqrt{g^2-k^2}} \ln \frac{\sqrt{1-g^2}}{\sqrt{1-k^2}+\sqrt{g^2-k^2}} + \frac{d}{b} \frac{1}{\sqrt{f^2-k^2}} \ln \frac{\sqrt{f^2-1}}{\sqrt{1-k^2}+\sqrt{f^2-k^2}} \right]$$

Equation (16) establishes the relationship between the various jet velocities and the amplifier setback. Another expression is needed to establish the symmetry of the geometrical configuration. This may be done by performing an integration from D to F along the free-streamline and writing the imaginary part equal to zero so as to ensure that the two sides of the control jets are along the same line and that there is no unsymmetry. Thus, writing

$$\mathcal{J}\left[\int dz\right] = 0 \tag{17}$$

or $$\mathcal{J}\left[\int_{-1}^{+1} e^{\Omega}\left(-\frac{1}{V_j}\frac{dw}{dt}\right)dt\right] = 0$$

and replacing $\frac{dw}{dt}$ from Eq. (13) and Ω from Eqs. (4) and (6), one has

$$\int_{-1}^{+1} \frac{\sqrt{t^2-1}}{\sqrt{t^2-k^2}}\left(\eta\frac{a}{\pi}\frac{1}{t} + \frac{\alpha b}{\pi}\frac{1}{t+c} + \frac{\gamma b}{\pi}\frac{1}{t-g} - \frac{d}{\pi}\frac{1}{t+f}\right)dt = 0 \tag{18}$$

Details of the integration are shown in Appendix III. The analysis yields:

$$\frac{2}{\pi(1+k)}\left\{\left[\left(\frac{1+ck}{k+c}\right)\alpha + \left(\frac{1-gk}{k-g}\right)\gamma - \left(\frac{1+fk}{k+f}\right)\frac{d}{b}\right]K\left(\frac{2\sqrt{k}}{k+1}\right)\right.$$

$$+\frac{\alpha(1-k)(c-1)}{(k+c)}\Pi\left(\frac{\pi}{2}, \frac{2(k+c)}{(k+1)(c+1)}, \frac{2\sqrt{k}}{k+1}\right) \tag{19}$$

$$+\frac{\gamma(1-k)(1+g)}{(g-k)}\Pi\left(\frac{\pi}{2}, \frac{2(k-g)}{(k+1)(1-g)}, \frac{2\sqrt{k}}{k+1}\right)$$

$$\left.-\frac{d}{b}\frac{(1-k)(f-1)}{(k+f)}\Pi\left(\frac{\pi}{2}, \frac{2(k+f)}{(k+1)(f+1)}, \frac{2\sqrt{k}}{k+1}\right)\right\} = 0$$

where $K(h)$ is the complete elliptic integral of the first kind and $\Pi\left(\frac{\pi}{2}, \alpha^2, h\right)$ is the complete elliptic integral of the third kind.

Since the parameter α^2 of the elliptic integral of the third kind shown in Eq. (19) was not always in the range of $0 < \alpha^2 < 1$, a subroutine program was written to reduce all the complete elliptic integrals of the third kind into the sum of complete and incomplete elliptic integrals of the first and second kind for which there are tables and subroutines available at the computer facility of the Naval Postgraduate School.

The reductions were made through the use of the transformations given in Ref. [4], and through the use of Heuman's Lambda and Jacobi's Zeta functions, as given in Ref. [5]. The aforementioned reductions are shown in Appendix IV. The evaluations of the resulting expressions for the discontinuity at t = -f is shown in Appendix V. The results obtained for $\frac{s}{a} = 1$ and $\frac{b}{a} = 1$ through the use of the expressions given above will be presented together with the experimental data in connection with the discussion of results.

III. EXPERIMENTAL EQUIPMENT AND PROCEDURE

The experimental apparatus consisted of a jet assembly, hot-wire aneomometer system, and a velocity calibrator.

A. JET ASSEMBLY

As shown in Fig. 2 and 3, the entire assembly consisted of three nozzles, one for the power jet and two for the control jets. Each nozzle was 1/4 inch wide and 2 inches high. This resulted in an aspect ratio of eight. The jet assembly was sandwiched between two 1/4 inch plexiglass plates.

The width of the control nozzle was adjustable from 1/4 inch to 1/2 inch. For all the tests reported here, the control and power jet nozzles, as well as the setback, were maintained at widths of 1/4 inch.

The smooth streamline contour of the nozzles gave an essentially uniform exit velocity profile. The special configuration adopted for the control jet walls prevented the jet from attaching to the side walls through the Coanda effect. In addition, two large holes, as shown in Fig. 2, were provided in the upper and lower cover-plates, in order to minimize the restriction to entrainment to the resultant jet.

The supply lines were 1-1/4 inch diameter Tygon tubing, connected to the three inlets. The flow was straightened via a one inch long honey-comb section before undergoing a contraction of ten to one.

Supply pressures were measured by means of inclined manometers through the use of wall pressure tabs located in the straight part of each nozzle.

The top and bottom plates had two slots cut out to enable the hot-wire anemometer mechanism to traverse along lines parallel to the power

nozzle axis. A graph paper, graduated in degrees, was placed under the bottom plate for the purpose of quickly measuring the jet deflection angle by means of a small light string attached to a needle. A more precise measurement of the jet deflection angle was, of course, made by means of the hot-wire anemometer.

Air was supplied to the system from a 50hp compressor at approximately 160 psi. Air first passed through a micro-filter to remove oil and dust and then through the primary pressure regulator. The three jets were independently supplied from this regulator. Each jet supply line had on it a series of pressure regulators, thus providing independently regulated flows into three rotameters. The rotameters were identical and each had a maximum capacity of 17.5 scfm. at 14.7 psia and 70°F. The actual flow rates were obtained from

$$Q = (\text{rotameter reading, \% of full flow}) \times (17.5) \times CF(P)$$

where CF(P) represents the pressure correction factor obtained from a chart provided by the manufacturer.

B. HOT-WIRE ANEMOMETER

A constant temperature hot-wire anemometer, manufactured by the Thermo-Systems, Model 1050, was used in the measurement of velocity and turbulence intensities. The wire used (wire #1272-T1.5) had a cold resistance of 7.30 ohms and an operating resistance of 10.95 ohms. The voltage across the bridge was measured with a digital voltmeter accurate to 0.01 volts.

A special probe holder was constructed and is shown in Fig. 4. This holder which was fitted into the slots in the jet assembly, enabled the probe to move along lines parallel to the power-nozzle axis in the mid-plane. A micrometer mechanism on the holder provided transverse movement of the hot-wire across the jet with an accuracy of 0.001 inch.

The hot-wire probe was calibrated with the Thermo-Systems Calibrator, Model 1125, shown in Fig. 4. An inclined manometer was connected to the reservoir of the calibrator to measure the stagnation pressure and the hot-wire was placed 1/16 inch above the 0.150 inch orifice of the calibrator. For the details of calibration analysis, see Appendix VI.

IV. EXPERIMENTAL PROCEDURE

The experiments were carried out for a combination of three power jet velocities and for four control jet bias velocities. The bias velocity was defined as (VC+VG)/2VA. For each combination, the velocity and turbulence distributions were measured at various distances from the pivoting point, and the results were reduced to actual data through the use of the computerized calibration curve. Most of the experiments were repeated for the purpose of checking the reproducibility of the data. Finally, the deflection angles were determined from the velocity profiles by connecting the peaks of each successive profile with the pivoting point. The deflection angles obtained in this manner did not deviate more than ± 0.5 degrees from those obtained through the use of the floating string and chart paper combination.

The supply pressure for each jet was measured, as previously cited, by means of inclined manometers. The stagnation pressure of the power jet was measured by one manometer, and the stagnation, as well as differential pressure of the control jets, through the use of two other manometers.

V. DISCUSSION OF RESULTS

In the following, first the experimental results obtained with the hot-wire anemometer will be discussed and then a comparison will be made between the theoretically and experimentally obtained deflection angle.

Figures 6 through 54 represent the velocity and turbulence intensity distributions as a function of x/a and U/VRO in terms of normalized control jet velocities, deflection angle, and the distance from the pivoting point. It is apparent from all of these figures that the control jets retain their identity up to a distance of 2a from the pivoting point. This region will be called the mixing region. For distances larger than approximately 2a, the velocity profiles acquire a nearly Guassian distribution. The turbulence intensity distribution exhibits essentially four peaks: two in the outer edges of the resultant jet because of the mixing of the jet with the ambient flow and two peaks in the regions where the control jets mix with the power jet. As the distances increase from the pivoting point, the turbulence intensity in the inner regions decreases and eventually reduces to a single minimum at the axis of the jet. It is therefore apparent that the application of the free-streamline theory to the mixing of jets of unequal velocities is not entirely valid in the mixing region since there are three independent free-streamline velocities. In the fully established region, the velocity profile is Gaussian and thus far from being uniform. Consequently, the use of the single jet velocity is not fully justified unless special precautions are taken to make sure that the gross continuity of the mass flow is satisfied by properly selecting the apparent jet width. In so doing, the maximum centerline velocity may be used as the free-streamline

velocity and the effective jet velocity may be calculated from the equation of continuity. The theoretical analysis presented herein makes good use of this fact and shows that the results so obtained are in good agreement with those obtained experimentally.

Figures 55 through 57 show a superposition of the velocity profiles and the evolution of the mixing from three independent jets to a single profile. Similar graphs are presented in Figs. 58 and 59 for the turbulence intensity. Figure 60 is a three-dimensional plot of the evolution of the velocity profiles as a function of the distance from the pivoting point.

The deflection angle is shown in Figs. 61 through 63 as a function of the sum and difference of the normalized control jets for all Reynolds numbers. It is immediately apparent that the deflection angle is a linear function of the normalized differential control jets velocity and that the deflection angle does not vary appreciably with the normalized average of the control jets. These results suggest that the characteristics of beam-deflection amplifiers be evaluated in terms of the parameters cited above rather than those previously used by other investigators. Although the experimental results presented herein are for equal control and power jet nozzles, there is every reason to believe that similar correlations will exist between the jet deflection angle and the two control jets parameters.

A comparison of the experimental results with those obtained theoretically for a normalized average control jet velocity of unity is shown in Fig. 64. As previously cited, the final jet width d used in the calculations was obtained by dividing the total flow rate by the maximum jet velocity. It is believed that there is at present no other

way of applying the free-streamline theory to the deflection of viscous jets for in the mixing region there are three different jet velocities and three fairly uniform velocity distributions and, in the fully established region, a single maximum with a Gaussian distribution. Thus, the only logical assumption to be made is that the free-streamline velocity used in the analysis is equal to the maximum of the fully established profile and that the effective jet width is determined by the equation of continuity. In reality, it appears that the maximum centerline velocity is somewhat higher than that predicted by the free-streamline theory and that the effective jet width is somewhat smaller than that used in the analysis. Be that as it may, no second-order corrections were applied to the analysis in order to preserve its generality. The extension of the analysis to other velocity ratios will be separately undertaken in the future.

The stagnation pressures at supply reservoirs of the three jets were determined as previously explained and are plotted in Fig. 65. Mean values rather than the actual data points are shown in this graph because the data points fell fairly consistently on straight lines. It is immediately apparent that the normalized differential control port pressures are linear functions of the deflection angle and depend weakly on the mean pressure of the control ports. A simple analysis of the jet deflection through the use of the momentum balance equation shows that the deflection angle so determined is considerably higher than that obtained experimentally or theoretically even when the pressure differences between various nozzles are taken into consideration.

VI. CONCLUSIONS

The foregoing theoretical and experimental study warrants the following conclusions:

(a) The jets preserve their identity in a region of approximately 2a from the pivoting point;

(b) The velocity profiles become Gaussian beyond the mixing region;

(c) The free streamline theory predicts the deflection angles fairly accurately provided that an effective jet width (calculated in terms of the mass flow and the maximum centerline velocity) is incorporated into the analysis;

(d) The previous models cited in the introduction do not predict, or are not capable of predicting, the jet deflection angle to an accuracy demanded by the beam deflection amplifiers; and finally,

(e) The normalized differential control reservoir pressures vary linearly with the deflection angle. It is thus believed that an analysis such as the one presented here, together with one experimentally determined parameter, is fully capable of predicting the performance of proportional amplifiers. The knowledge of the jet deflection angle and the Gaussian shape of the velocity profile provide through a simple integration the determination of the amounts of flow at a given amplifier receiver.

APPENDIX I

EVALUATION OF THE INTEGRAL

$$\Omega = \int \frac{M t\,dt}{(t^2-k^2)\sqrt{t^2-1}} + N \tag{20}$$

Letting $x^2 = t^2 - k^2$

$x\,dx = t\,dt$

one has

$$\Omega = M \int \frac{dx}{x\sqrt{x^2+(k^2-1)}} + N$$

The general solution of this integral, irrespective of whether the radicals are real or imaginary, is given in Grobner 233.3b [Ref. 6] as,

$$\Omega = -\frac{M}{\sqrt{k^2-1}} \ln \frac{(k^2-1)+\sqrt{(k^2-1)(x^2+(k^2-1))}}{x} + N \tag{21}$$

replacing t and rearranging, we have

$$\Omega = -\frac{M}{i\sqrt{k^2-1}} \ln \frac{(k^2-1)+\sqrt{k^2-1}\ \sqrt{t^2-1}}{\sqrt{t^2-k^2}} + N \tag{22}$$

or

$$\Omega = -\frac{M}{i\sqrt{k^2-1}} \ln \frac{\sqrt{k^2-1}+\sqrt{t^2-1}}{\sqrt{t^2-k^2}} + N_1 \tag{23}$$

or

$$\Omega = -\frac{M}{i\sqrt{k^2-1}} \ln \frac{\sqrt{1-k^2}+i\sqrt{t^2-1}}{\sqrt{t^2-k^2}} + N_2 \tag{24}$$

or

$$\Omega = M_2 \ln \frac{\sqrt{1-k^2}+i\sqrt{t^2-1}}{\sqrt{t^2-k^2}} + N_2 \tag{25}$$

The constants M_2 and N_2 may be determined, for the different regions of the t plane, as follows:

a. At the point D, $\quad t = -1 \;,\; \frac{V_j}{q} = 1 \;,\; \theta = 0$

i) approaching from left to D $\quad t = -1 - \varepsilon$

$$0 + i0 = \lim_{\varepsilon \to 0} \left[\frac{-M}{i\sqrt{1-k^2}} \ln \frac{\sqrt{1-k^2} + i\sqrt{(-1-\varepsilon)^2 - 1}}{\sqrt{(-1-\varepsilon)^2 - k^2}} \right] + N_2$$

$$= M_2 \ln \frac{\sqrt{1-k^2}}{\sqrt{1-k^2}} + N_2$$

Then $\quad N_2 = 0$

ii) approaching from right to D $\quad t = -1 + \varepsilon$

$$0 + i0 = \lim_{\varepsilon \to 0} \left[\frac{-M}{i\sqrt{1-k^2}} \ln \frac{\sqrt{1-k^2} + i\sqrt{(-1+\varepsilon)^2 - 1}}{\sqrt{(-1+\varepsilon)^2 - k^2}} \right] + N_2$$

$$= \frac{-M}{i\sqrt{1-k^2}} \ln \frac{\sqrt{1-k^2}}{\sqrt{1-k^2}} + N_2$$

Then $\quad N_2 = 0$

Furthermore, since at $\quad t = -\infty \;,\; \theta = \frac{\pi}{2}$

one has $\quad 0 + i\frac{\pi}{2} = \frac{-M}{i\sqrt{1-k^2}} \ln(0 + i)$

Then

$$M_2 = \frac{-M}{i\sqrt{1-k^2}} = 1$$

b. At the point B, $t = -k$, $\frac{V_j}{q} = \infty$

i) approaching from left to B, $t = 0$, $t = -k - \epsilon$

$$\infty + i\,0 = M_2 \lim_{\epsilon \to 0} \left[\ln \frac{\sqrt{1-k^2} + i\sqrt{(-k-\epsilon)^2 - 1}}{\sqrt{(-k-\epsilon)^2 - k^2}} \right] + N_2$$

$$\infty + i0 = M_2 \lim_{\epsilon \to 0} \left[\ln \frac{2\sqrt{1-k^2}}{\sqrt{2k\epsilon + \epsilon^2}} \right] + N_2$$

$$\infty + i0 = M_2 \infty + N_2$$

Thus $N_2 = 0$

and $M_2 = 1$

ii) approaching from right to B, $\theta = \frac{\pi}{2}$, $t = -k + \epsilon$

$$\infty + i\frac{\pi}{2} = M_2 \lim_{\epsilon \to 0} \left[\ln \frac{\sqrt{1-k^2} + i\sqrt{(-k+\epsilon)^2 - 1}}{\sqrt{(-k+\epsilon)^2 - k^2}} \right] + N_2$$

$$\infty + i\frac{\pi}{2} = M_2 \lim_{\epsilon \to 0} \left[\ln \frac{2\sqrt{1-k^2}}{\sqrt{-2\epsilon k}} \right] + N_2$$

$$\infty + i\frac{\pi}{2} = M_2 \lim_{\epsilon \to 0} \left[\ln \frac{2\sqrt{1-k^2}}{i\sqrt{2\epsilon k}} \right] + N_2$$

$$\infty + i\frac{\pi}{2} = M_2 \left[\ln \infty - i\frac{\pi}{2} \right] + N_2$$

Thus $M_2 = 1$ and $N_2 = i\pi$

c. At the point H, $t = +k$, $\frac{V_j}{q} = \infty$

i) approaching from left, $\theta = \frac{\pi}{2}$, $t = k - \varepsilon$

$$\infty + i\frac{\pi}{2} = M_2 \lim_{\epsilon \to 0} \left[\ln \frac{\sqrt{1-k^2} + i\sqrt{(k-\varepsilon)^2 - 1}}{\sqrt{(k-\epsilon)^2 - k^2}} \right] + N_2$$

$$\infty + i\frac{\pi}{2} = M_2 \lim_{\epsilon \to 0} \left[\ln \frac{2\sqrt{1-k^2}}{i\sqrt{2\varepsilon k}} \right] + N_2$$

$$\infty + i\frac{\pi}{2} = M_2 \left[\ln \infty - i\frac{\pi}{2} \right] + N_2$$

Thus $M_2 = 1$ and $N_2 = i\pi$

ii) approaching from right, $\theta = \pi$, $t = k + \varepsilon$

$$\infty + i\pi = M_2 \lim_{\varepsilon \to 0} \left[\ln \frac{\sqrt{1-k^2} + i\sqrt{(k+\varepsilon)^2 - 1}}{\sqrt{(k+\varepsilon)^2 - k^2}} \right] + N_2$$

$$\infty + i\pi = M_2 \lim_{\varepsilon \to 0} \left[\ln \frac{2\sqrt{1-k^2}}{\sqrt{2k\varepsilon}} \right] + N_2$$

$$\infty + i\pi = M_2 \ln \infty + N_2$$

Thus $M_2 = 1$ and $N_2 = i\pi$

d. At the point F, $t = +1$, $\theta = \pi$, $\frac{v_2}{t} = 1$

i) Where approaching from left $t = 1 - \varepsilon$

$$0 + i\pi = M_2 \lim_{\varepsilon \to 0} \left[\ln \frac{\sqrt{1-k^2} + i\sqrt{(1-\varepsilon)^2 - 1}}{\sqrt{(1-\varepsilon)^2 - k^2}} \right] + N_2$$

$$0 + i\pi = M_2 \lim_{\varepsilon \to 0} \left[\ln \frac{\sqrt{1-k^2} + \sqrt{\varepsilon}}{\sqrt{1-k^2}} \right] + N_2$$

Thus $M_2 = 1$ and $N_2 = i\pi$

ii) approaching from right, $t = 1 + \varepsilon$

$$0 + i\pi = M_2 \lim_{\varepsilon \to 0} \left[\ln \frac{\sqrt{1-k^2} + i\sqrt{(1+\varepsilon)^2 - 1}}{\sqrt{(1+\varepsilon)^2 - k^2}} \right] + N_2$$

$$0 + i\pi = M_2 \lim_{\varepsilon \to 0} \left[\ln \frac{\sqrt{1-k^2} + i\sqrt{2\varepsilon + \varepsilon^2}}{\sqrt{1-k^2 + 2\varepsilon + \varepsilon^2}} \right] + N_2$$

$$0 + i\pi = M_2 \ln \frac{\sqrt{1-k^2}}{\sqrt{1-k^2}} + N_2$$

Thus $M_2 = -1$ and $N_2 = i\pi$

Furthermore, where as $t \to +\infty$, $\theta = \frac{\pi}{2}$ or $\lim$

$$0 + i\frac{\pi}{2} = M_2 \ln(0 + i) + N_2$$

$$0 + i\frac{\pi}{2} = M_2 \left(i\frac{\pi}{2} \right) + N_2$$

Thus $M_2 = -1$ and $N_2 = i\pi$

Finally, Ω reduces to

$$\Omega = \ln \frac{\sqrt{1-k^2} + i\sqrt{t^2-1}}{\sqrt{t^2-1}} \qquad \text{for} \quad t \leq -k \tag{26}$$

$$\Omega = \ln \frac{\sqrt{1-k^2} + i\sqrt{t^2-1}}{-\sqrt{t^2-k^2}} \qquad \text{for} \quad -k \leq t \leq 1 \tag{27}$$

$$\Omega = -\ln \frac{\sqrt{1-k^2} + i\sqrt{t^2-1}}{-\sqrt{t^2-k^2}} \qquad \text{for} \quad 1 \leq t \tag{28}$$

Evidently, Eq. (28) is equivalent to

$$\Omega = \ln \frac{-\sqrt{1-k^2} + i\sqrt{t^2-1}}{\sqrt{t^2-k^2}} \tag{29}$$

APPENDIX II

EVALUATION OF THE INTEGRAL

$$\int \frac{\sqrt{1-k^2}}{\pi}\left[\frac{a}{k}+\frac{\alpha b}{t+c}+\frac{\gamma' b}{t-g}-\frac{d}{t+f}\right]\frac{dt}{\sqrt{t^2-k^2}} \tag{30}$$

Working each term of the integral separately, one has

A1. From CRC Table, formula - 134

$$\int \frac{dt}{t\sqrt{t^2-k^2}} = \frac{1}{k}\sec^{-1}\frac{t}{k}+C = \frac{1}{k}\cos^{-1}\frac{k}{t}+C \tag{31}$$

A2. From Grobner and Hofreiter [Ref. 6] formula - 231.10a

$$\int \frac{dt}{(t+c)\sqrt{t^2-k^2}} = -\frac{1}{\sqrt{c^2-k^2}}\ln\frac{\sqrt{(t^2-k^2)(c^2-k^2)}-k^2-ct}{(t+c)\sqrt{c^2-k^2}}+C_1$$

$$= -\frac{1}{\sqrt{c^2-k^2}}\ln\frac{\sqrt{(t^2-k^2)(c^2-k^2)}-k^2-ct}{t+c}+C_2 \tag{32}$$

A3. Using the same method as A2

$$\int \frac{dt}{(t-g)\sqrt{t^2-k^2}} = -\frac{1}{\sqrt{g^2-k^2}}\ln\frac{\sqrt{(t^2-k^2)(g^2-k^2)}-k^2-gt}{t-g}+C_3 \tag{33}$$

A4. Using the same method as A2

$$\int \frac{dt}{(t-g)\sqrt{t^2-k^2}} = -\frac{1}{\sqrt{f^2-k^2}}\ln\frac{\sqrt{(t^2-k^2)(f^2-k^2)}-k^2-ft}{t+f}+C_4 \tag{34}$$

LIMIT PROCESS

Equations (31), (32) and (33) have no discontinuity at t = - f

For Eq. (31), one has

$$\frac{1}{k}\left[\left(\cos^{-1}\frac{k}{-\infty}-\cos^{-1}\frac{k}{-1}\right)-\left(\cos^{-1}\frac{k}{+1}-\cos^{-1}\frac{k}{+\infty}\right)\right]$$

which reduces to

$$\frac{2}{k}\sin^{-1}k \tag{35}$$

For Eq. (32) we have

$$\lim_{Q\to\infty}\left[-\frac{1}{\sqrt{c^2-k^2}}\ln\frac{\left(\sqrt{(Q^2-k^2)(c^2-k^2)}-k^2+cQ\right)\left(\sqrt{(Q^2-k^2)(c^2-k^2)}-k^2-cQ\right)(c+1)(c-1)}{(c-Q)(c+Q)\left(\sqrt{(1-k^2)(c^2-k^2)}-k^2+c\right)\left(\sqrt{(1-k^2)(c^2-k^2)}-k^2-c\right)}\right]$$

which reduces to

$$-\frac{2}{\sqrt{c^2-k^2}}\ln\frac{\sqrt{1-c^2}}{\sqrt{1-k^2}+\sqrt{c^2-k^2}} \tag{36}$$

For Eq. (33), using the same procedure as above, one has

$$-\frac{2}{\sqrt{g^2-k^2}}\ln\frac{\sqrt{1-g^2}}{\sqrt{1-k^2}+\sqrt{g^2-k^2}} \tag{37}$$

For Eq. (34) the inclusion of the discontinuity at t = -f yields

$$\lim_{\substack{\varepsilon\to 0\\ Q\to\infty}}\left\{-\frac{1}{\sqrt{f^2-k^2}}\ln\frac{\left[\sqrt{(f^2-k^2)(f^2-k^2)}-k^2+f(f-\varepsilon)\right]\left[\sqrt{(Q^2-k^2)(f^2-k^2)}-k^2+fQ\right]}{(f-f+\varepsilon)(f-Q)(f+Q)\left[\sqrt{(1-k^2)(f^2-k^2)}-k^2+f\right]}\right.$$

$$\left.\cdot\frac{\left[\sqrt{(Q^2-k^2)(f^2-k^2)}-k^2-fQ\right](f-1)(f-f-\varepsilon)(f+1)}{\left[\sqrt{(f^2-k^2)(f^2-k^2)}-k^2+f(f+\varepsilon)\right]\left[\sqrt{(1-k^2)(f^2-k^2)}-k^2-f\right]}\right\}$$

which after simplification reduces to

$$-\frac{2}{\sqrt{f^2-k^2}}\ln\frac{\sqrt{f^2-1}}{\sqrt{1-k^2}+\sqrt{f^2-k^2}} \tag{38}$$

Replacing Eqs. (35), (36), (37) and (38) in Eq. (15) one has

$$a + 2s = d\sin\beta + \frac{2\sqrt{1-k^2}}{\pi}\left[\eta\frac{a}{k}\sin^{-1}k - \frac{\alpha b}{\sqrt{c^2-k^2}}\ln\frac{\sqrt{1-c^2}}{\sqrt{1-k^2}+\sqrt{c^2-k^2}}\right.$$

$$\left. - \frac{\delta b}{\sqrt{g^2-k^2}}\ln\frac{\sqrt{1-g^2}}{\sqrt{1-k^2}+\sqrt{g^2-k^2}} + \frac{d}{\sqrt{f^2-k^2}}\ln\frac{\sqrt{f^2-1}}{\sqrt{1-k^2}+\sqrt{f^2-k^2}}\right] \qquad (39)$$

APPENDIX III

EVALUATION OF THE INTEGRAL

$$\int_{-1}^{+1} \sqrt{\frac{t^2-1}{t^2-k^2}} \left(\gamma \frac{a}{\pi} \frac{1}{t} + \frac{\alpha b}{\pi} \frac{1}{t+c} + \frac{\gamma b}{\pi} \frac{1}{t-g} - \frac{d}{\pi} \frac{1}{t+f} \right) dt \tag{40}$$

Consider the following typical integral

$$\int_{-1}^{+1} \sqrt{\frac{t^2-1}{t^2-k^2}} \; \frac{dt}{t+p} \tag{41}$$

Multiplying by $\sqrt{t^2-1}$ the numerator and the denominator, we have

$$\int_{-1}^{+1} \frac{(t^2-1)\, dt}{\sqrt{(t^2-1)(t^2-k^2)}\cdot(t+p)}$$

Dividing (t^2-1) by $(t + p)$, we can express the integral as

$$\int_{-1}^{+1} \frac{t\, dt}{\sqrt{(t^2-1)(t^2-k^2)}} - p \int_{-1}^{+1} \frac{dt}{\sqrt{(t^2-1)(t^2-k^2)}} + (p^2-1) \int_{-1}^{+1} \frac{dt}{(t+p)\sqrt{(t^2-k^2)(t^2-1)}} \tag{42}$$

Note that the first integral in Eq. (42) is an odd function of t. Thus its integration from -1 to +1 reduces to zero. The same result is obtained for the third integral when p = 0.

From Gröbner [Ref. 6] formulas 244.8a 4 and 244.8a 7 one has

$$\int \frac{dt}{\sqrt{(t^2-1)(t^2-k^2)}} = \frac{2}{1+k} F(\varphi, h) \tag{43}$$

and

$$\int \frac{dt}{(t+p)\sqrt{(t^2-1)(t^2-k^2)}} = \frac{1}{(k+p)(k+1)} \left\{ 2F(\varphi,h) + \frac{2(k-1)}{(1+p)} \Pi\left(\varphi, \frac{2(k+p)}{(k+1)(p+1)}, h \right) \right\} \tag{44}$$

where

$$h = \frac{2\sqrt{k}}{1+k} \tag{45}$$

and φ is given by

$$\sin^2\varphi = \frac{(k+1)(t-1)}{2(t-k)} \tag{46}$$

and $F(\varphi, h)$ is defined by $\int_0^{\sin\varphi} \frac{dx}{\sqrt{(1-x^2)(1-h^2x^2)}}$

and $\Pi(\varphi, \alpha^2, h)$ is defined as $\int_0^{\sin\varphi} \frac{dx}{(1-\alpha^2x^2)\sqrt{(1-x^2)(1-h^2x^2)}}$

In taking the limit of Eqs. (43) and (44), it must be noted that the integral from -1 to +1 is to be performed by going from -1 to $-\infty$, to $+\infty$ to +1. Replacing the value of t in Eq. (46), it is seen that φ goes from $\frac{\pi}{2}$ to zero when t goes from -1 to +1, in the sense described above. Replacing Eqs. (43) and (44) in Eq. (42) and noting that φ goes from $\frac{\pi}{2}$ to zero, we have:

$$\int_{-1}^{+1} \sqrt{\frac{t^2-1}{t^2-k^2}}\, \frac{dt}{t+p} = \frac{2}{1+k}\left\{\frac{1+pk}{k+p} K(h) + \frac{(1-k)(p-1)}{(k+p)} \Pi\left(\frac{\pi}{2}, \frac{2(k+p)}{(k+1)(p+1)}, h\right)\right\} \tag{47}$$

where $K(h)$ is the complete elliptic integral of the first kind and h is as defined by Eq. (45).

Replacing Eq. (47) in Eq. (40) and replacing ρ by its appropriate value, we have

$$\int_{-1}^{+1} \sqrt{\frac{t^2-1}{t^2-k^2}} \left(\gamma \frac{a}{\pi} \frac{1}{t} + \frac{\alpha b}{\pi} \frac{1}{t+c} + \frac{\gamma b}{\pi} \frac{1}{t-g} - \frac{d}{\pi} \frac{1}{t+f} \right) dt =$$

$$\frac{2b}{\pi(1+k)} \left\{ \left[\left(\frac{1+ck}{k+c} \right) \alpha + \left(\frac{1-gk}{k-g} \right) \gamma - \left(\frac{1+fk}{k+f} \right) \frac{d}{b} \right] \cdot K(h) \right.$$

$$+ \frac{\alpha(1-k)(c-1)}{(k+c)} \Pi \left(\frac{\pi}{2}, \frac{2(k+c)}{(k+1)(c+1)}, h \right)$$

$$+ \frac{\gamma(1-k)(1+g)}{(g-k)} \Pi \left(\frac{\pi}{2}, \frac{2(k-g)}{(k+1)(1-g)}, h \right)$$

$$\left. - \frac{d}{b} \frac{(1-k)(f-1)}{(k+f)} \Pi \left(\frac{\pi}{2}, \frac{2(k+f)}{(k+1)(f+1)}, h \right) \right\} \qquad (48)$$

The singularity at t = -f is evaluated separately in Appendix V.

APPENDIX IV

EVALUATION OF COMPLETE ELLIPTIC INTEGRAL OF THE THIRD KIND

In the general case of Complete Elliptic Integrals of third kind

$$\Pi\left(\tfrac{\pi}{2}, \alpha^2, h\right) \tag{49}$$

According to C. Heuman [Ref. 5] they can be reduced to combinations of first and second kind elliptic integrals, depending on the value of α^2, that is depending on whether the integrals are hyperbolic or circular. In the present case

$$\alpha^2 = \frac{2(k+p)}{(k+1)(1+p)} \tag{50}$$

where p can be f, c, or -g and

$$h = \frac{2\sqrt{h}}{k+1} \tag{51}$$

a. For the case of p = f, we have $\alpha^2 > 1$

$$\Pi\left(\tfrac{\pi}{2}, \alpha^2, h\right) = -\frac{\alpha K Z(\beta, h)}{\sqrt{(\alpha^2-1)(\alpha^2-h^2)}} \tag{52}$$

where

$$\beta = \sin^{-1}\left(\frac{1}{\alpha}\right)$$

b. For the case of p = c, we have $h^2 < \alpha^2 < 1$

and the transformation becomes

$$\Pi\left(\tfrac{\pi}{2}, \alpha^2, h\right) = \frac{\pi}{2}\frac{\alpha \Lambda_0\left(\xi, h\right)}{\sqrt{(\alpha^2-h^2)(1-\alpha^2)}} \tag{53}$$

where

$$\xi = \sin^{-1}\sqrt{\frac{\alpha^2-h^2}{\alpha^2(1-h^2)}}$$

c. For the case of p = -g, we have $\alpha^2 < 0$

and the transformation becomes:

$$\Pi\left(\tfrac{\pi}{2}, \alpha^2, h\right) = \frac{h^2 K}{h^2-\alpha^2} - \frac{\pi}{2}\frac{\alpha^2 \Lambda_0(\phi,h)}{\sqrt{\alpha^2(1-\alpha^2)(\alpha^2-h^2)}} \tag{54}$$

where

$$\phi = \sin^{-1}\sqrt{\frac{\alpha^2}{\alpha^2-h^2}}$$

where the Heuman's Lambda function Λ_0 is defined as

$$\Lambda_0(\beta,h) = \frac{2}{\pi}\left[E\,F(\beta,h') + K\,E(\beta,h') - K\,F(\beta,h')\right] \tag{55}$$

and the Jacobi's Zeta function Z is defined as

$$Z(\beta,h) = E(\beta,h) - \frac{E}{K}F(\beta,h) \tag{56}$$

where

$E(\beta,h)$ is the elliptic integral of the second kind (57)

$F(\beta,h)$ is the elliptic integral of the first kind (58)

and $E = E\left(\tfrac{\pi}{2},h\right)$ (59)

$K = F\left(\tfrac{\pi}{2},h\right)$ (60)

and $h'^2 = 1-h^2$

Subroutine CEL3 was written to calculate the complete elliptic integrals of the third kind for all the cases of α^2 cited above.

APPENDIX V

EVALUATION OF THE DISCONTINUITY OF THE INTEGRAL

$$\int_{-1}^{+1} \frac{dt}{(t+f)\sqrt{(t^2-k^2)(t^2-1)}} \tag{61}$$

Since there is a discontinuity at t = -f, we have to go to the limiting process as follows

$$\int_{-1}^{+1} f(t) = \int_{-1}^{-f+\varepsilon} f(t) + \int_{-f-\varepsilon}^{+1} f(t) \qquad \text{as } \varepsilon \to 0 \tag{62}$$

As calculated in Appendix IV

$$\int \frac{dt}{(t+f)\sqrt{(t^2-k^2)(t^2-1)}} = \frac{2}{(1+k)(f+k)}\left\{ F(\varphi,h) - \frac{(1-k)}{(f+1)}\Pi\left(\varphi, \frac{2(k+f)}{(1+k)(1+f)}, h\right)\right\} \tag{63}$$

where

$$\sin^2\varphi = \frac{(t-1)(1+k)}{2(t-k)} \tag{64}$$

When taking $\int_{-1}^{+1} f(t)\,dt$, we have $\int_{\frac{\pi}{2}}^{0} f(\varphi)$ which means that $F(\varphi,h)$ reduces to K (complete elliptic integral of the first kind) and $\Pi(\varphi,\alpha^2,h)$ reduces to $\Pi(\alpha^2,h)$ (complete elliptic integral of the third kind). The only term which has a discontinuity is $\Pi(\varphi,\alpha^2,h)$ since $F(\varphi,h)$ is continuous.

At $t = -f+\varepsilon$

$$\varphi_1 = \sin^{-1}\sqrt{\frac{(1+k)(1+f-\varepsilon)}{2(f+k-\varepsilon)}}$$

and at $t = -f-\varepsilon$

$$\varphi_2 = \sin^{-1}\sqrt{\frac{(1+k)(1+f+\varepsilon)}{2(f+k+\varepsilon)}}$$

Then Eq. (62) becomes

$$B(0) - B(\varphi_2) + B(\varphi_1) - B\left(\frac{\pi}{2}\right) \tag{65}$$

Let us examine in particular, $B(\varphi_1) - B(\varphi_2)$, or

$$\Pi(\varphi_1, \alpha^2, h) - \Pi(\varphi_2, \alpha^2, h) \tag{66}$$

Transforming $\Pi(\varphi, \alpha^2, h)$ into a combination of first kind elliptict integrals and Zeta and Theta functions, according to [Ref. 4], we have

$$\Pi(\varphi, \alpha^2, h) = - \frac{\alpha\left[F(\varphi,h)\,Z(A,h) - \Omega_4\right]}{\sqrt{(\alpha^2-1)(\alpha^2-h^2)}} \tag{67}$$

where

$$\Omega_4 = \frac{1}{2} \ln \frac{\sin\left[\omega(A) + v\right]}{\sin\left[\omega(A) - v\right]} + \sum_{m=1}^{\infty} q^m \frac{\sin 2mv \sin 2m\omega(A)}{m \sinh 2mp}$$

$$A = \sin^{-1}\left(\frac{1}{\alpha}\right)$$

$$v = \frac{\pi}{2K} F(\varphi, h)$$

$$p = \frac{\pi}{2K} K(h')$$

$$\omega(\xi) = \frac{\pi}{2K} F(\xi, h)$$

$$q = e^{-2p}$$

when we take $B(\varphi_1) - B(\varphi_2)$ where $B(\varphi)$ is given by Eq. (67), we are left with

$$B(\varphi_1) - B(\varphi_2) = - \frac{\alpha\left[\Omega_4(\varphi_1) - \Omega_4(\varphi_2)\right]}{\sqrt{(\alpha^2-1)(\alpha^2-h^2)}} \tag{68}$$

Examining Ω_4 further we find that every term is independent of ξ except v , which is a function of φ . Thus Eq. (68) may be written as

$$B(\varphi_1) - B(\varphi_2) = - \frac{\alpha}{2\sqrt{(\alpha^2-1)(\alpha^2-h^2)}} \left[\ln \frac{\sin\left[\frac{\pi}{2K}\left\{F(A,h) + F(\varphi_1,h)\right\}\right]}{\sin\left[\frac{\pi}{2K}\left\{F(A,h) - F(\varphi_1,h)\right\}\right]} - \ln \frac{\sin\left[\frac{\pi}{2K}\left\{F(A,h) + F(\varphi_2,h)\right\}\right]}{\sin\left[\frac{\pi}{2K}\left\{F(A,h) - F(\varphi_2,h)\right\}\right]} \right] \tag{69}$$

Simplifying, Eq. (69) reduces to

$$= -\frac{\frac{\alpha}{2}}{\sqrt{(\alpha^2-1)(\alpha^2-1)}} \ln \frac{\sin\left[\frac{\pi}{2K}\left\{F(A,h)+F(\varphi_1,h_1)\right\}\right]\cdot\sin\left[\frac{\pi}{2K}\left\{F(A,h)-F(\varphi_2,h_1)\right\}\right]}{\sin\left[\frac{\pi}{2K}\left\{F(A,h)-F(\varphi_1,h)\right\}\right]\cdot\sin\left[\frac{\pi}{2K}\left\{F(A,h)+F(\varphi_2,h_1)\right\}\right]}$$

in the limit as $\varepsilon \to 0$, $\varphi_1 \to \varphi_2 \to \varphi$

The ratio inside the $\ln$ will reduce to unity unless $F(A, h_1) = \pm F(\varphi, h)$

Replacing A by

$$A = \sin^{-1}\frac{1}{\alpha} = \sin^{-1}\sqrt{\frac{(1+k)(1+f)}{2(k+f)}}$$

and φ by

$$\varphi = \sin^{-1}\sqrt{\frac{(1+k)(1+f)}{2(k+f)}}$$

Then $A = \varphi$

Thus we have an undetermined case of the type $\ln \frac{0}{0}$

Defining

$$F(\varphi_1, h) = F_1$$

$$F(\varphi_2, h) = F_2$$

$$F(A, h) = F$$

$$\frac{\pi}{2K} = a$$

$$-\frac{\alpha/2}{\sqrt{(\alpha^2-1)(\alpha^2-h^2)}} = b$$

and using L'Hopital's rule, we have

$$= \lim_{\varepsilon\to 0} b \ln \frac{\sin(aF+aF_1)}{\sin(aF+aF_2)} + \lim_{\varepsilon\to 0} b \ln \frac{\sin(aF-aF_2)}{\sin(aF-aF_1)} \qquad (70)$$

which is equal to

$$= \lim_{\varepsilon\to 0} b \ln \frac{\sin(aF-aF_2)}{\sin(aF-aF_1)}$$

Using L'Hopital's rule

$$= \lim_{\varepsilon \to 0} b \ln \frac{\cos(aF - aF_2)\frac{\partial F_2}{\partial \varepsilon}}{\cos(aF - aF_1)\frac{\partial F_1}{\partial \varepsilon}}$$

or

$$= \lim_{\varepsilon \to 0} b \ln \frac{\frac{\partial F_2}{\partial \varepsilon}}{\frac{\partial F_1}{\partial \varepsilon}} \tag{71}$$

From Hildebrand (Adv. Calc. for Eng.) page 352, one has

$$\frac{\partial F(\varphi, h)}{\partial \varepsilon} = f(\sin\varphi)\,\frac{\partial \sin\varphi}{\partial \varepsilon} \tag{72}$$

where

$$f(\sin\varphi_1) = f(\varepsilon) = \frac{1}{\sqrt{(1-k^2)\left(1 - \frac{k^2(1+k)(1+f+\varepsilon)}{2(f+k+\varepsilon)}\right)}} \tag{73}$$

Then

$$\frac{\partial \sin(\varphi_1)}{\partial \varepsilon} = \sqrt{\frac{(k+1)}{2}}\,\frac{(k-1)}{2(f+k+\varepsilon)^{3/2}\sqrt{f+1+\varepsilon}} \tag{74}$$

and

$$\frac{\partial \sin(\varphi_2)}{\partial \varepsilon} = -\sqrt{\frac{(k+1)}{2}}\,\frac{(1-k)}{2(f+k-\varepsilon)^{3/2}\sqrt{f+1-\varepsilon}} \tag{75}$$

Now replacing Eqs. (72), (73), (74) and (75) in Eq. (71), and letting $\varepsilon \to 0$, one has

$$B(\varphi_1) - B(\varphi_2) = 0$$

APPENDIX VI

DERIVATION OF TURBULENCE - INTENSITY EQUATION

On a hot-wire anemometer the heat transfer equilibrium equation is given by

$$\frac{I^2 R_w}{R_w - R_g} = A + B\sqrt{U} \tag{76}$$

where I = current through the wire

R_w = operating resistance

R_g = cold resistance

A and B = constants

U = instantaneous velocity of the fluid

From (76) at $U = 0$ $I = I_o$

So

$$\frac{I^2 R_w}{R_w - R_g} = \frac{I_o^2 R_w}{R_w - R_g} + B\sqrt{U}$$

Multiplying both sides of the equation by R_w and replacing I^2R^2 by E^2 we obtain

$$E^2 = E_o^2 + B R_w (R_w - R_g)\sqrt{U}$$

or

$$E^2 = E_o^2 + C\sqrt{U} \tag{77}$$

Since the wire is kept at a constant temperature R_w and R_g are constants. Taking the derivative with respect to time, one has

$$2E\frac{dE}{dt} = \frac{C\sqrt{U}}{2U}\frac{du}{dt} \tag{78}$$

From Eq. (77) $$c\sqrt{U} = E^2 - E_o^2$$

Then Eq. (78) becomes $$\frac{1}{U}\frac{dU}{dt} = \frac{4E}{E^2 - E_o^2}\frac{dE}{dt}$$

where $\frac{dU}{dt} = \sqrt{\overline{u^2}}$ = velocity variation

and $\frac{dE}{dt} = \sqrt{\overline{e^2}}$ = voltage variation

Finally we have

$$\frac{\sqrt{\overline{u^2}}}{U} = \frac{4E}{E^2 - E_o^2}\sqrt{\overline{e^2}}$$

in other words, turbulence intensity is equal to $\frac{4E}{E^2 - E_o^2}$ times RMS reading.

TABLE I

Point in the z-plane	Corresponding Value in the t-plane	Corresponding Value in the -plane
A	0	$-\ln \frac{V_A}{V_j} + i\frac{\pi}{2}$
B	-k	$+\infty + i \begin{cases} c \\ \pi/2 \end{cases}$
C	-c	$-\ln \frac{V_C}{V_j} + i\,0$
D	-1	$0 + i\,0$
E	f	$0 + i\beta$
F	1	$0 + i\pi$
G	g	$-\ln \frac{V_G}{V_j} + i\pi$
H	k	$+\infty + i \begin{cases} \pi \\ \pi/2 \end{cases}$

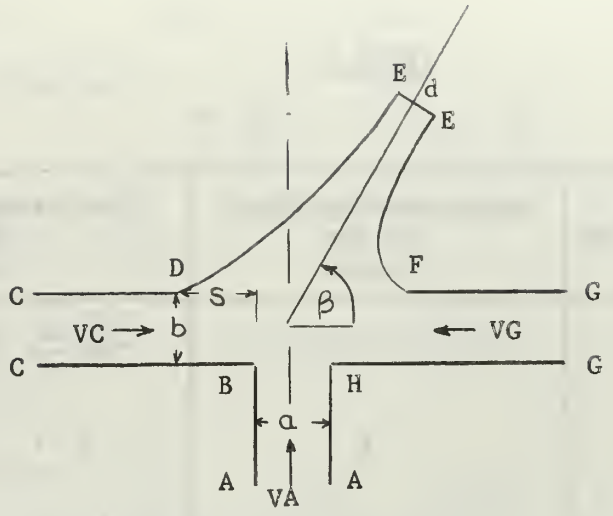

Figure 1a z-plane

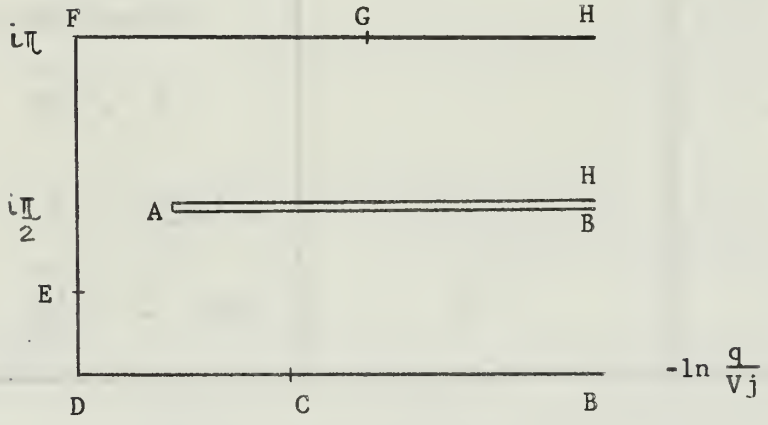

Figure 1b -plane

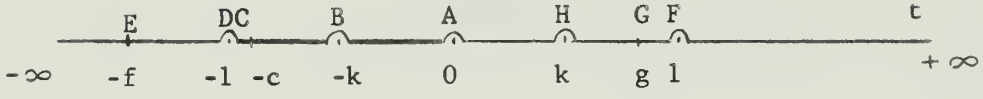

Figure 1c t-plane

Figure 1 Transformations Planes

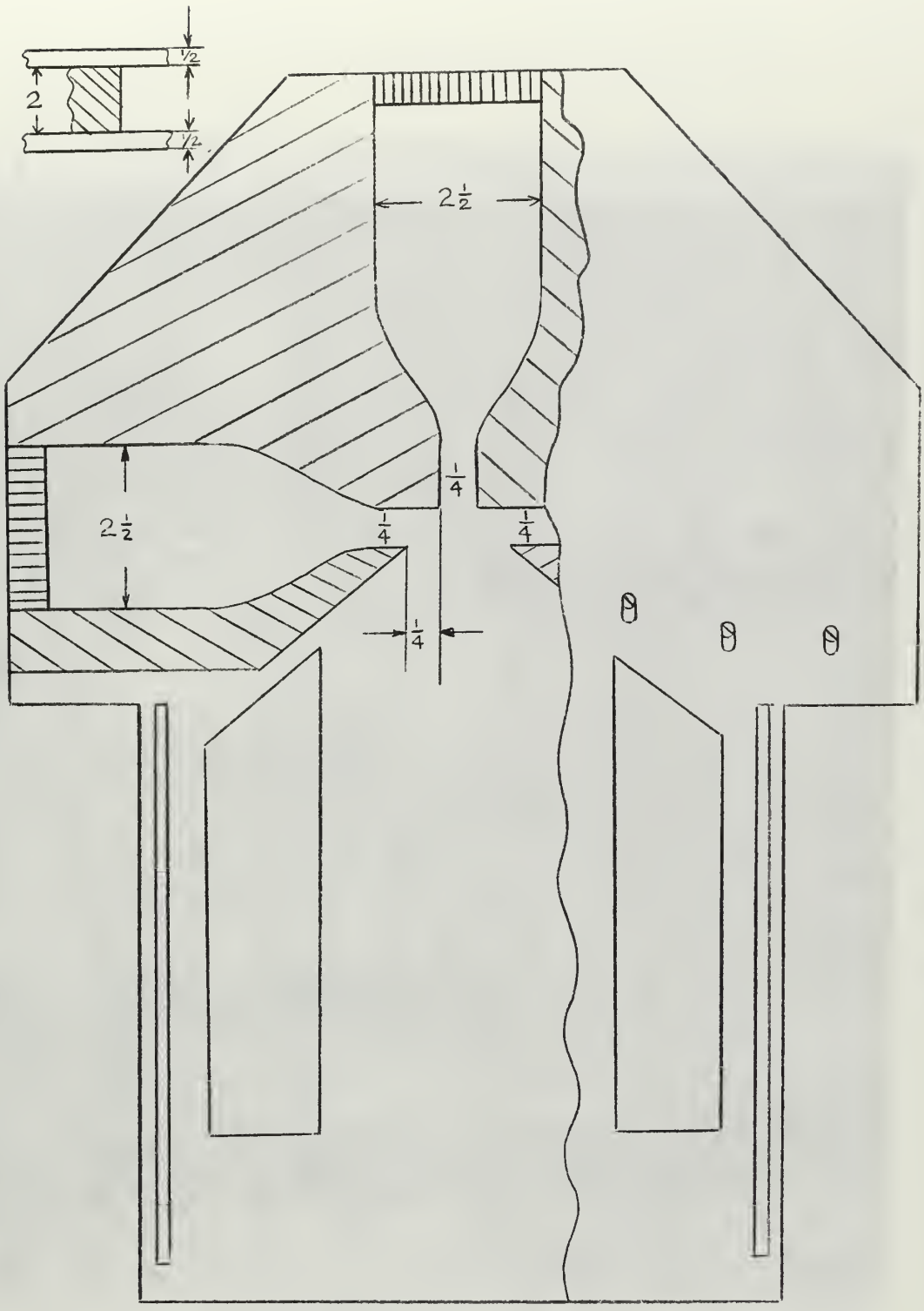

Figure 2 Jet Assembly

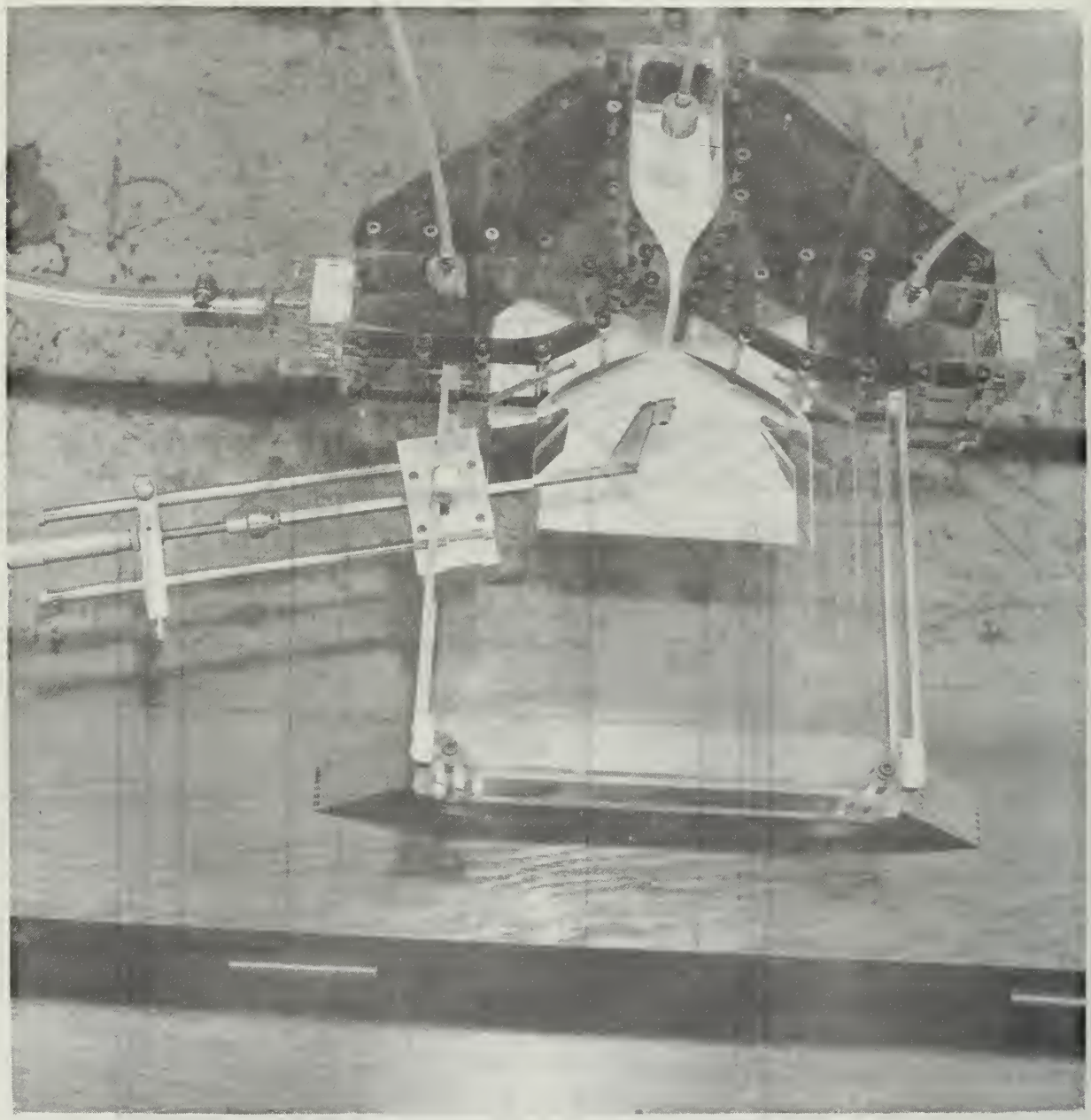

Figure 3 Jet Assembly

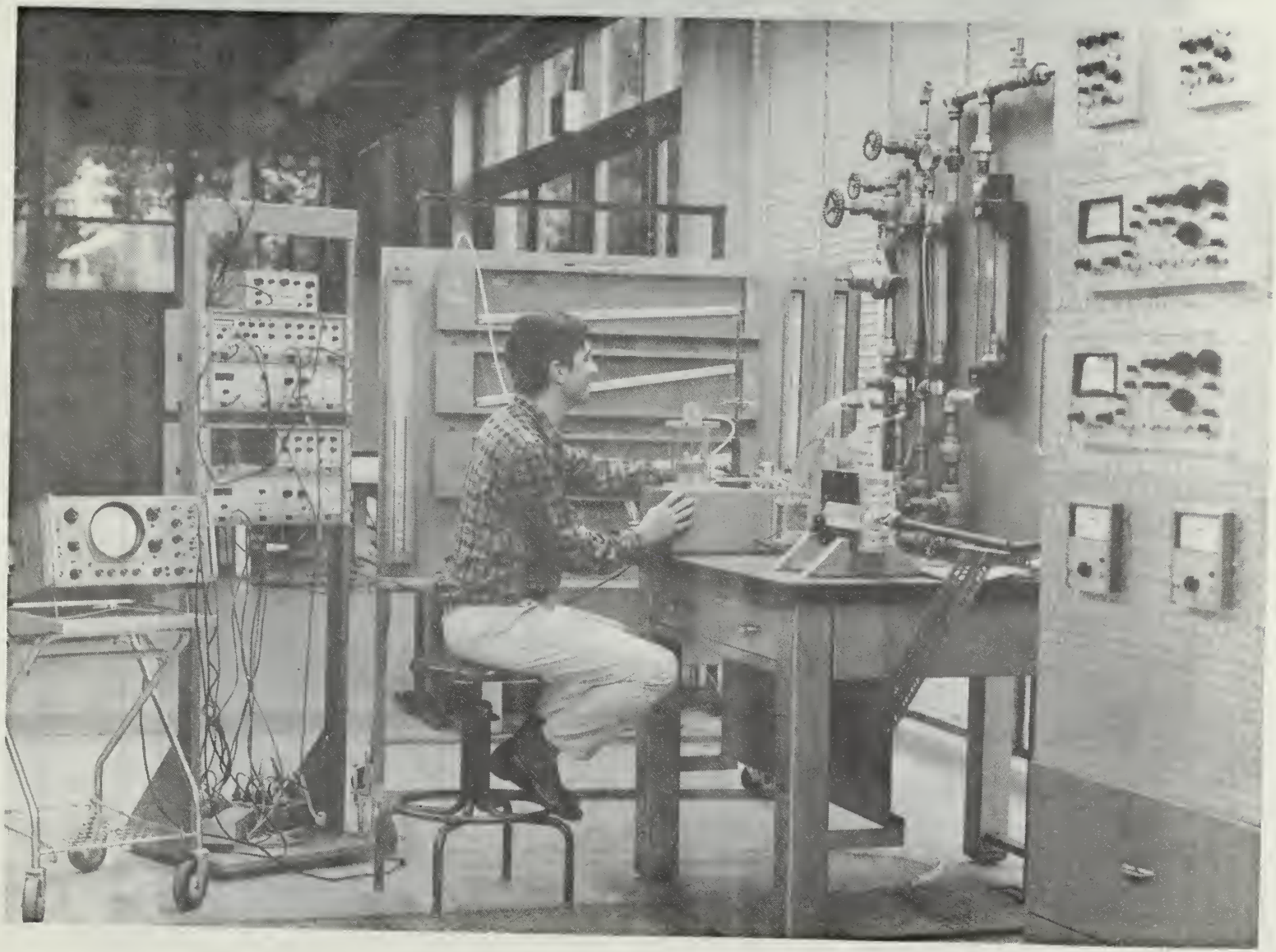

Figure 4 Calibration Equipment

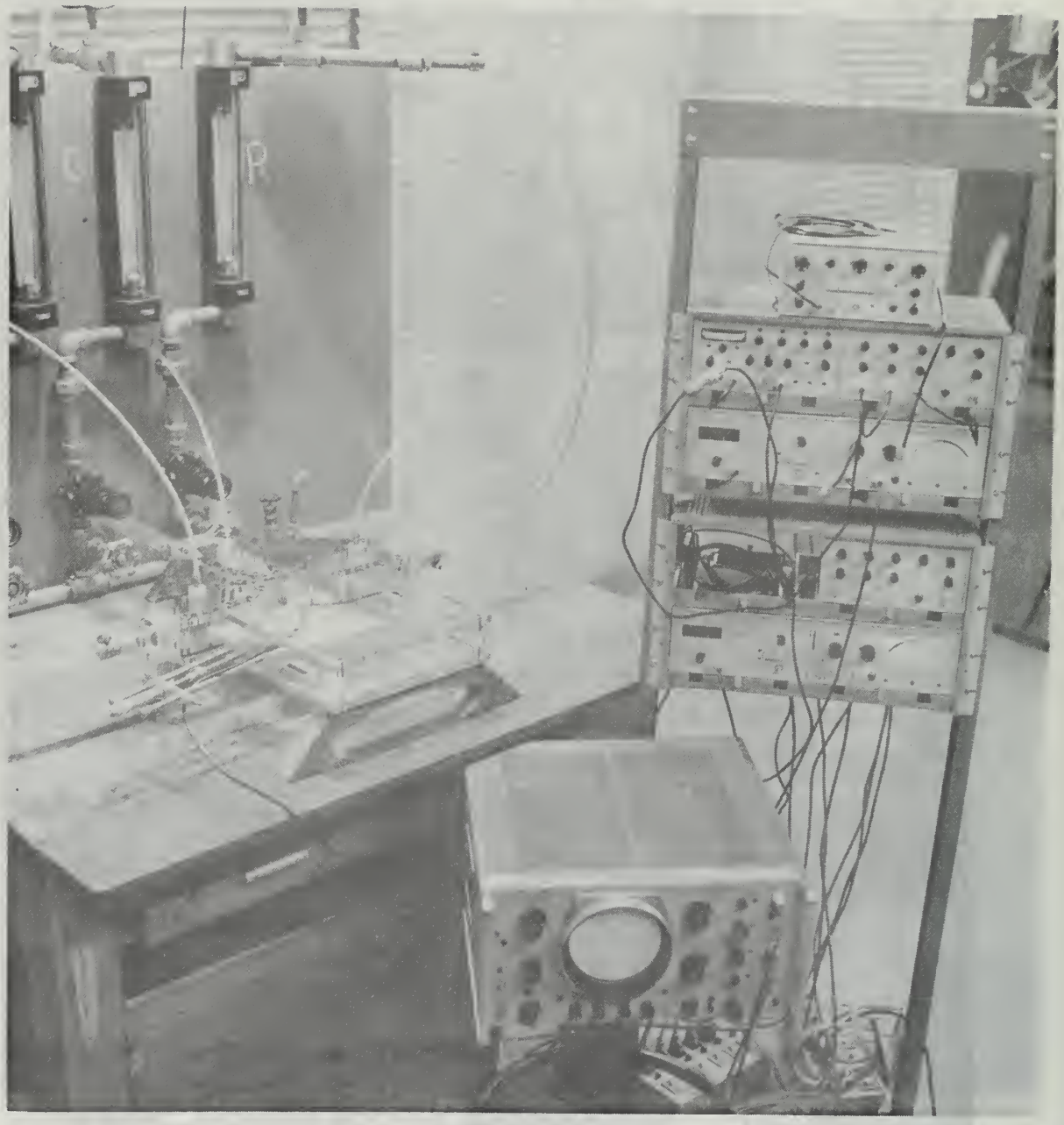

Figure 5 General Setup of Experiment

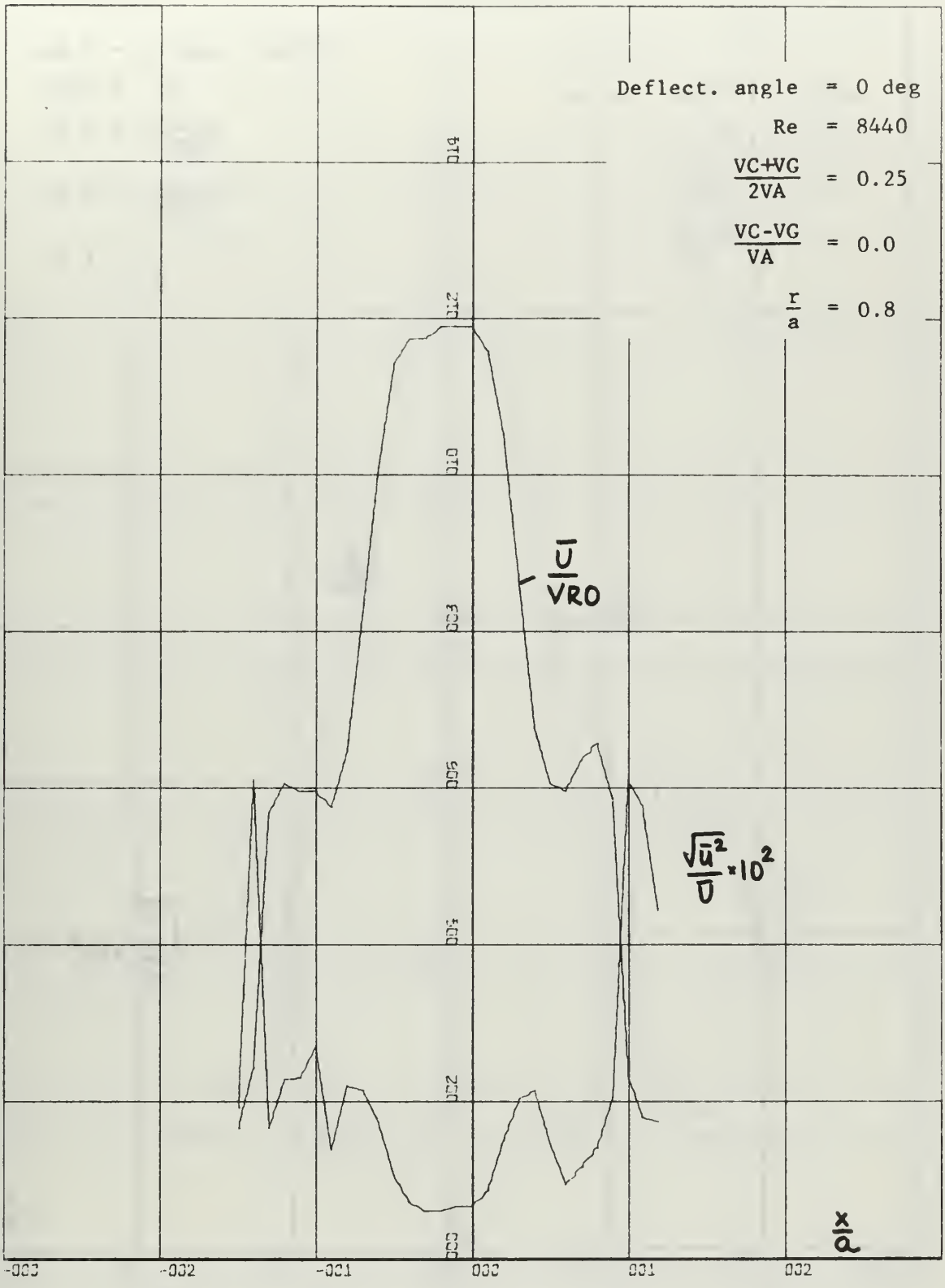

FIGURE 6 VELOCITY PROFILE AND TURBULENCE INTENSITY

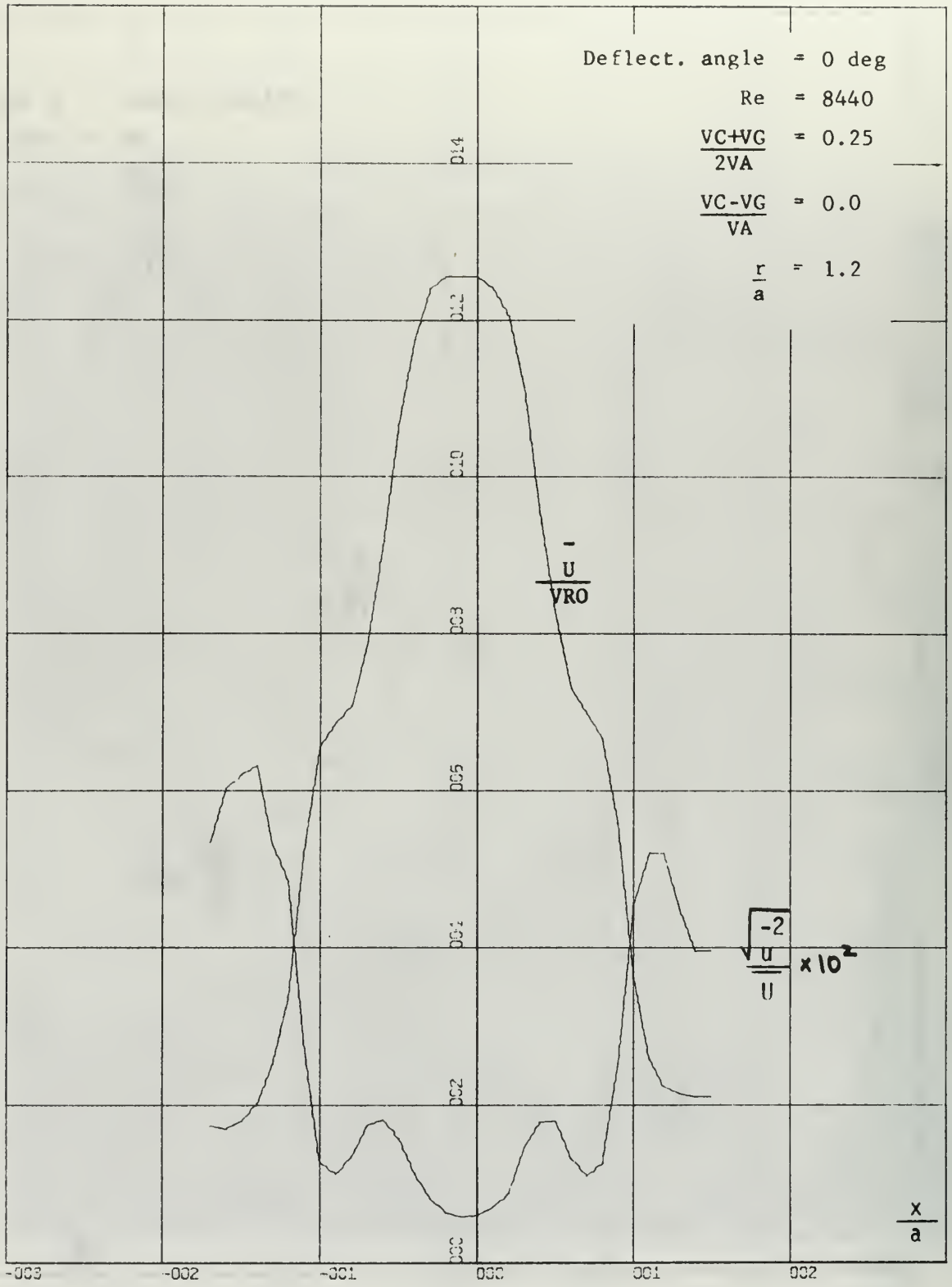

FIGURE 7 VELOCITY PROFILE AND TURBULENCE INTENSITY

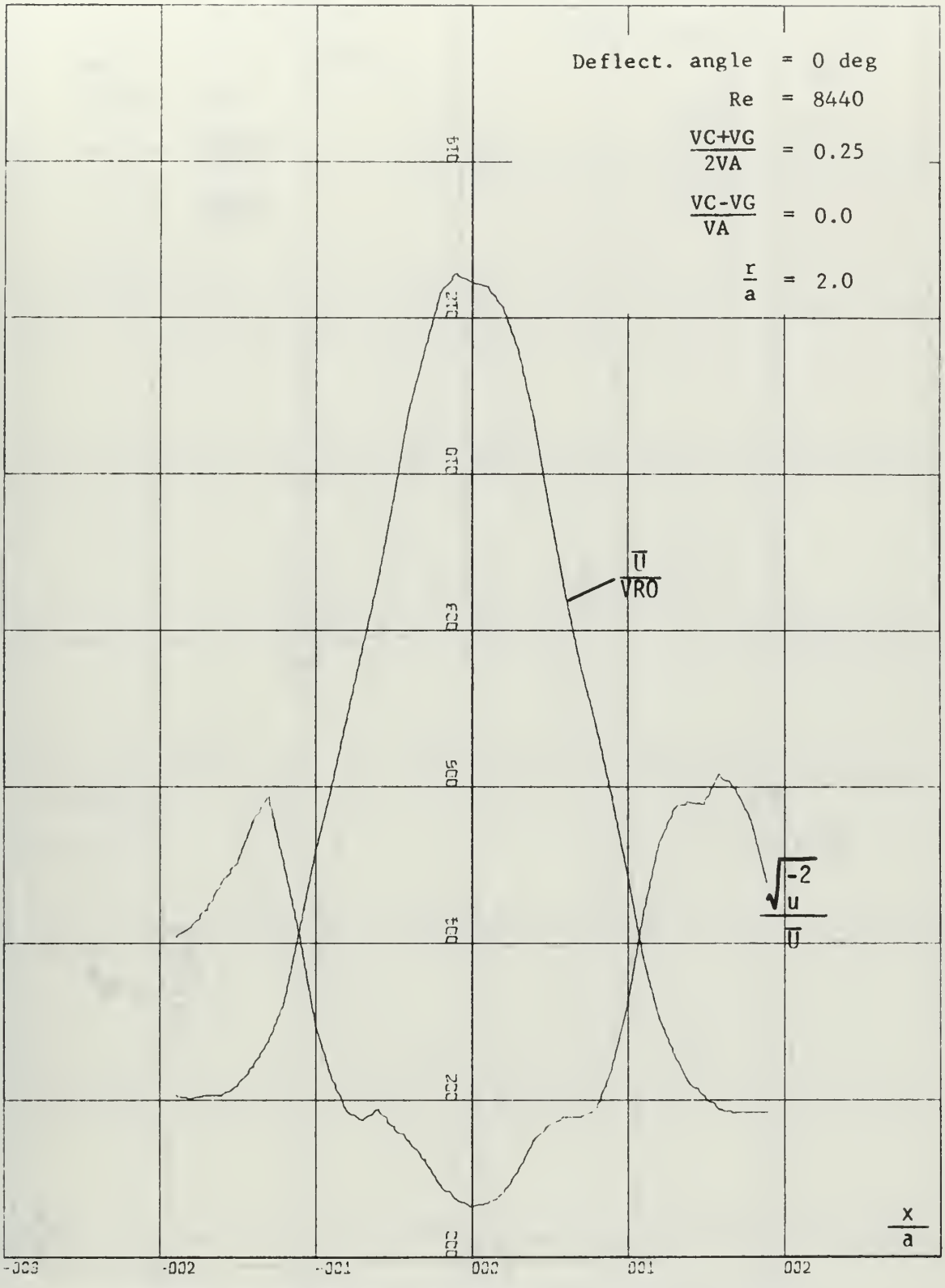

FIGURE 8 VELOCITY PROFILE AND TURBULENCE INTENSITY

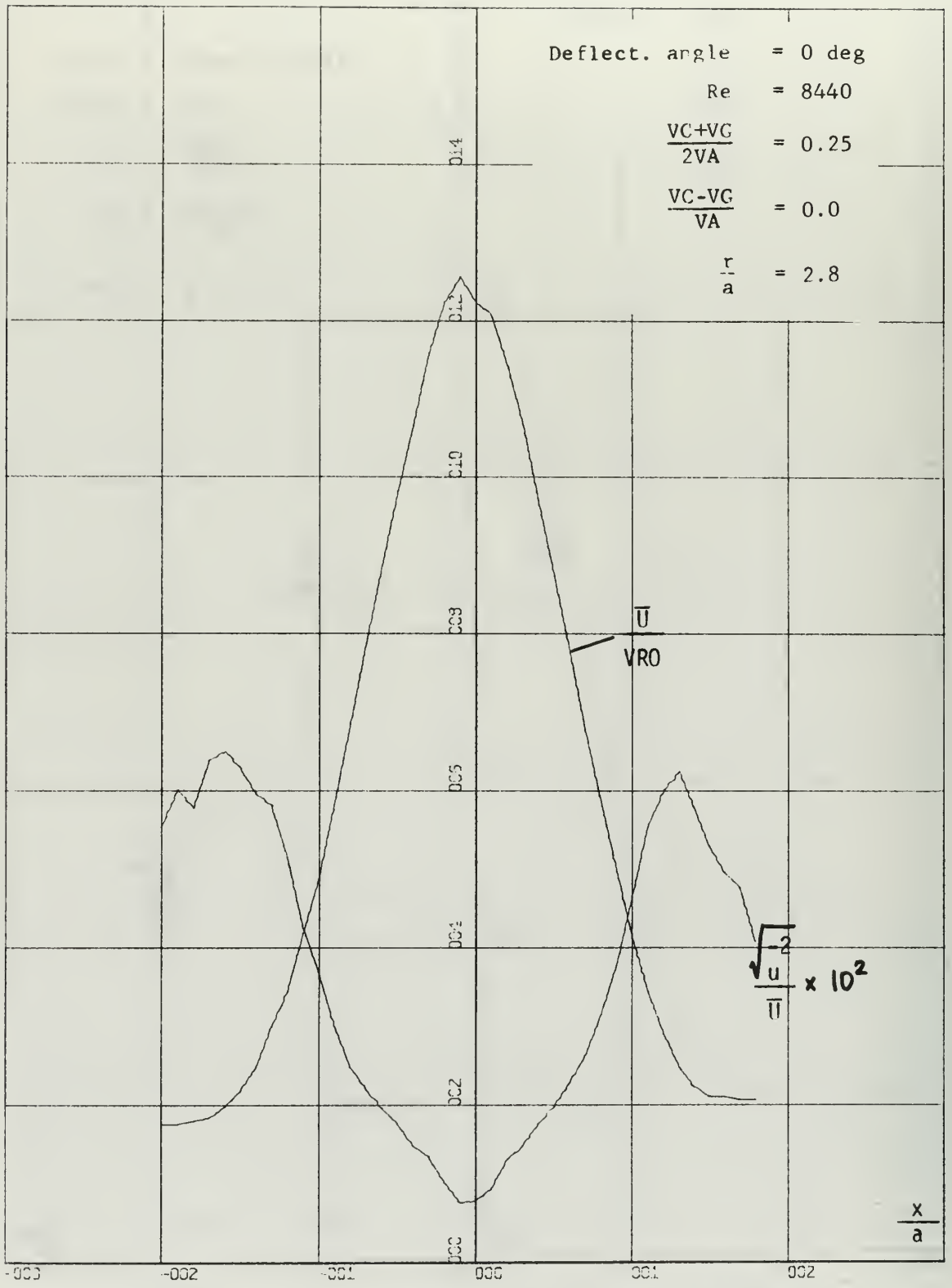

FIGURE 9 VELOCITY PROFILE AND TURBULENCE INTENSITY

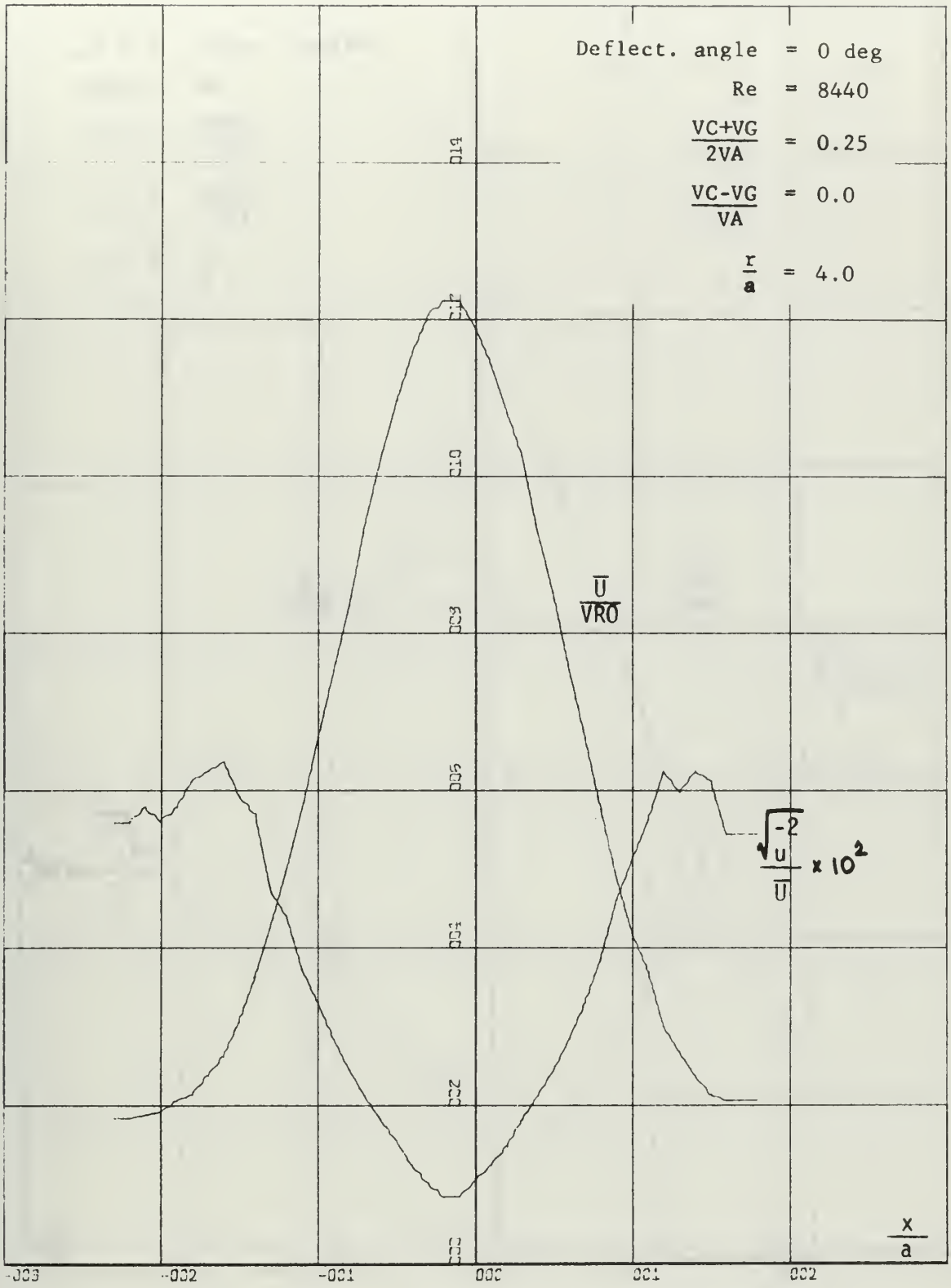

FIGURE 10 VELOCITY PROFILE AND TURBULENCE INTENSITY

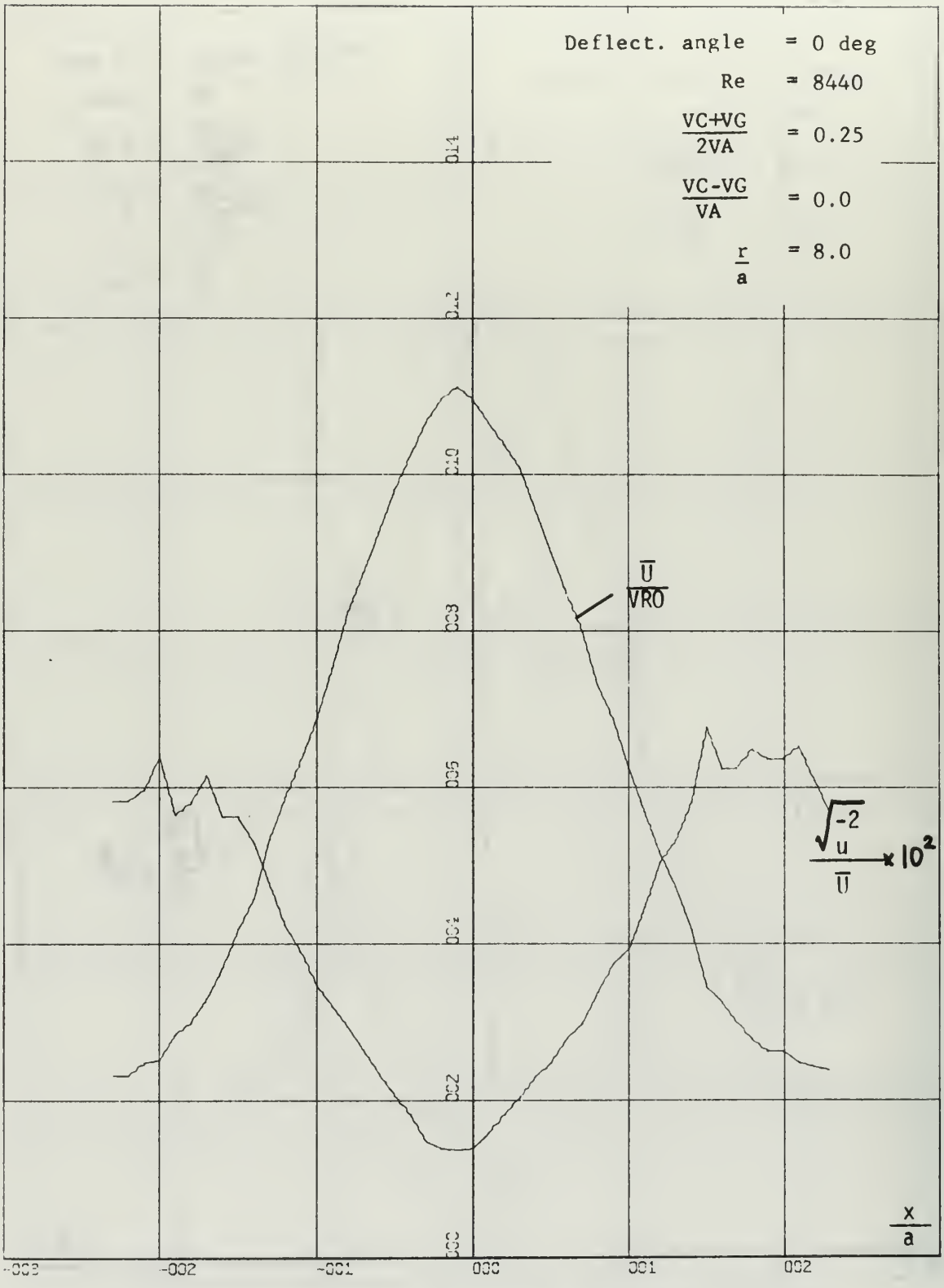

FIGURE 11 VELOCITY PROFILE AND TURBULENCE INTENSITY

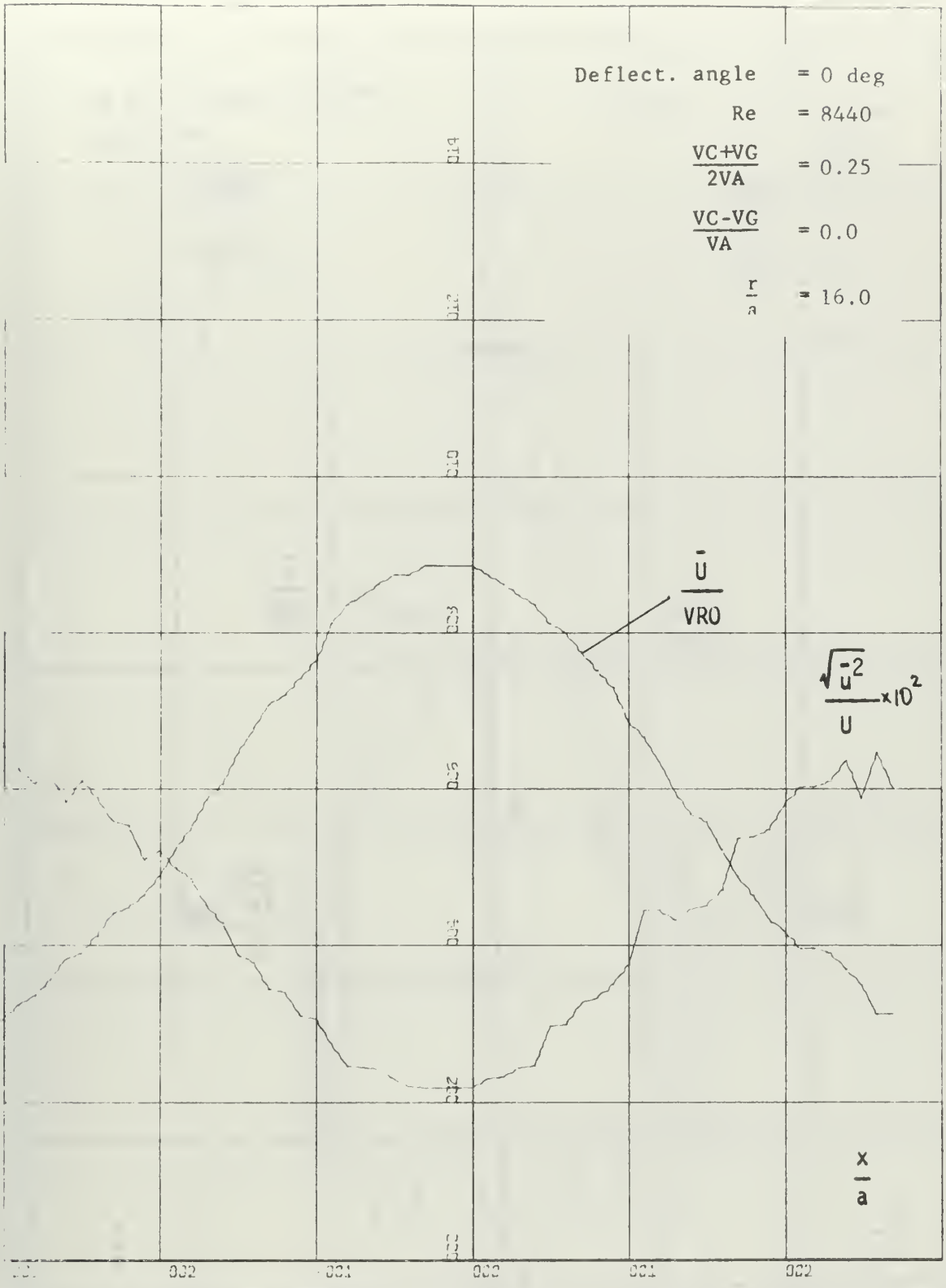

FIGURE 12 VELOCITY PROFILE AND TURBULENCE INTENSITY

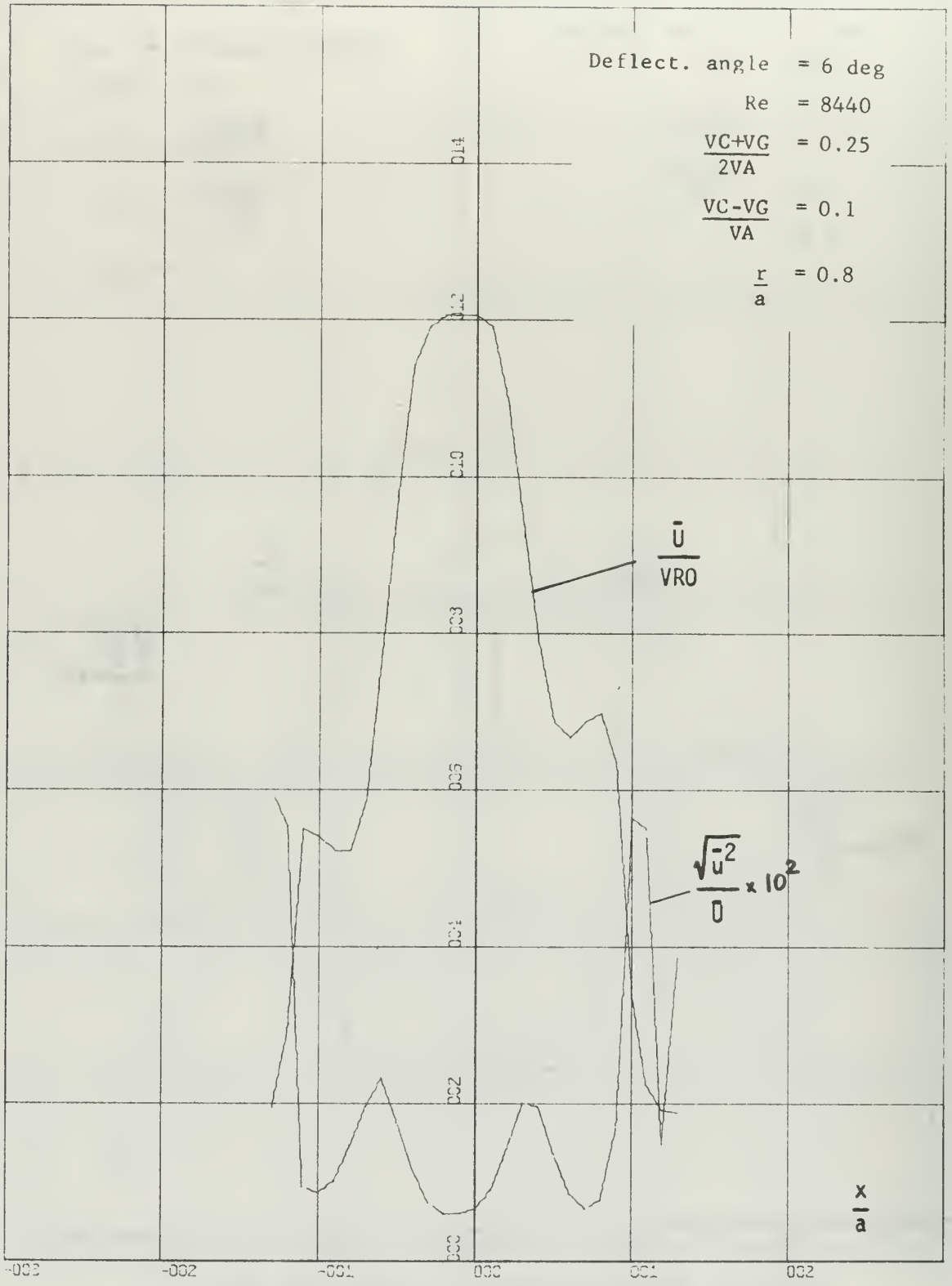

FIGURE 13 VELOCITY PROFILE AND TURBULENCE INTENSITY

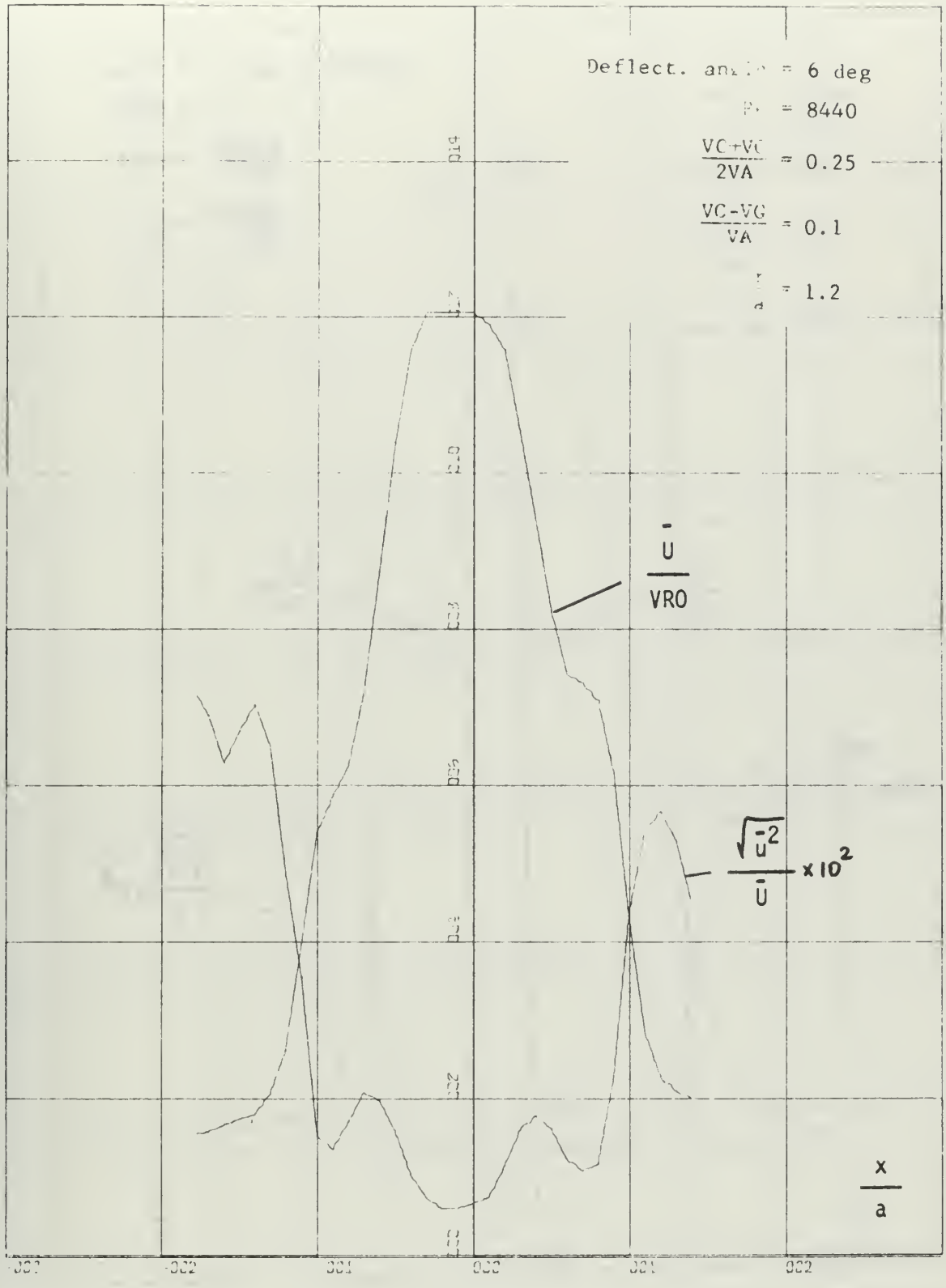

FIGURE 14 VELOCITY PROFILE AND TURBULENCE INTENSITY

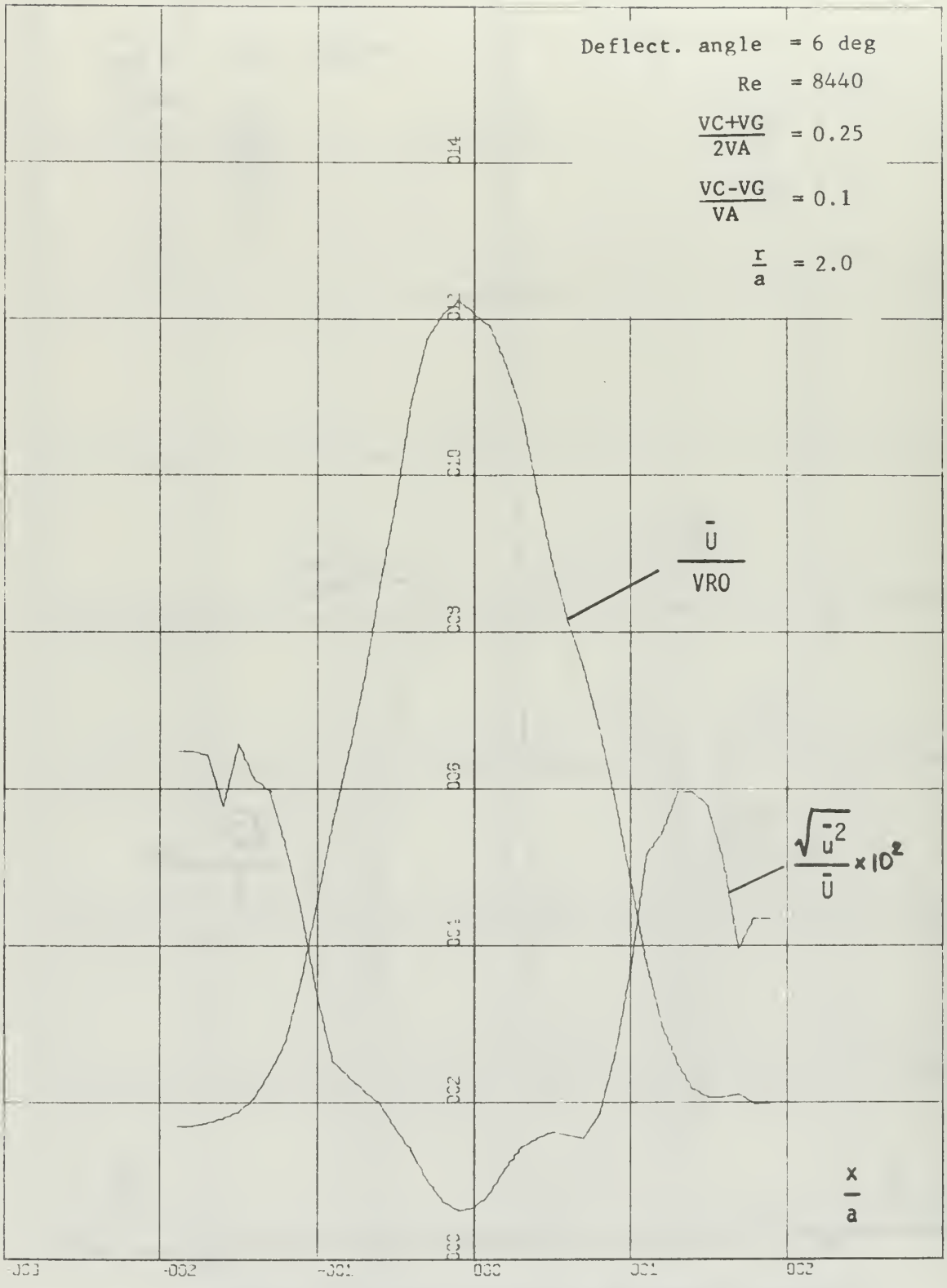

FIGURE 15 VELOCITY PROFILE AND TURBULENCE INTENSITY

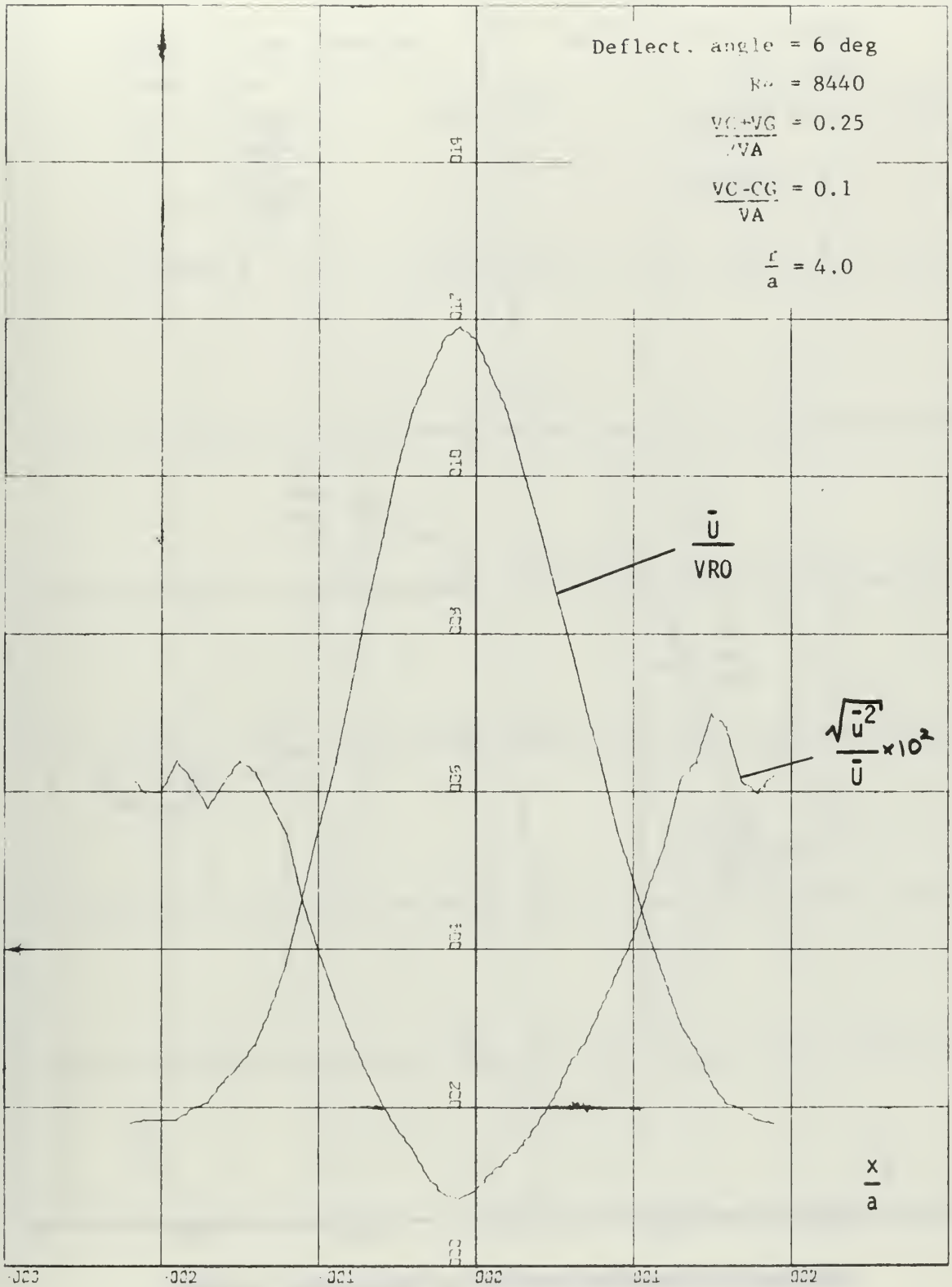

FIGURE 16 VELOCITY PROFILE AND TURBULENCE INTENSITY

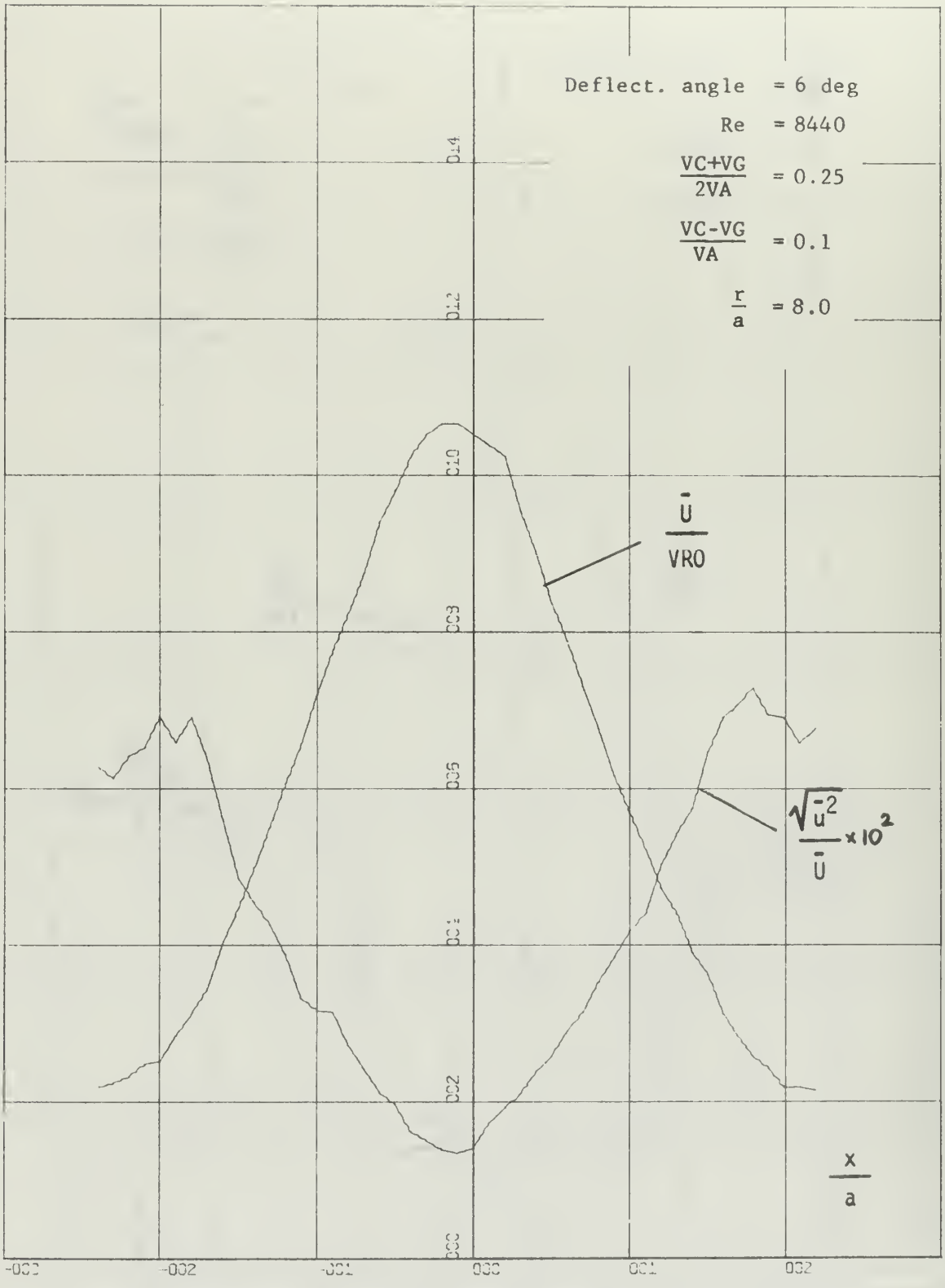

FIGURE 17 VELOCITY PROFILE AND TURBULENCE INTENSITY

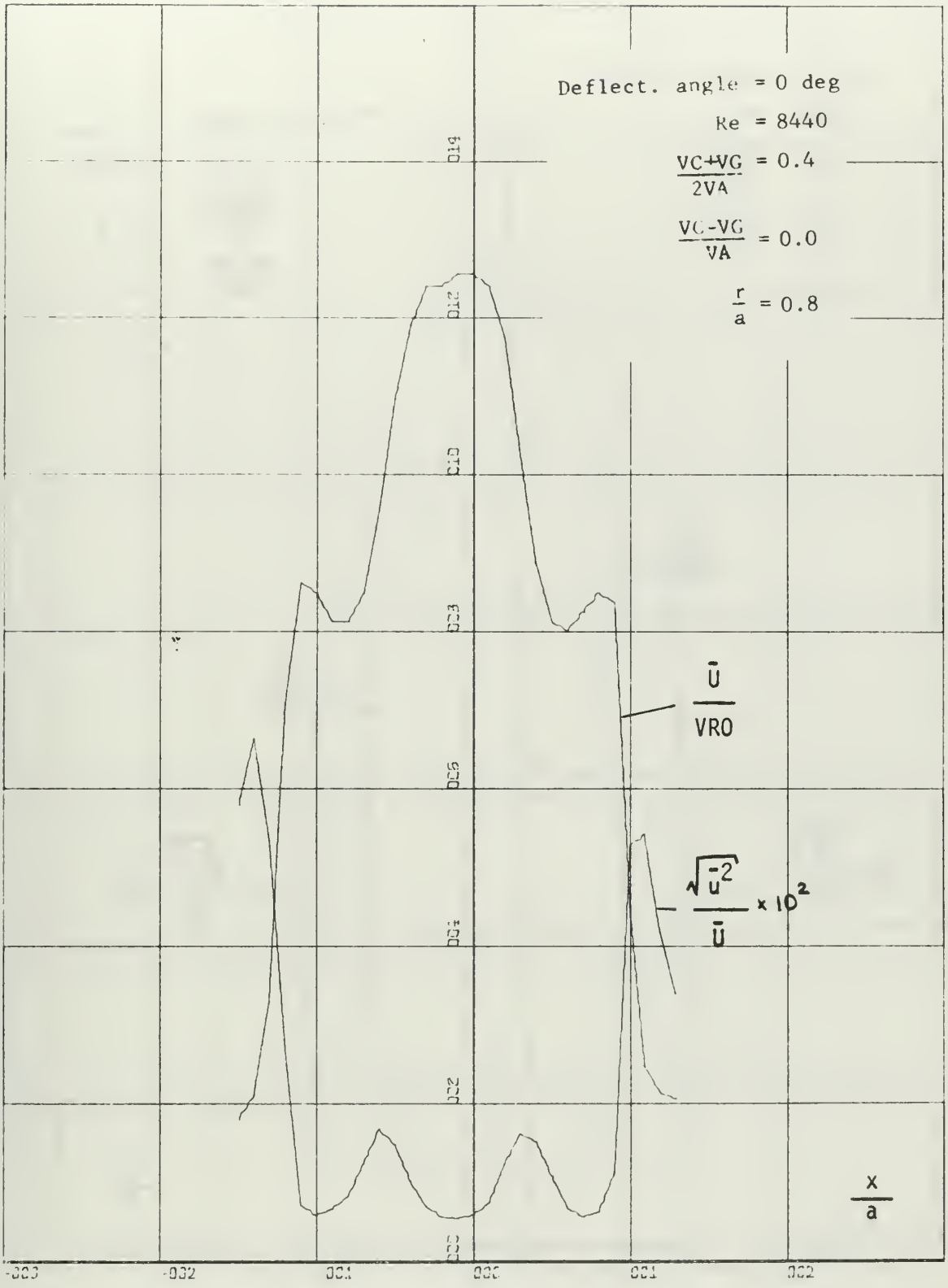

FIGURE 18 VELOCITY PROFILE AND TURBULENCE INTENSITY

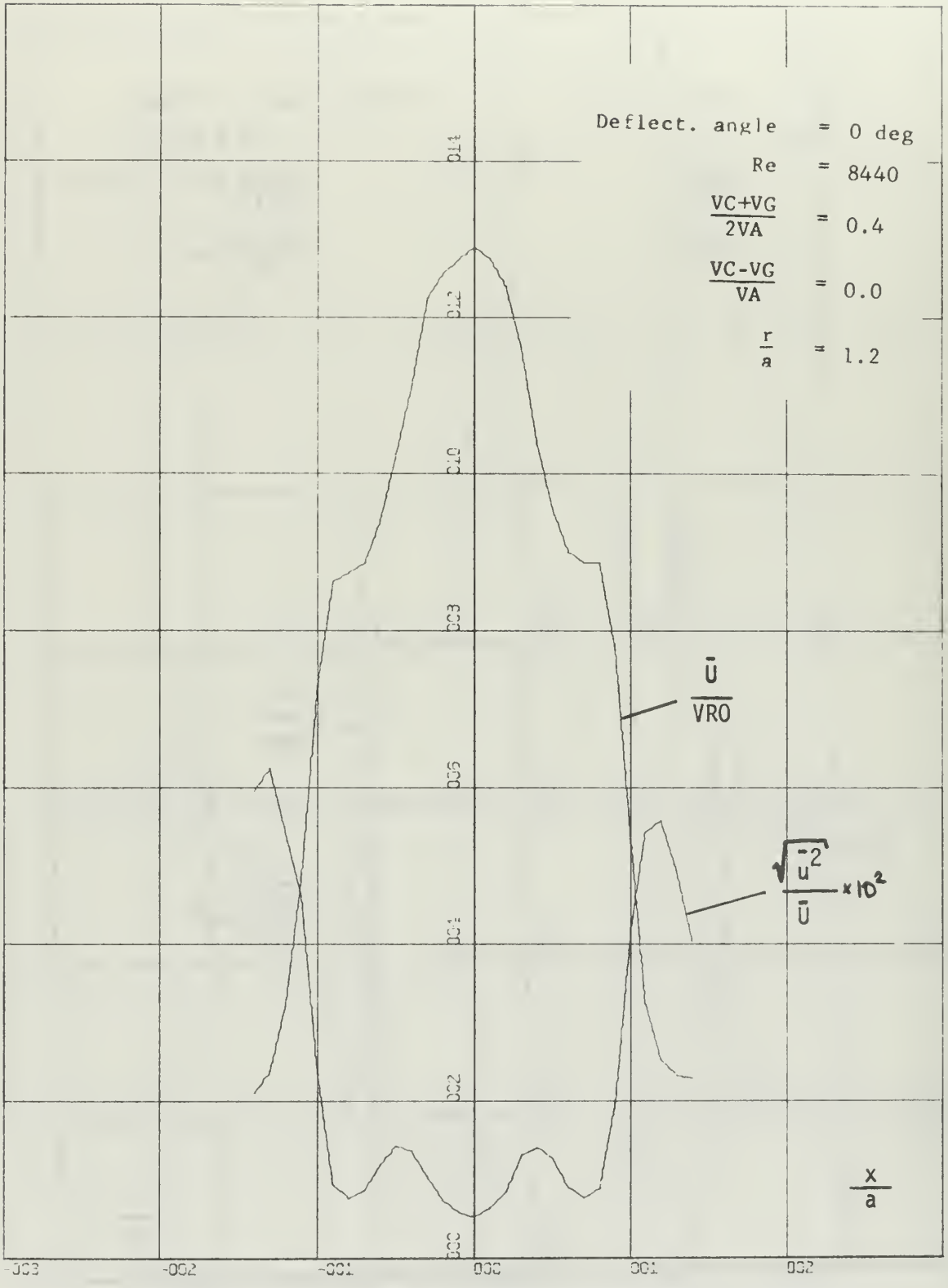

FIGURE 19 VELOCITY PROFILE AND TURBULENCE INTENSITY

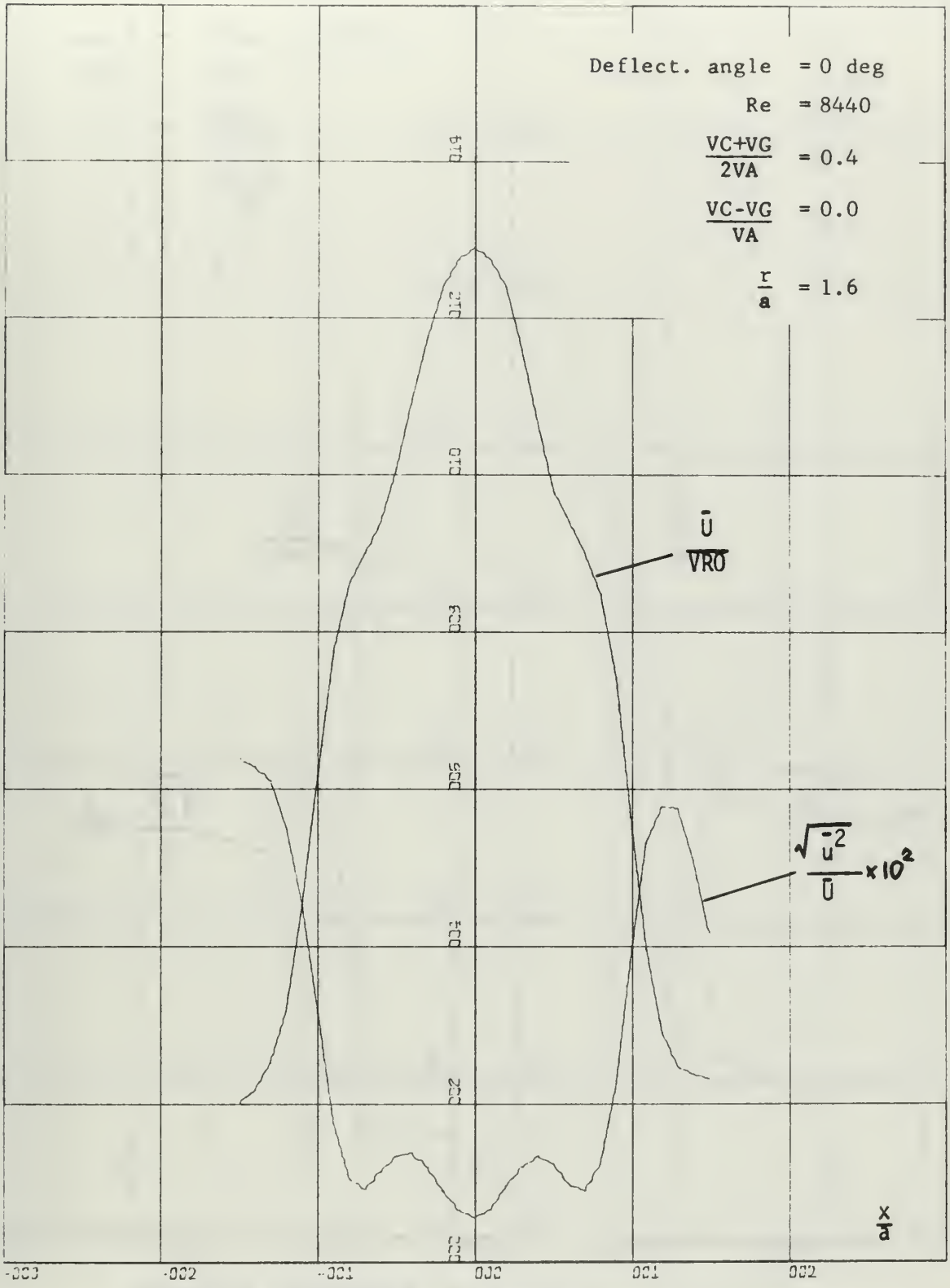

FIGURE 20 VELOCITY PROFILE AND TURBULENCE INTENSITY

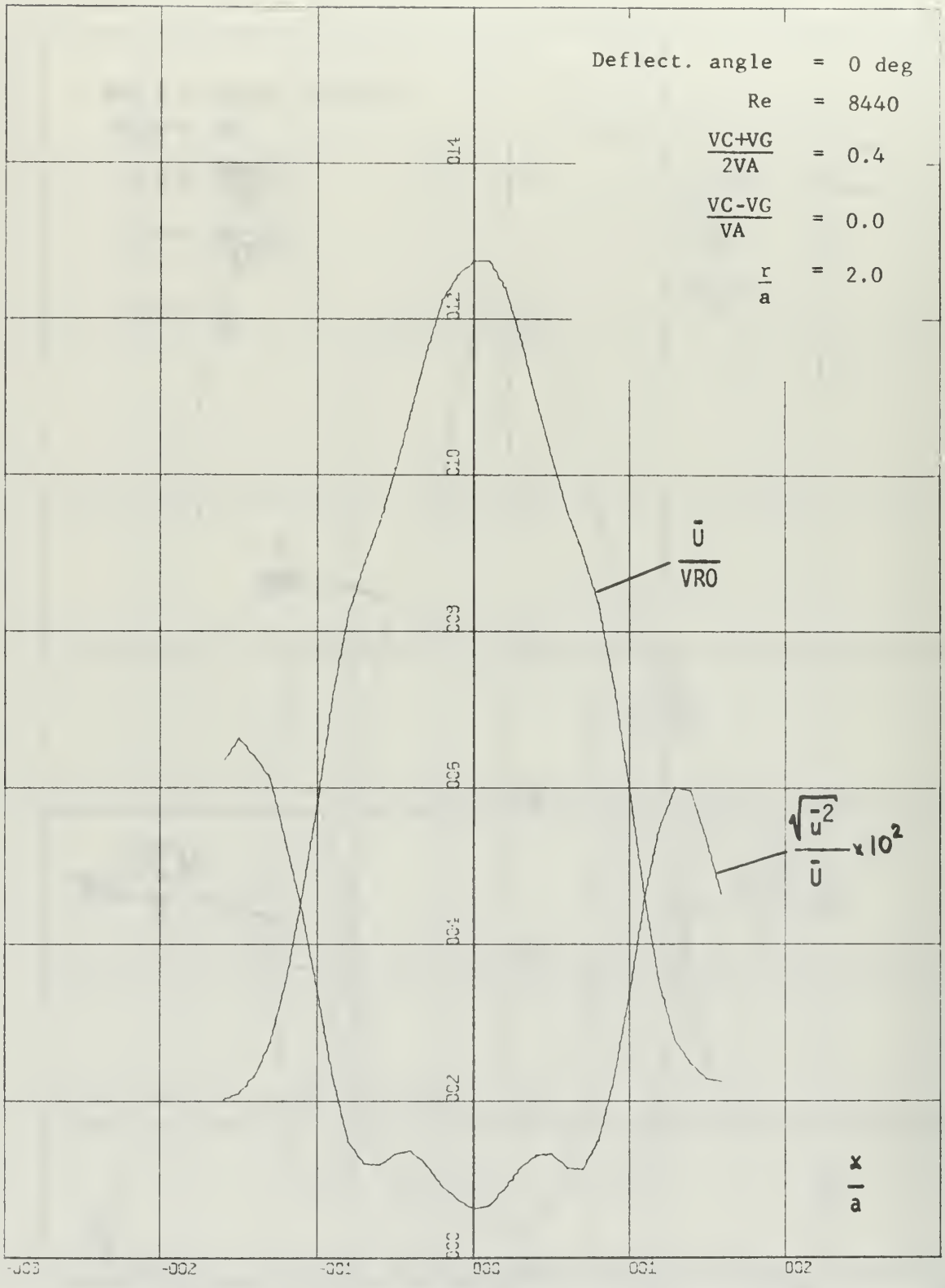

FIGURE 21 VELOCITY PROFILE AND TURBULENCE INTENSITY

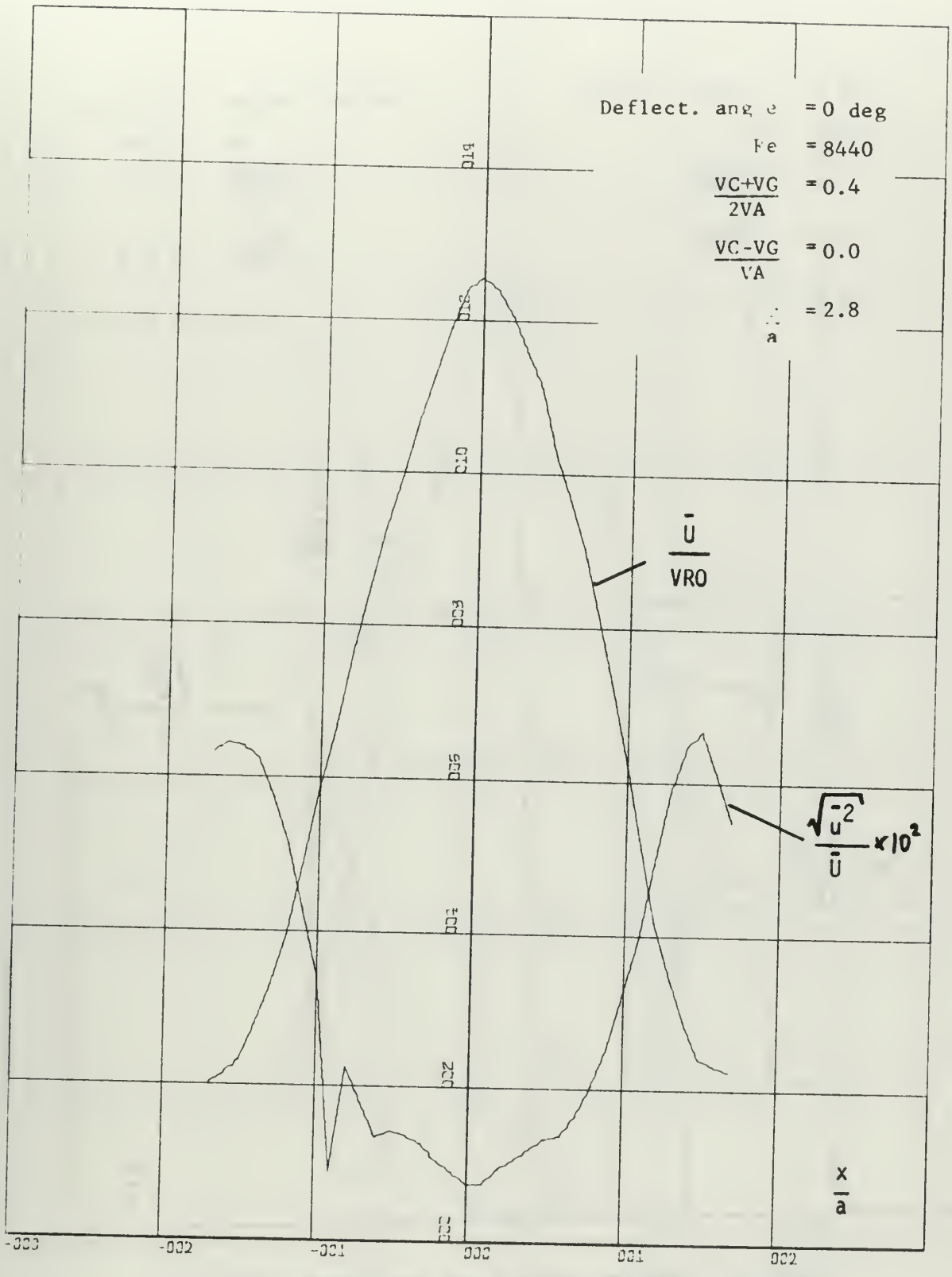

FIGURE 22 VELOCITY PROFILE AND TURBULENCE INTENSITY

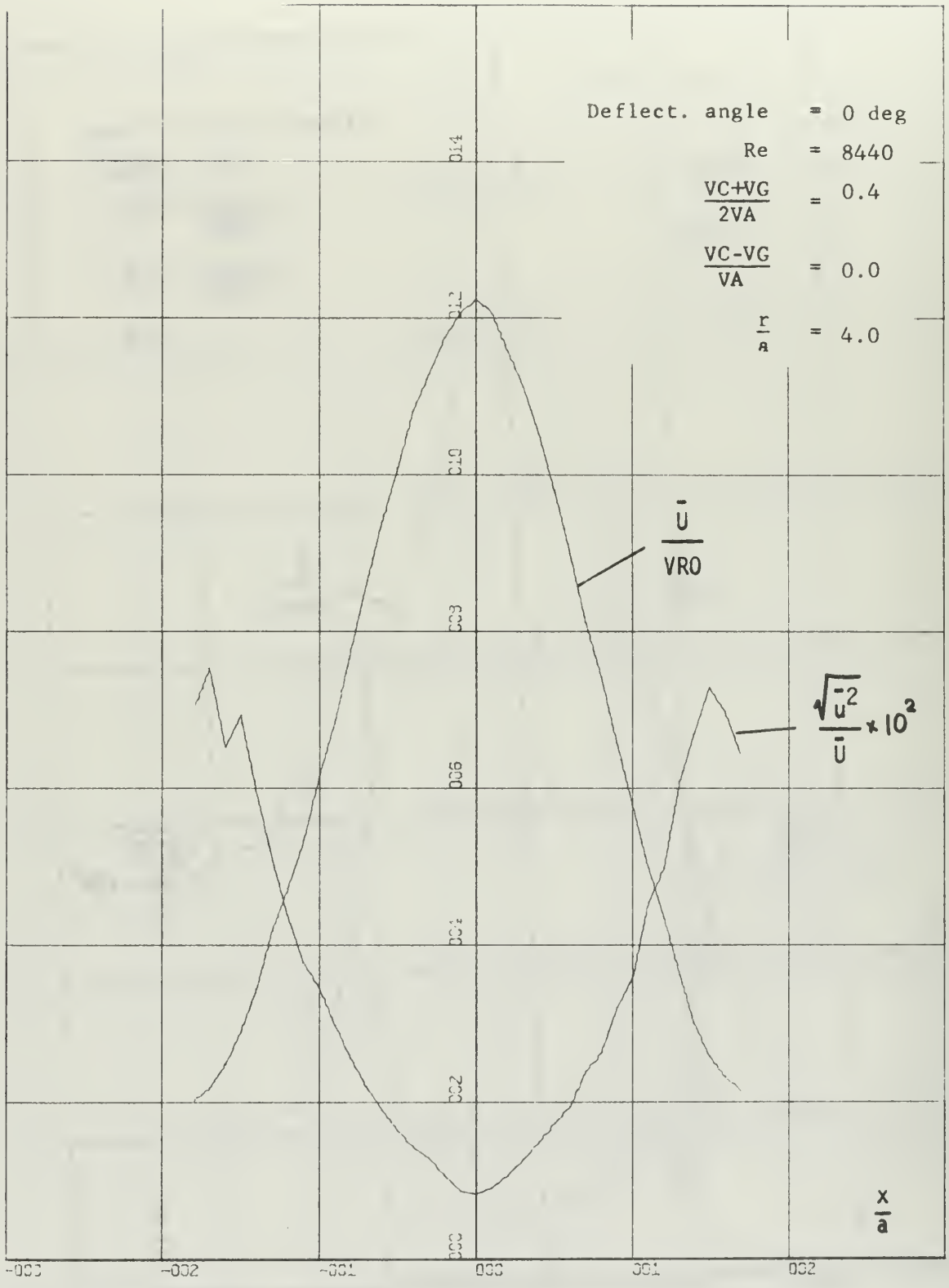

FIGURE 23 VELOCITY PROFILE AND TURBULENCE INTENSITY

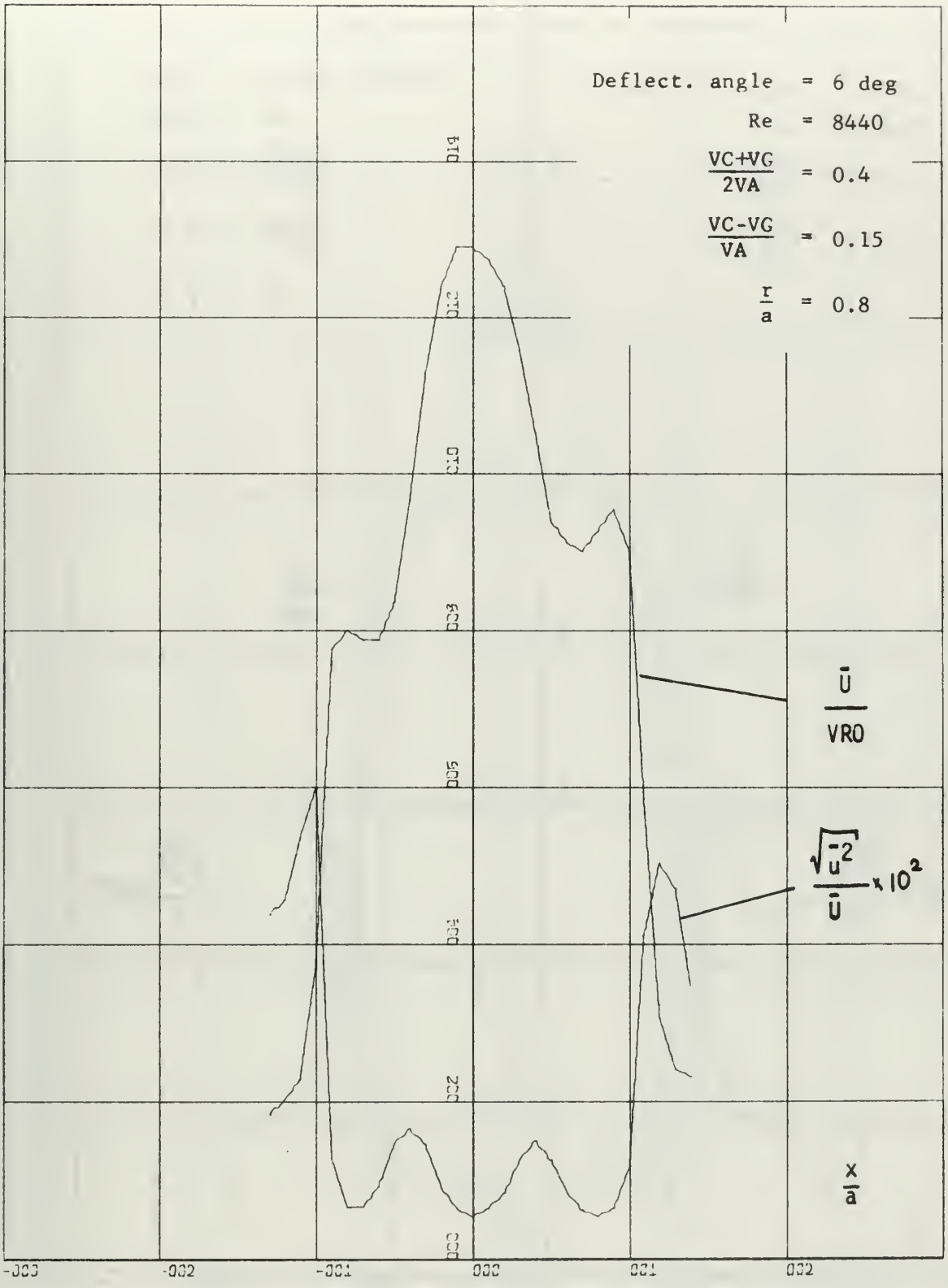

FIGURE 24 VELOCITY PROFILE AND TURBULENCE INTENSITY

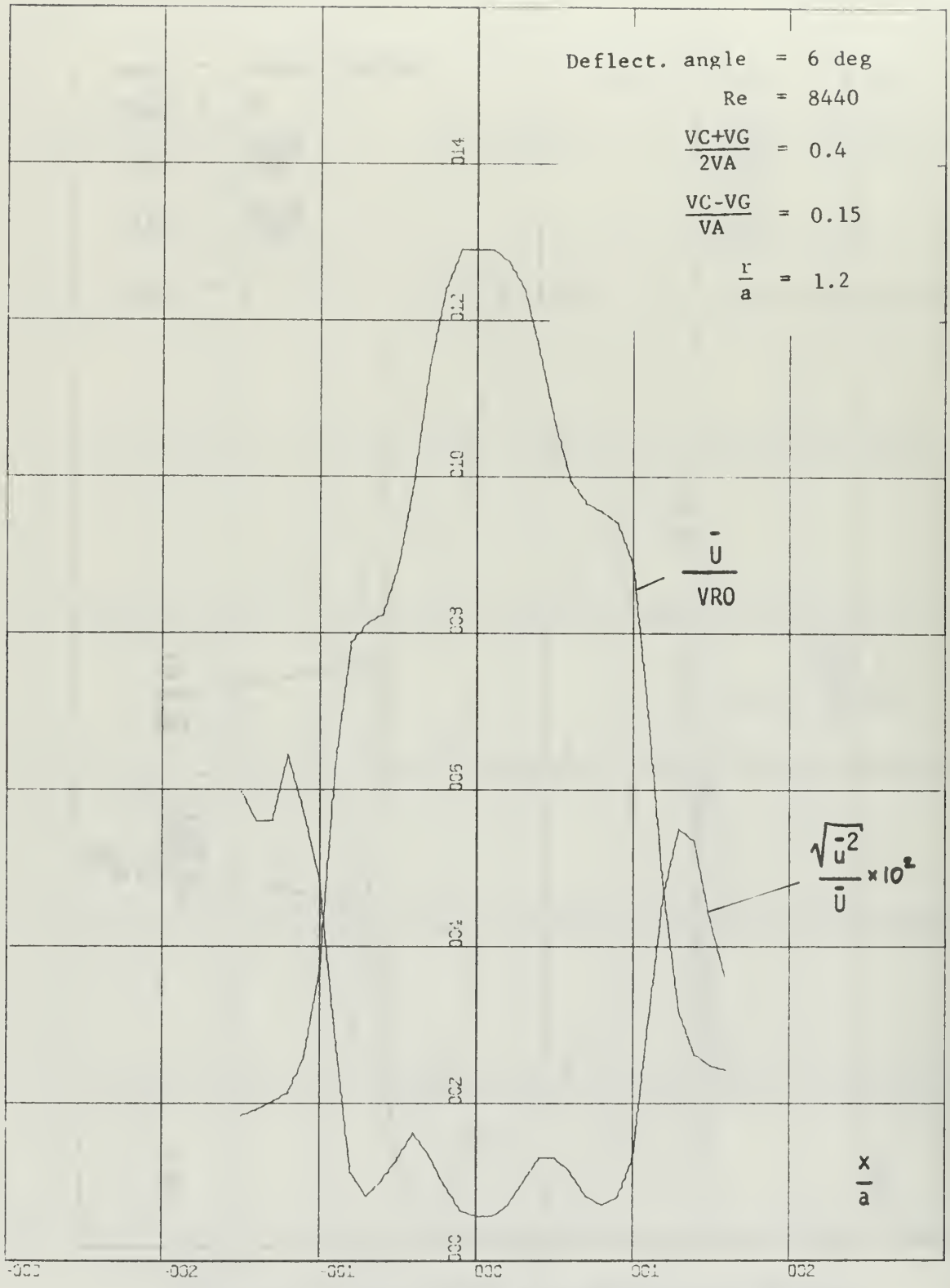

FIGURE 25 VELOCITY PROFILE AND TURBULENCE INTENSITY

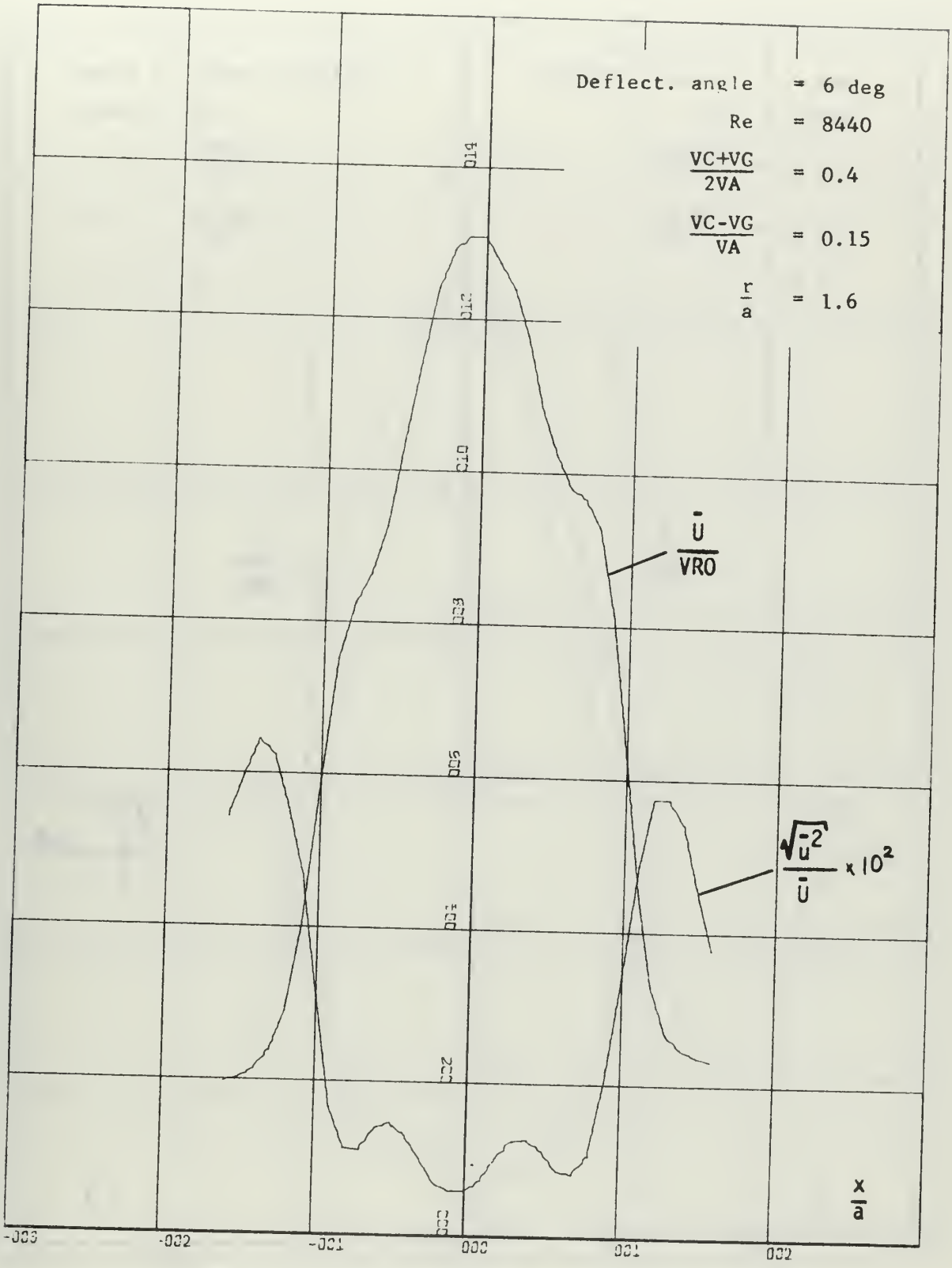

FIGURE 26 VELOCITY PROFILE AND TURBULENCE INTENSITY

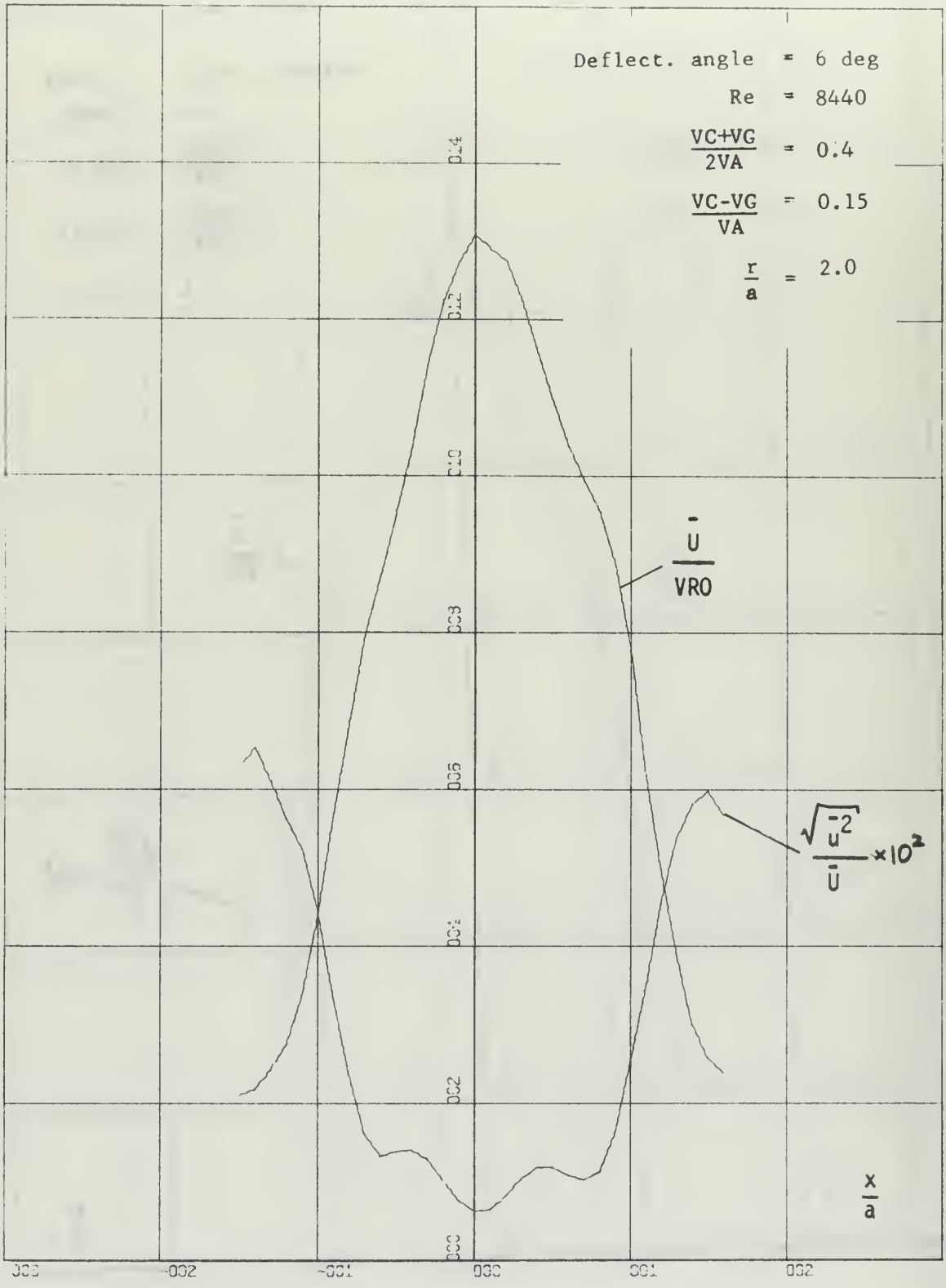

FIGURE 27 VELOCITY PROFILE AND TURBULENCE INTENSITY

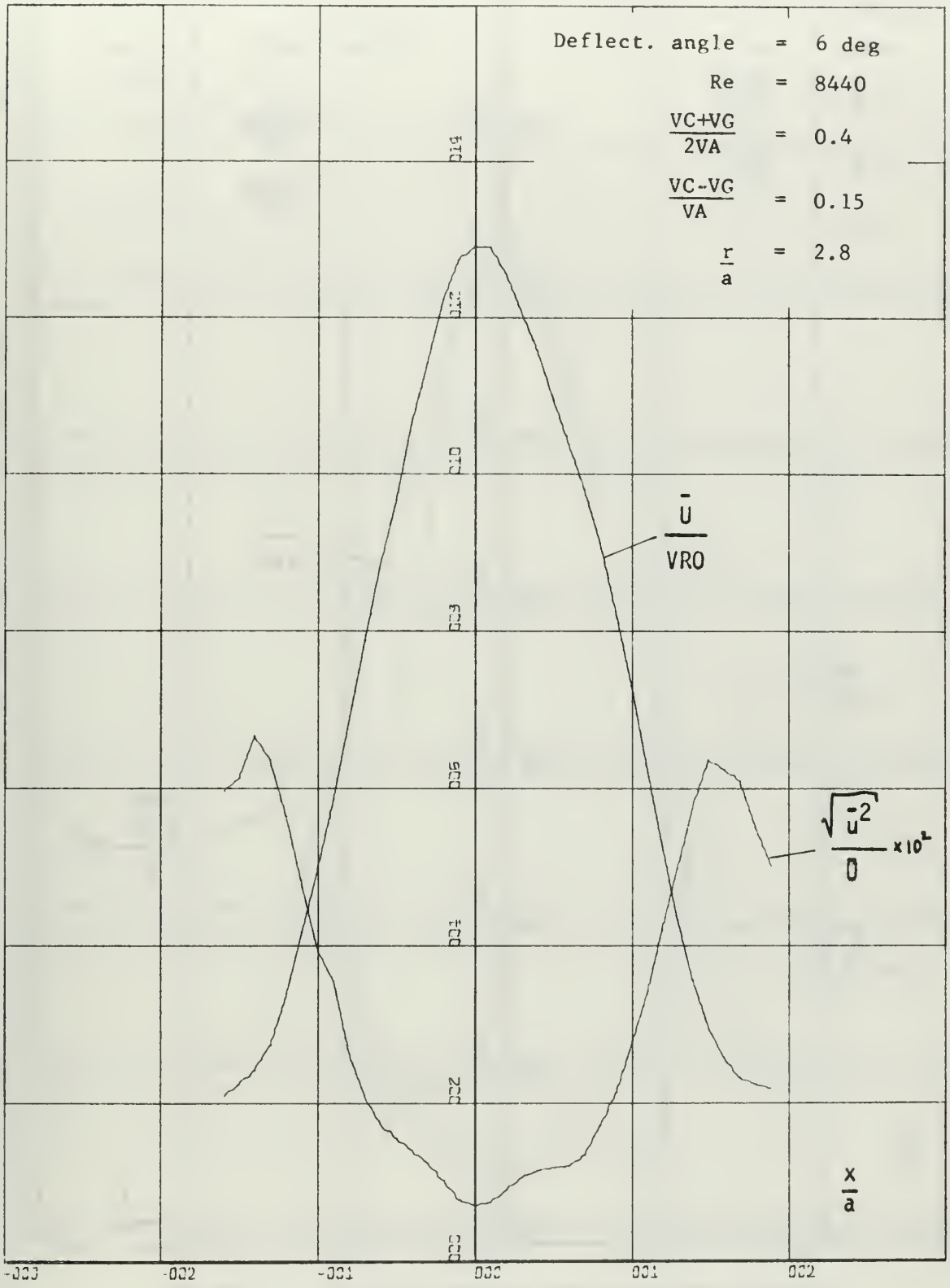

FIGURE 28 VELOCITY PROFILE AND TURBULENCE INTENSITY

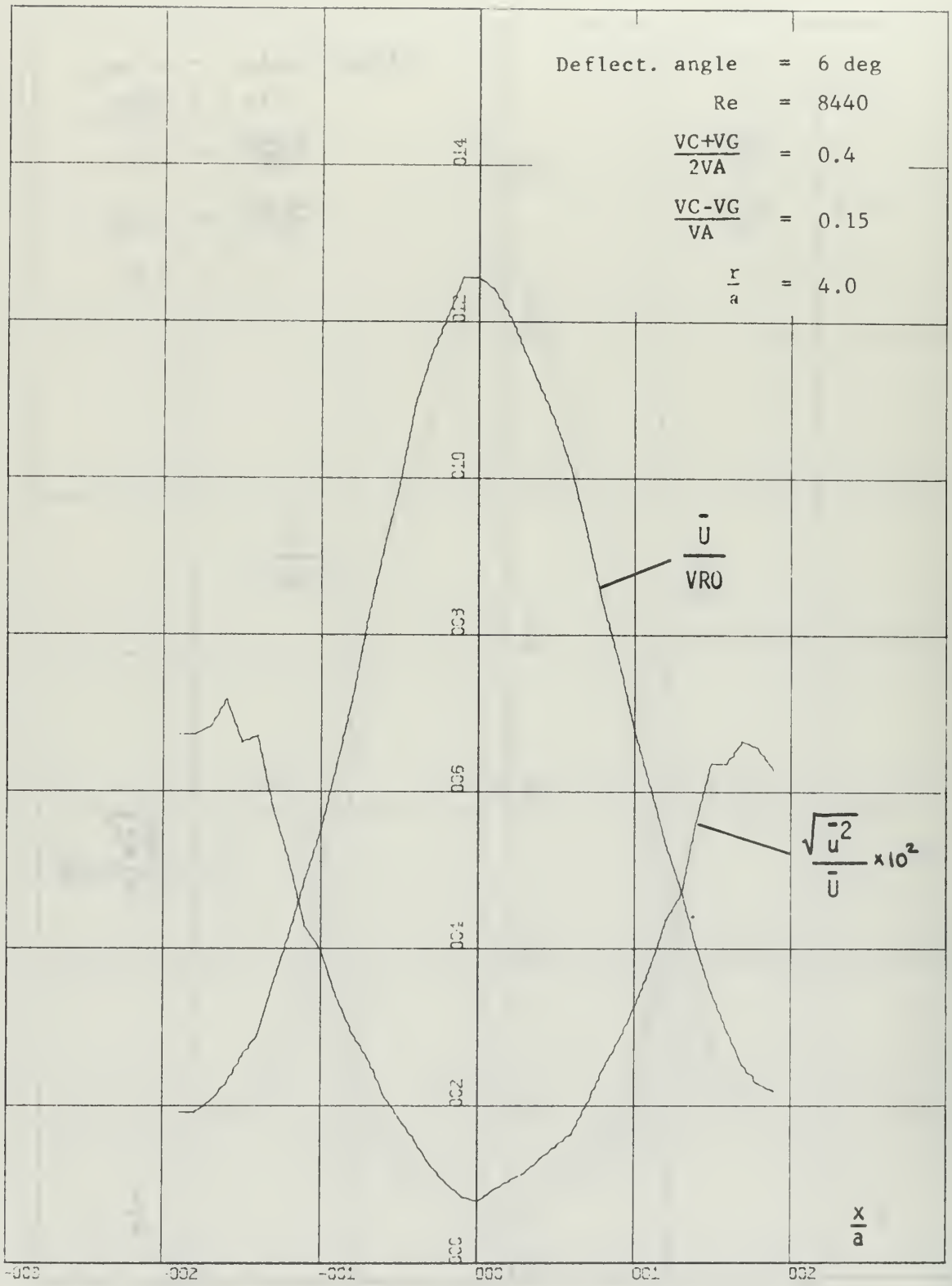

FIGURE 29 VELOCITY PROFILE AND TURBULENCE INTENSITY

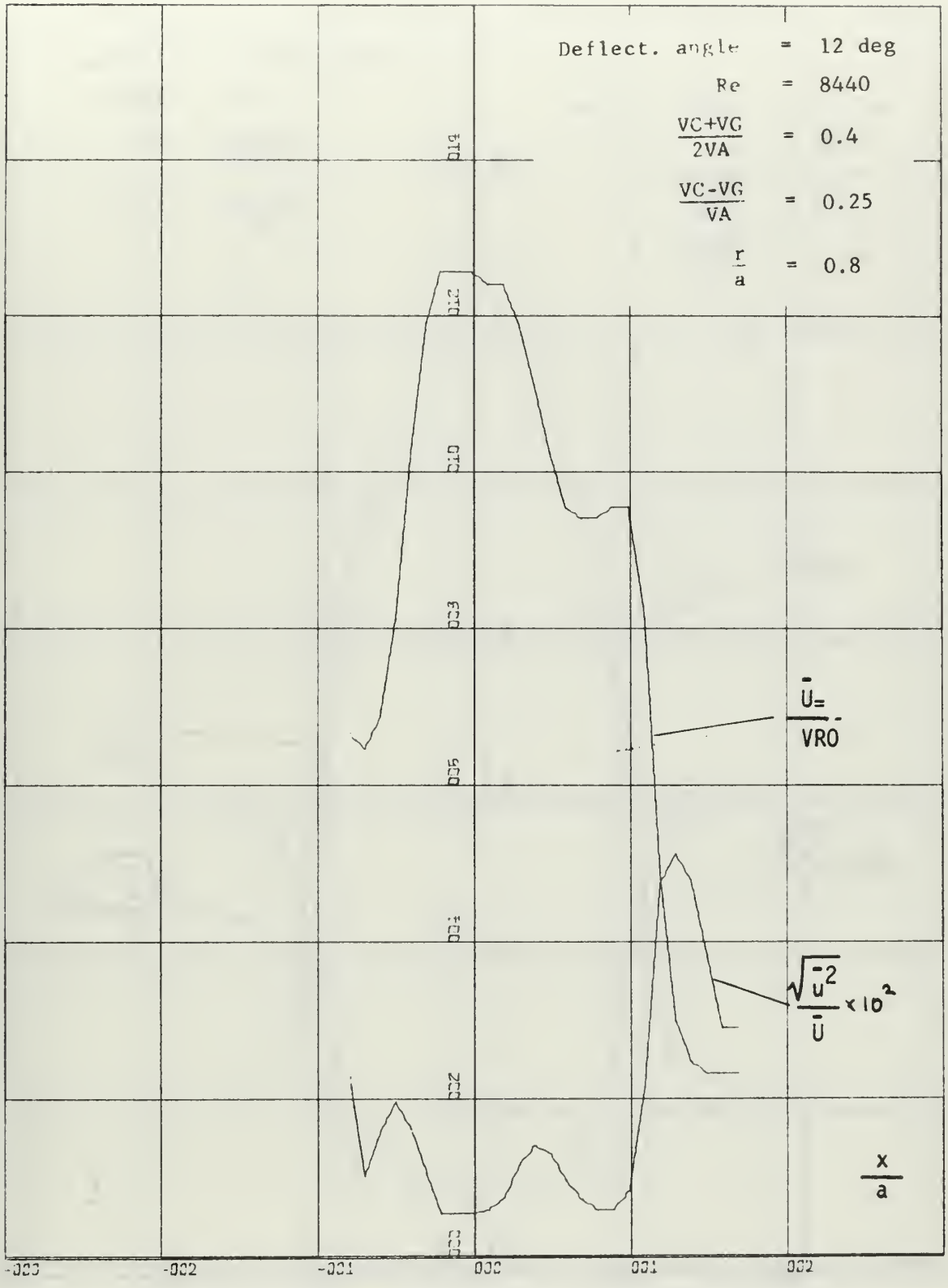

FIGURE 30 VELOCITY PROFILE AND TURBULENCE INTENSITY

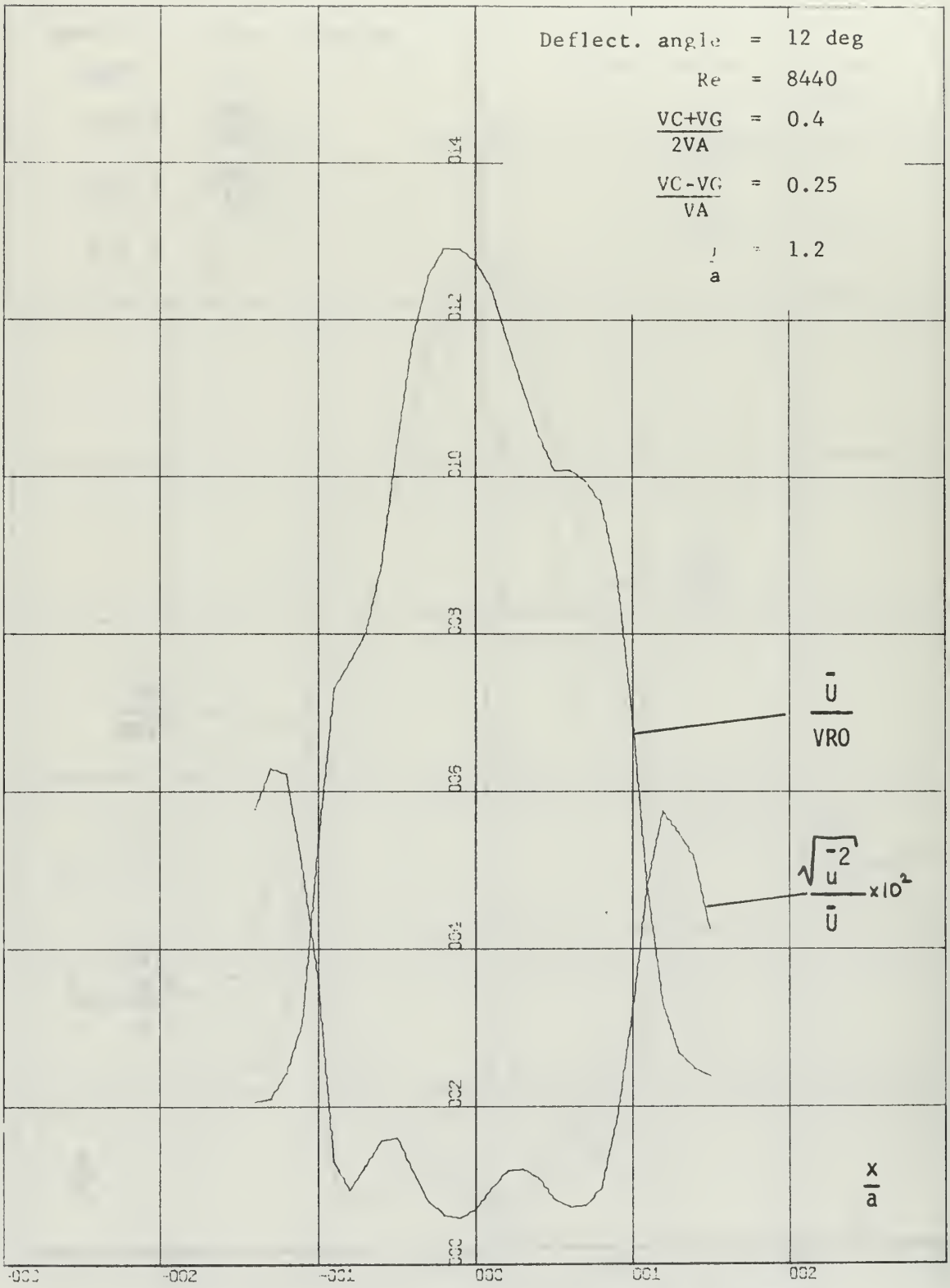

FIGURE 31 VELOCITY PROFILE AND TURBULENCE INTENSITY

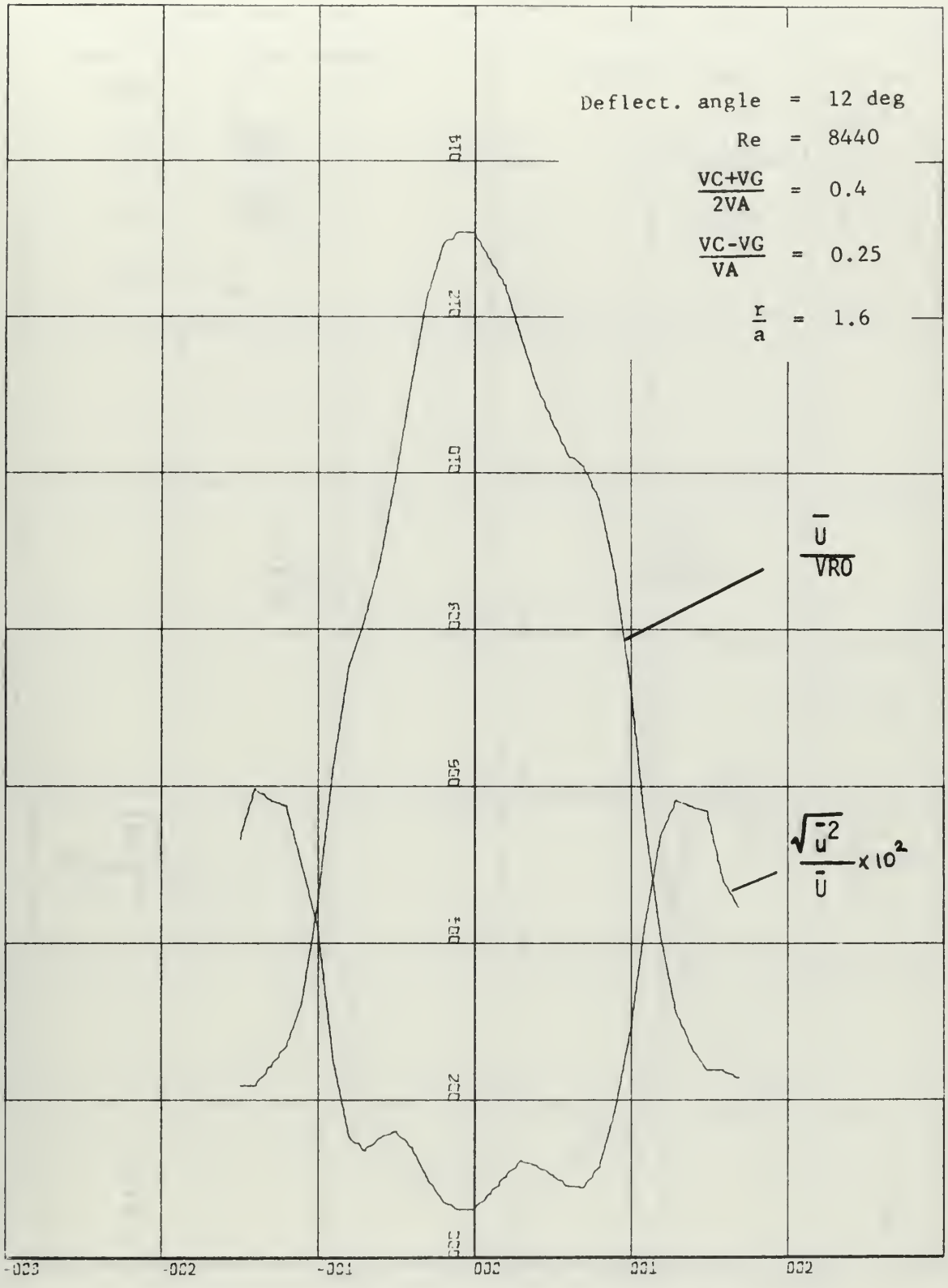

FIGURE 32 VELOCITY PROFILE AND TURBULENCE INTENSITY

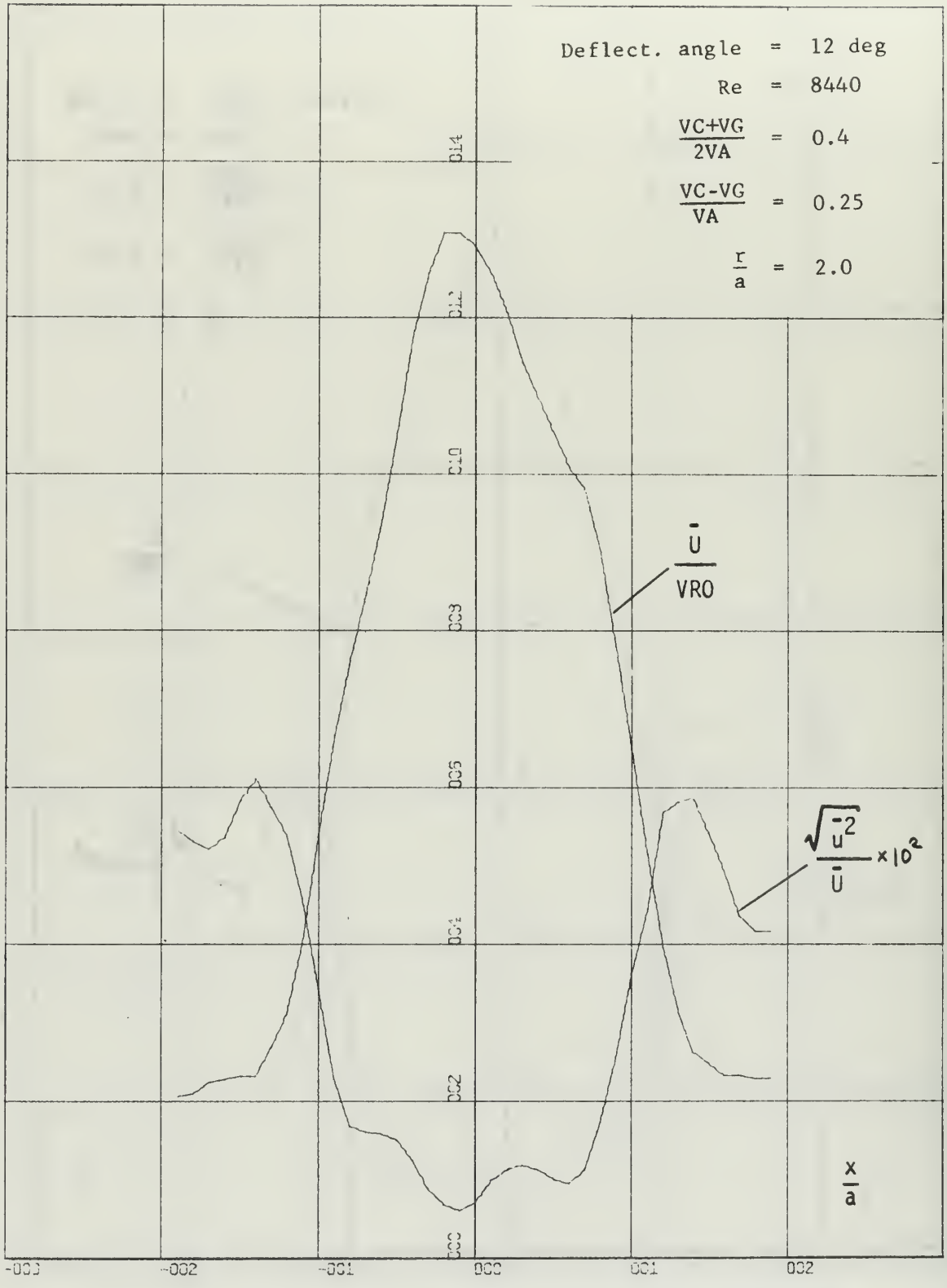

FIGURE 33 VELOCITY PROFILE AND TURBULENCE INTENSITY

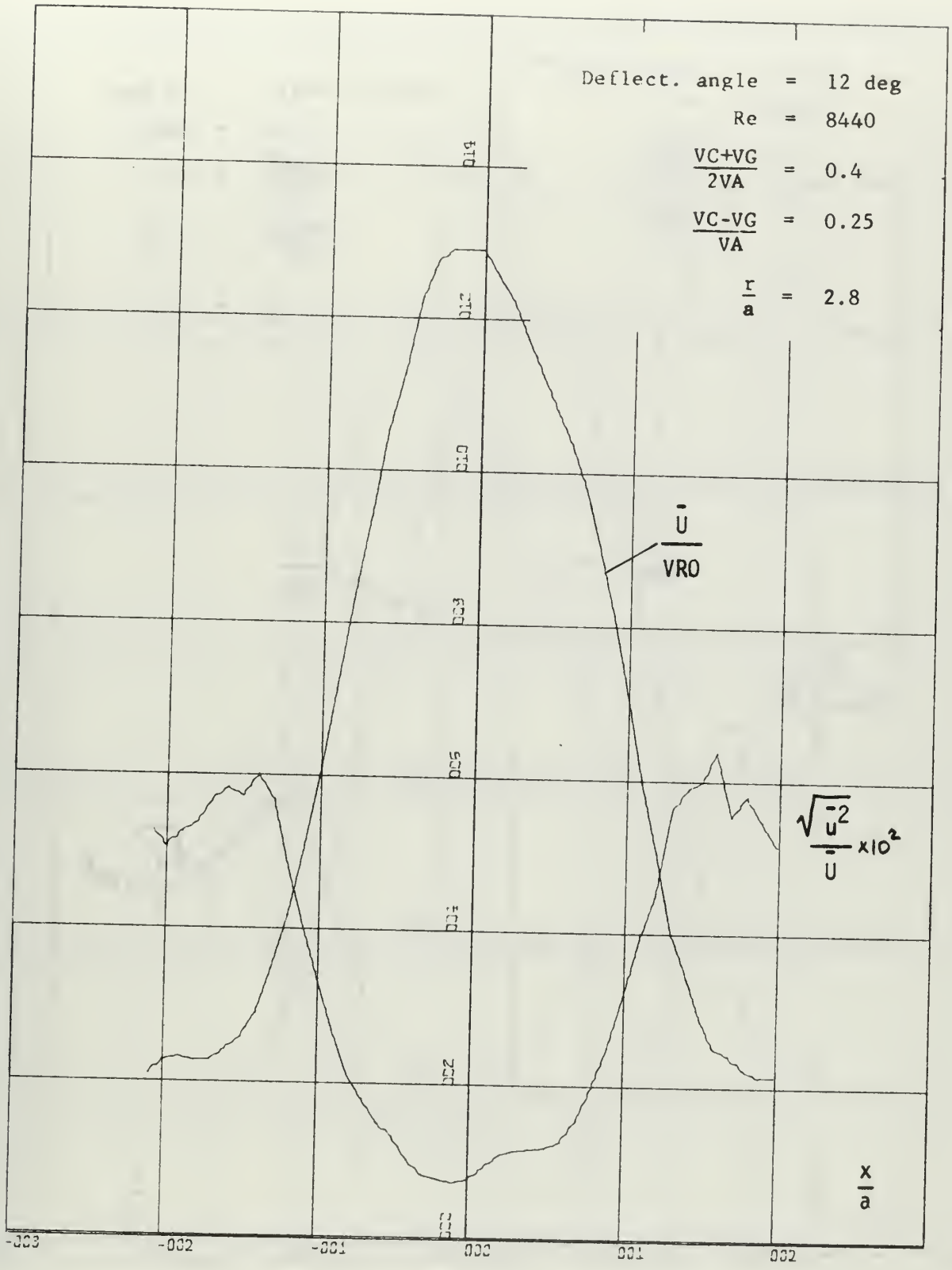

FIGURE 34 VELOCITY PROFILE AND TURBULENCE INTENSITY

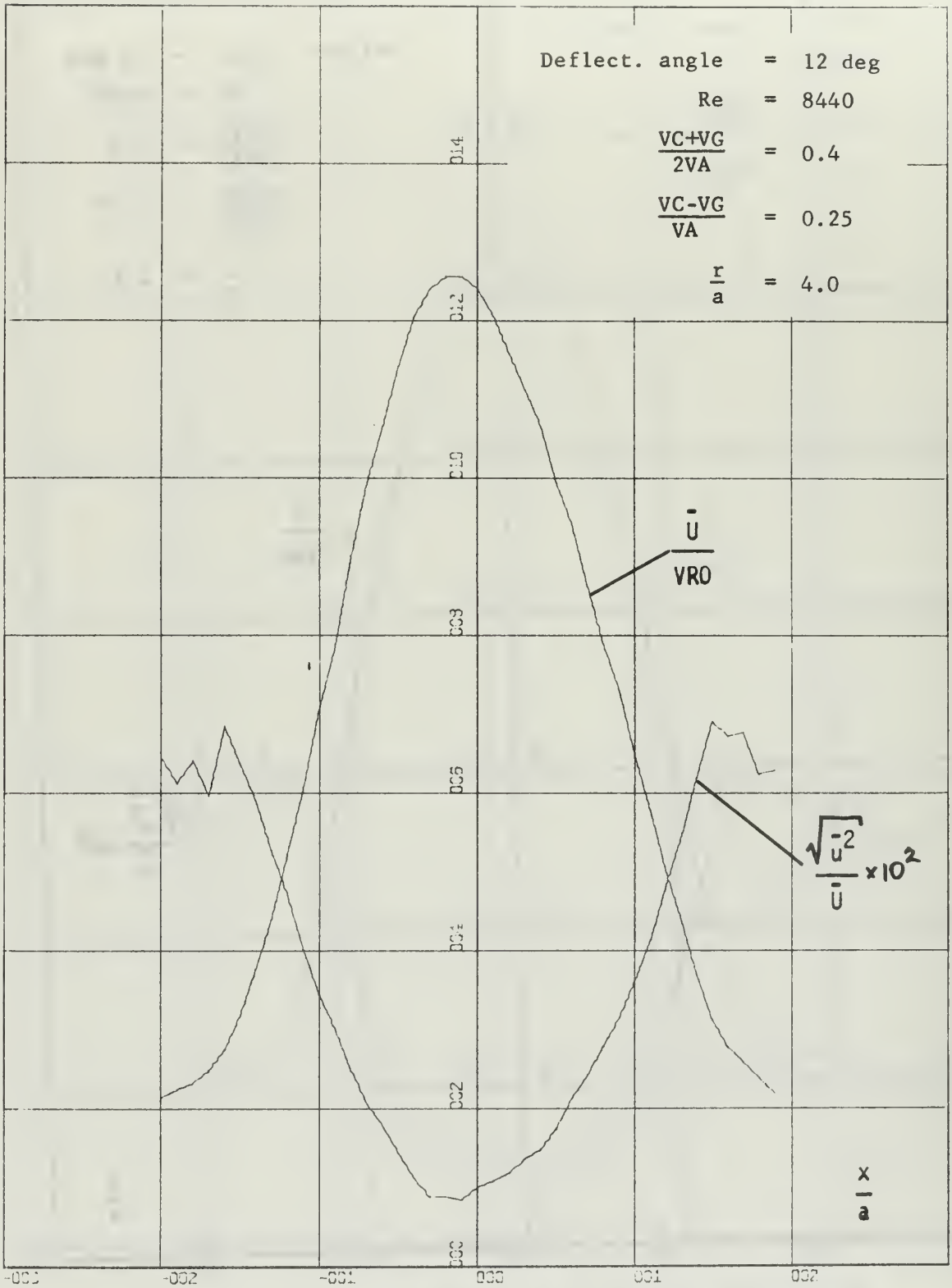

FIGURE 35 VELOCITY PROFILE AND TURBULENCE INTENSITY

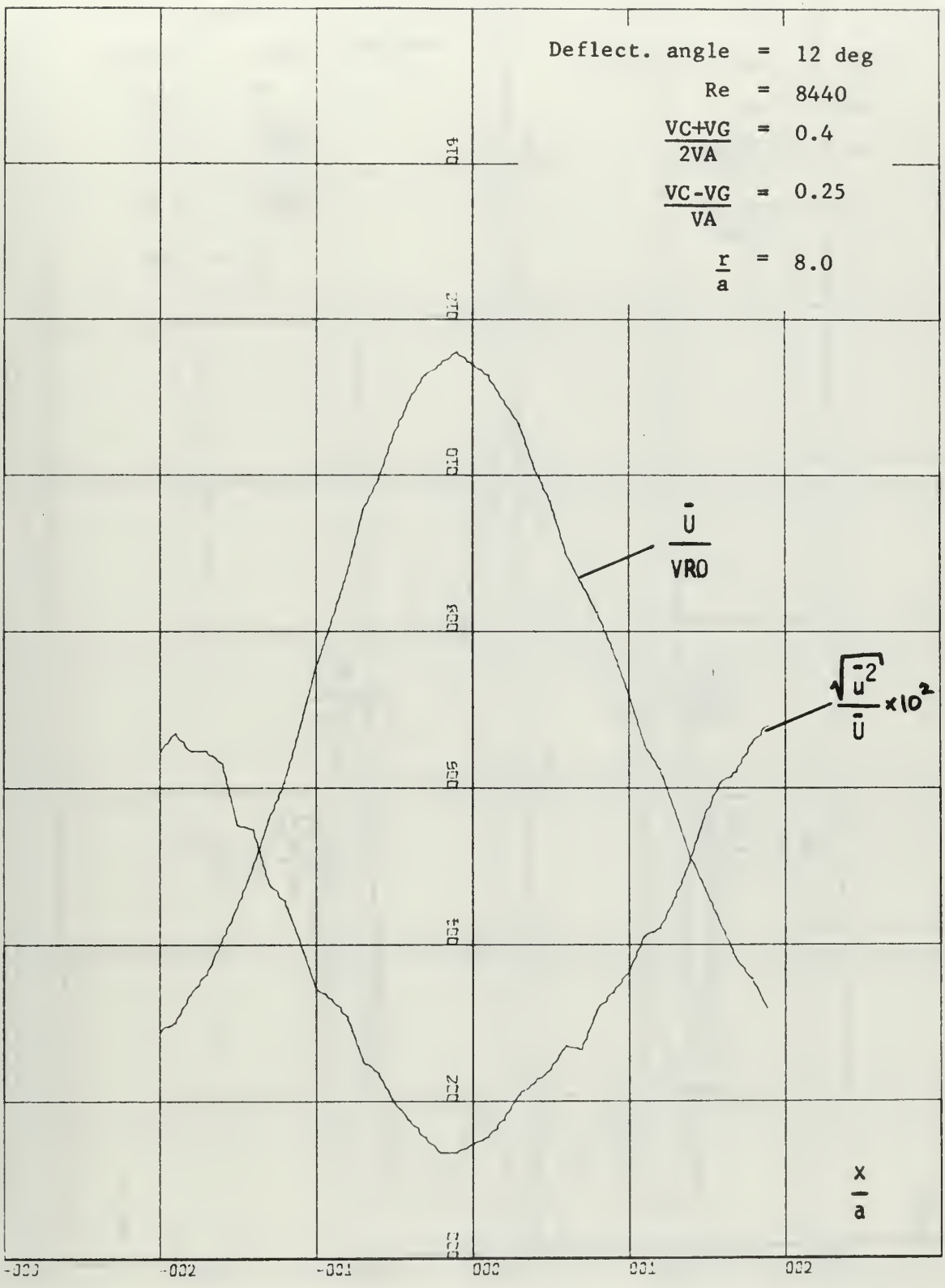

FIGURE 36 VELOCITY PROFILE AND TURBULENCE INTENSITY

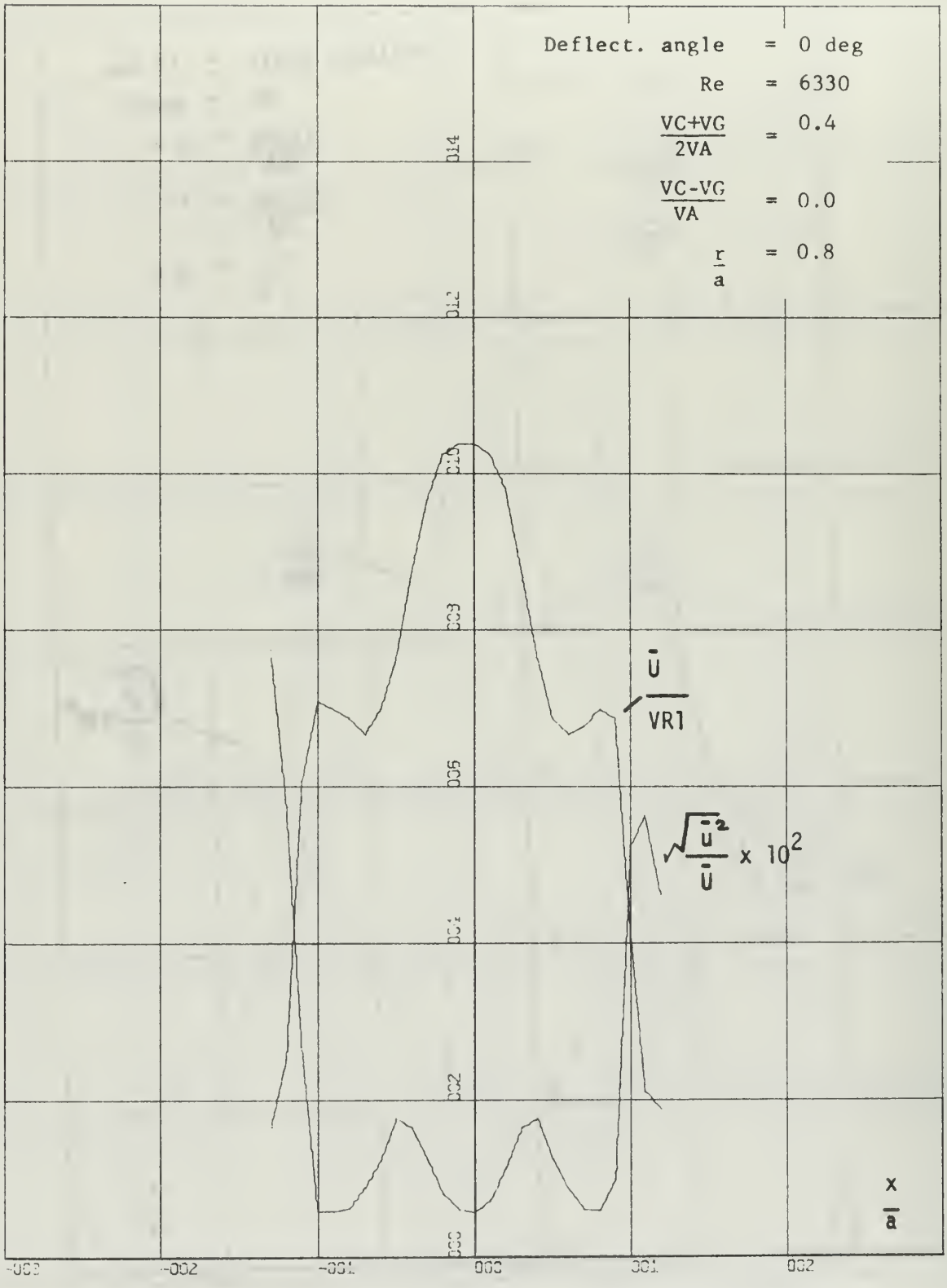

FIGURE 37 VELOCITY PROFILE AND TURBULENCE INTENSITY

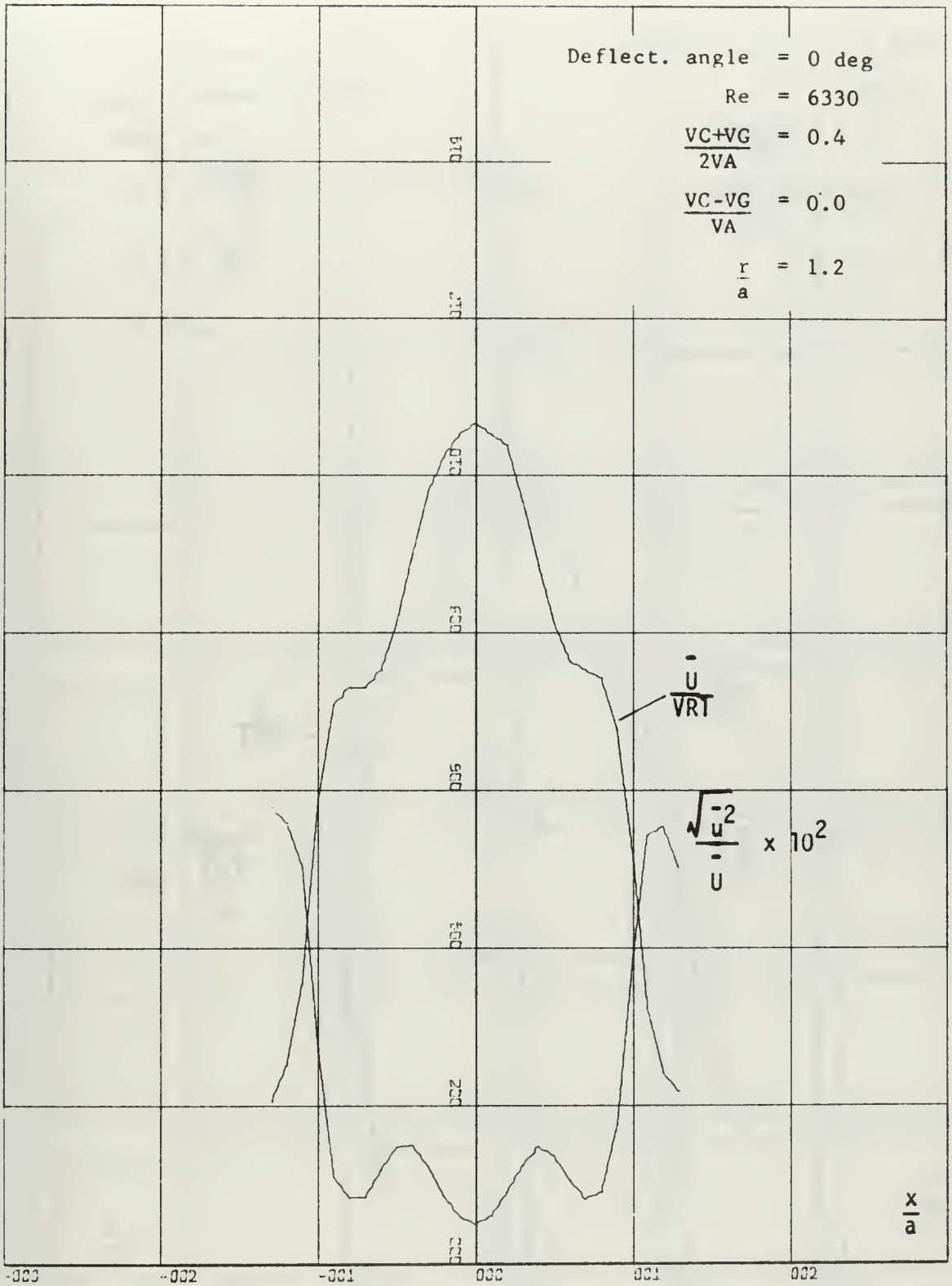

FIGURE 38 VELOCITY PROFILE AND TURBULENCE INTENSITY

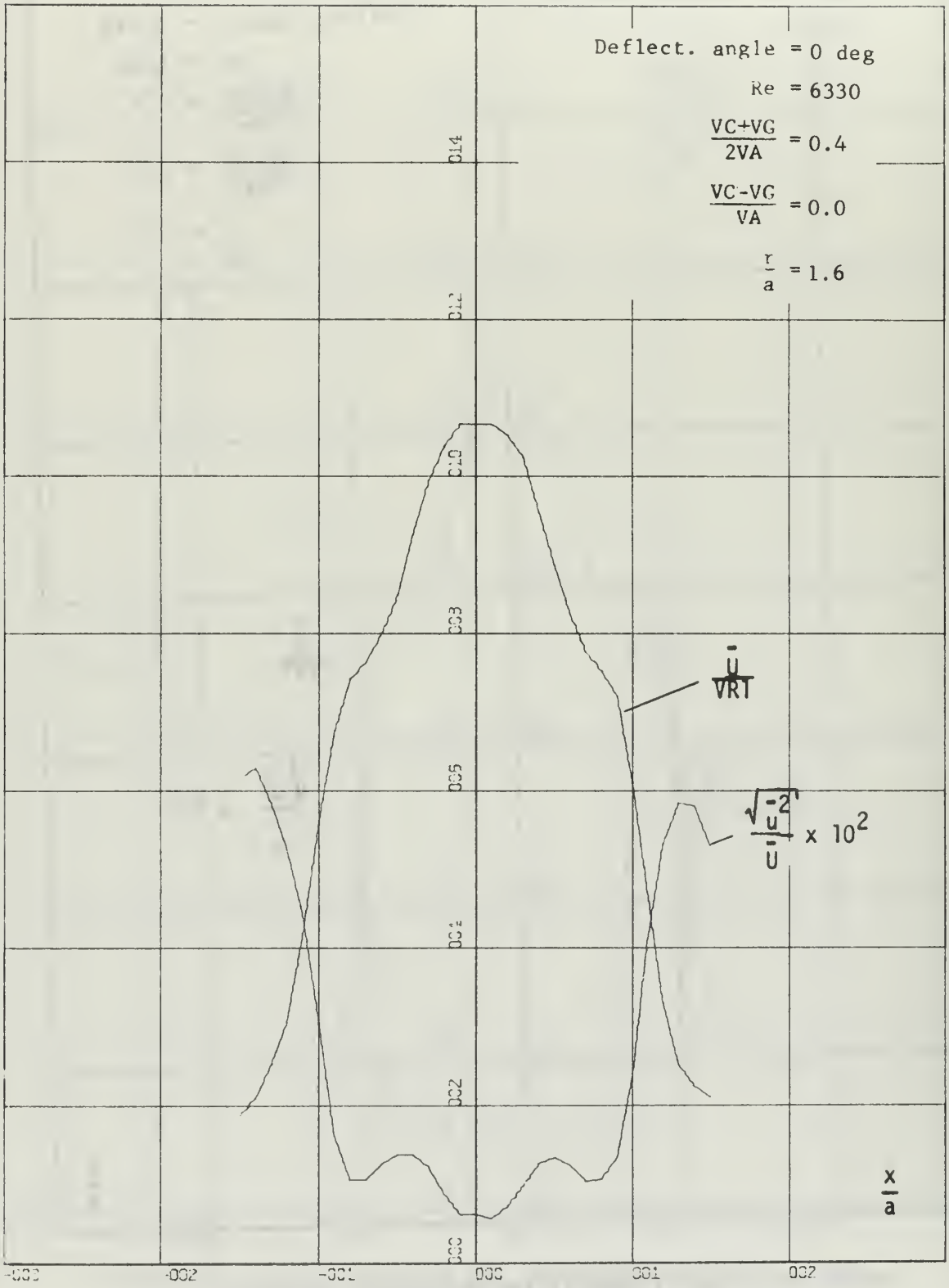

FIGURE 39 VELOCITY PROFILE AND TURBULENCE INTENSITY

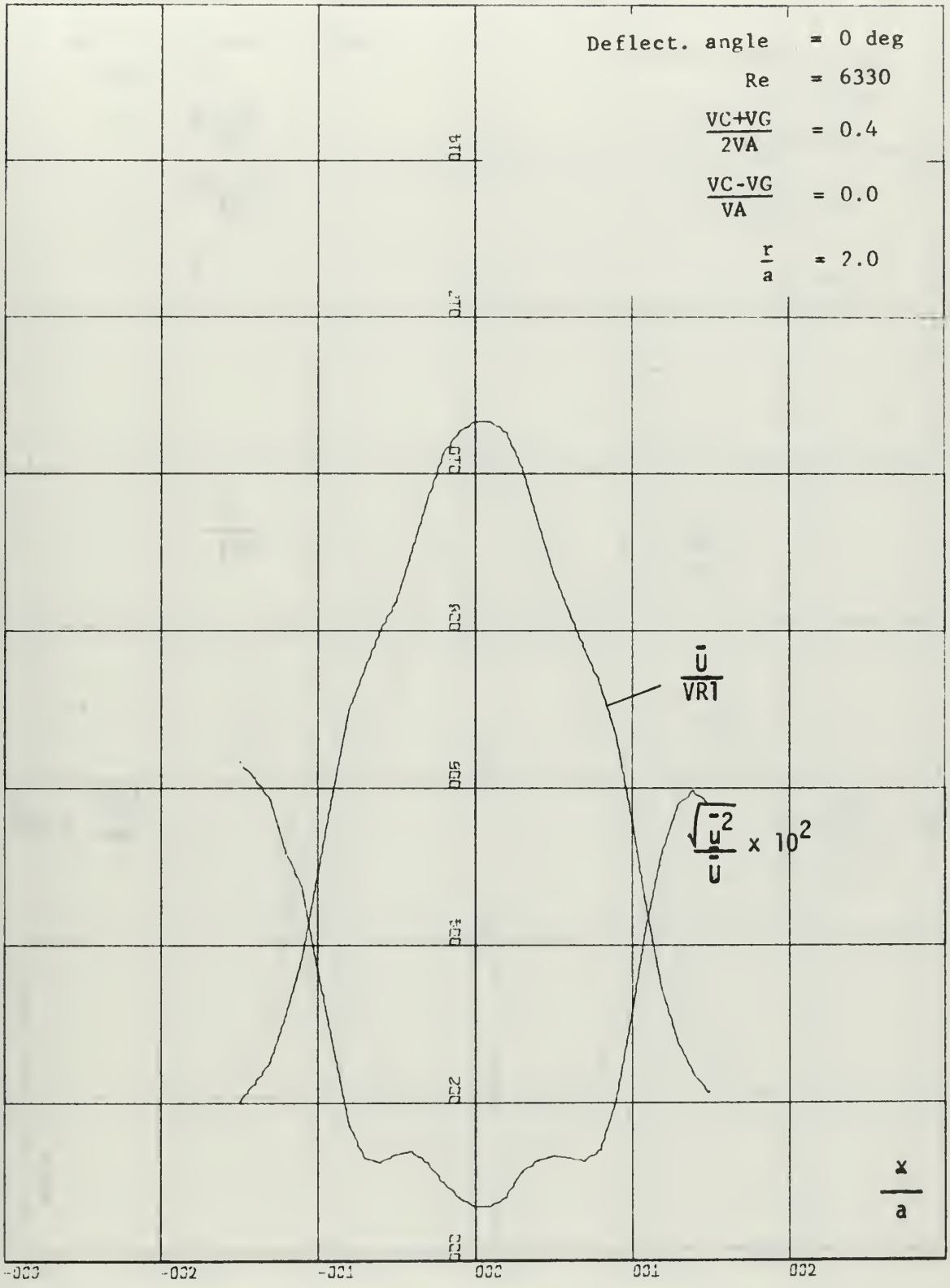

FIGURE 40 VELOCITY PROFILE AND TURBULENCE INTENSITY

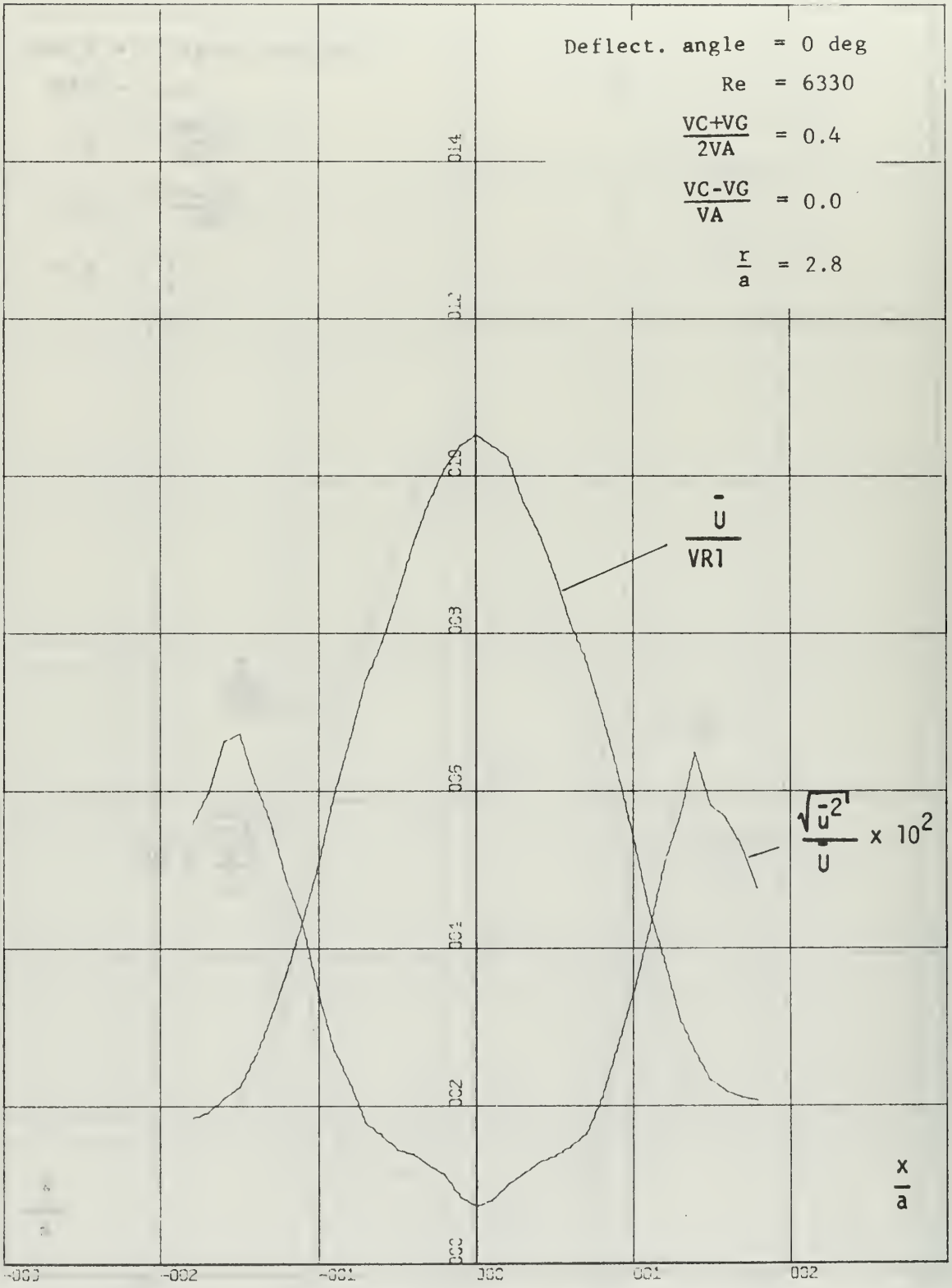

FIGURE 41 VELOCITY PROFILE AND TURBULENCE INTENSITY

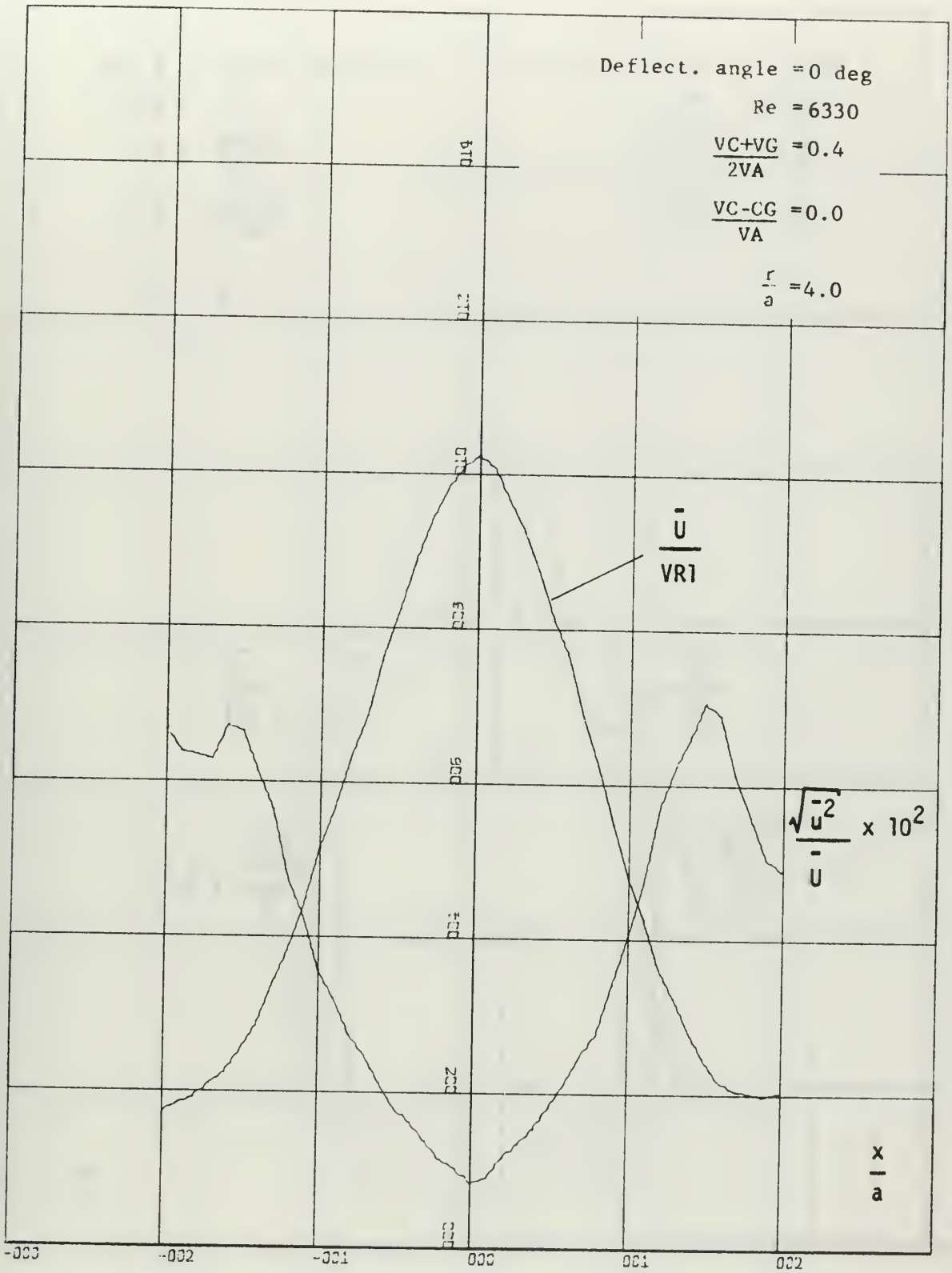

FIGURE 42 VELOCITY PROFILE AND TURBULENCE INTENSITY

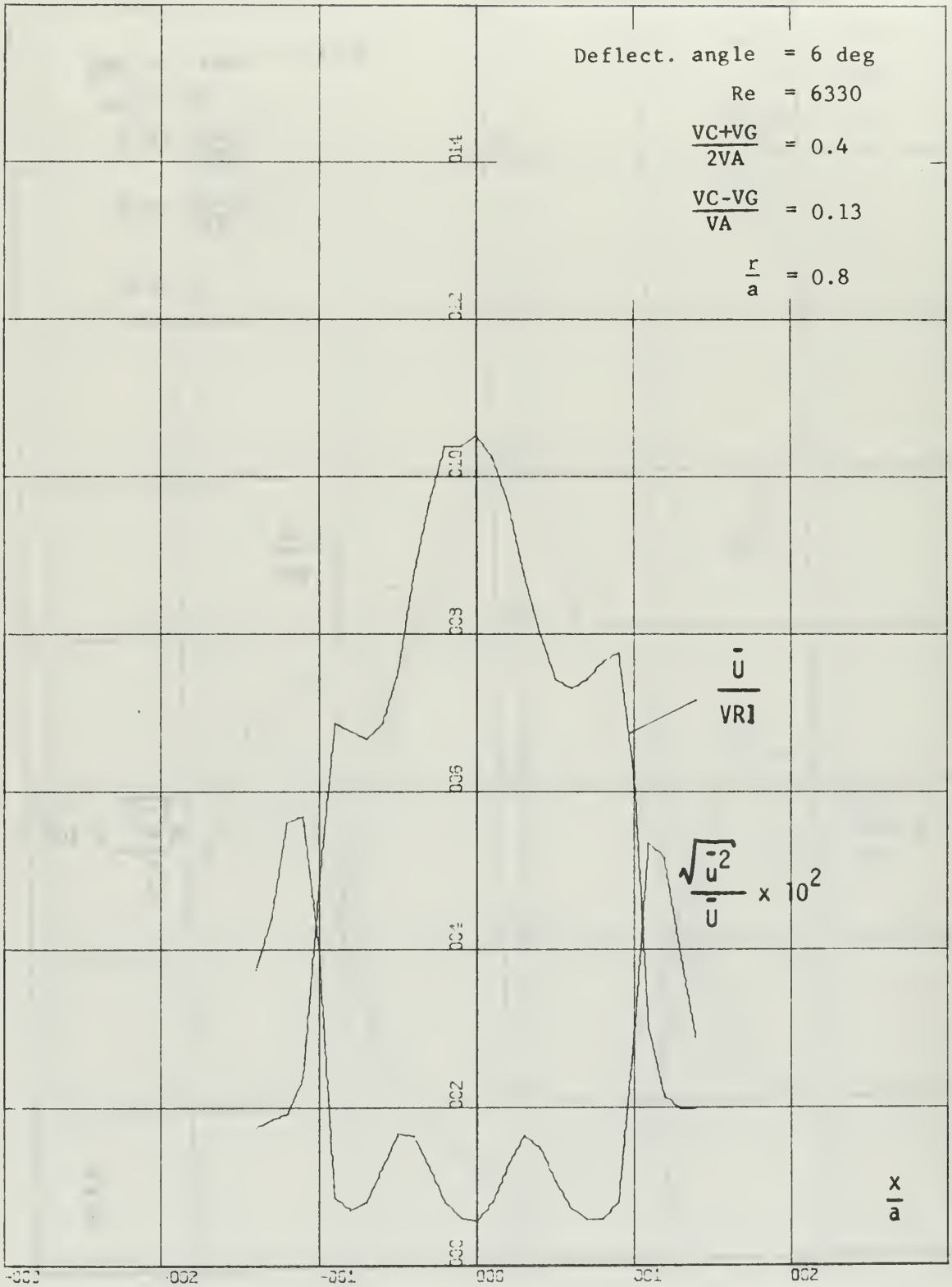

FIGURE 43 VELOCITY PROFILE AND TURBULENCE INTENSITY

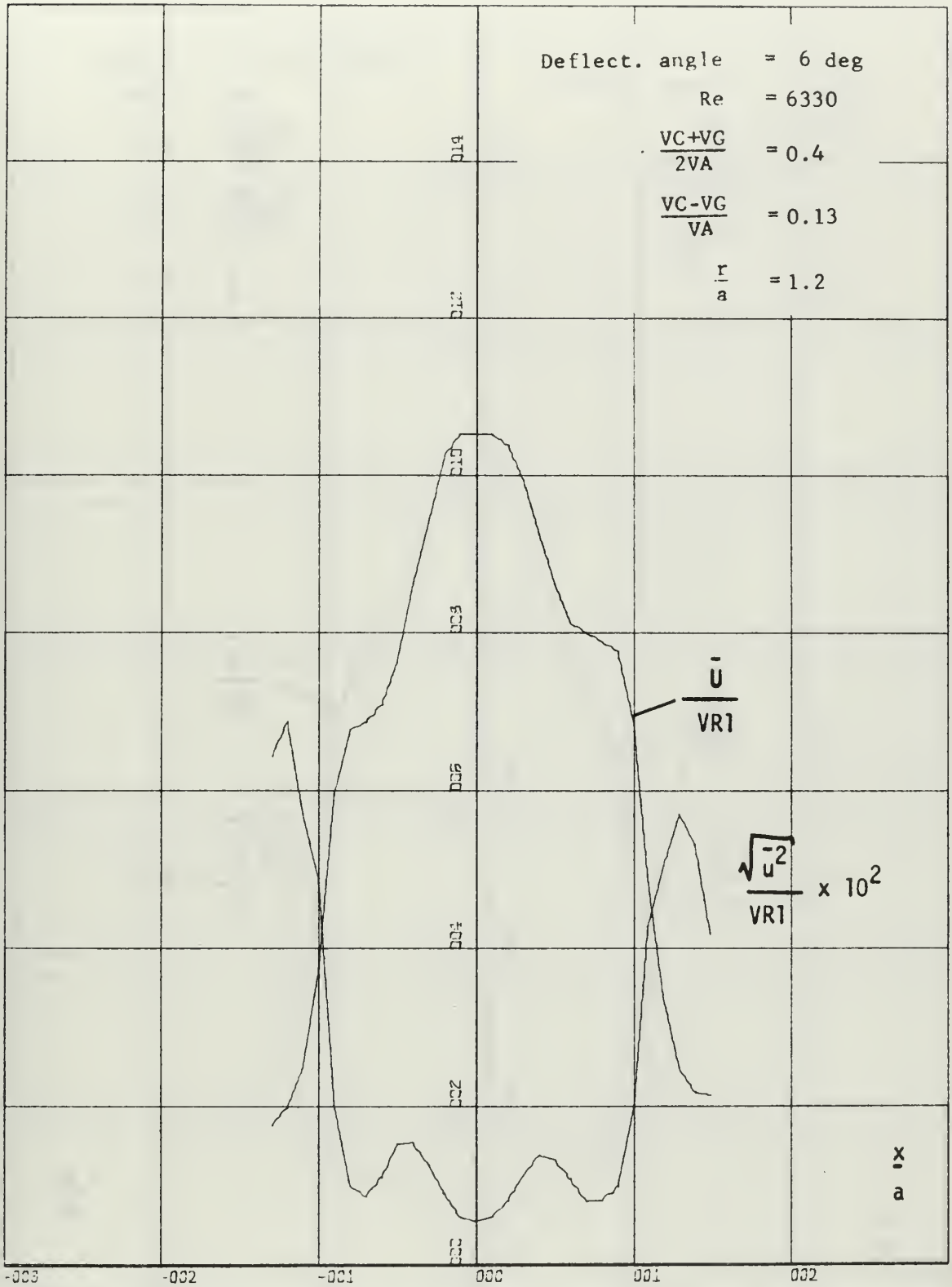

FIGURE 44 VELOCITY PROFILE AND TURBULENCE INTENSITY

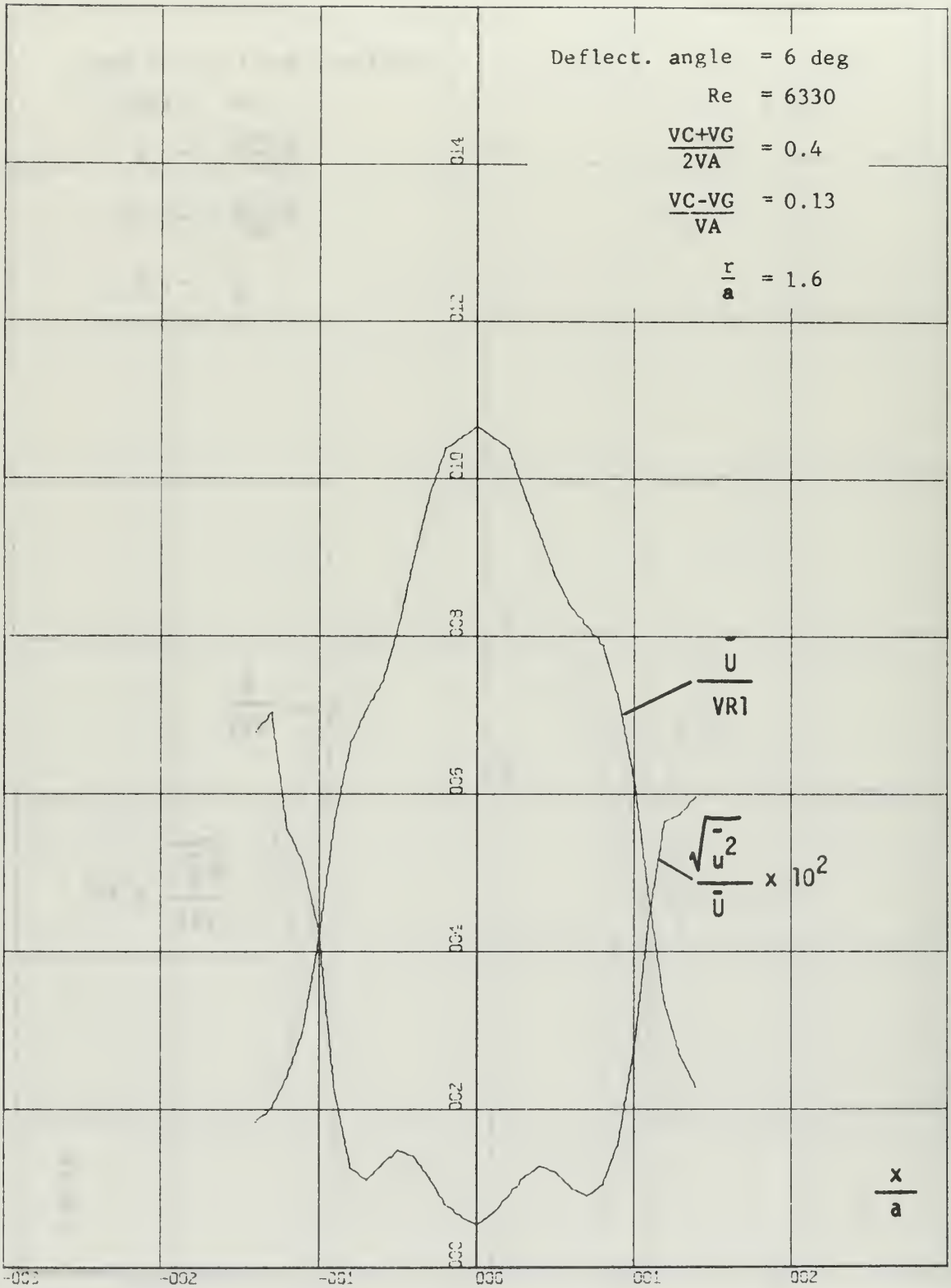

FIGURE 45 VELOCITY PROFILE AND TURBULENCE INTENSITY

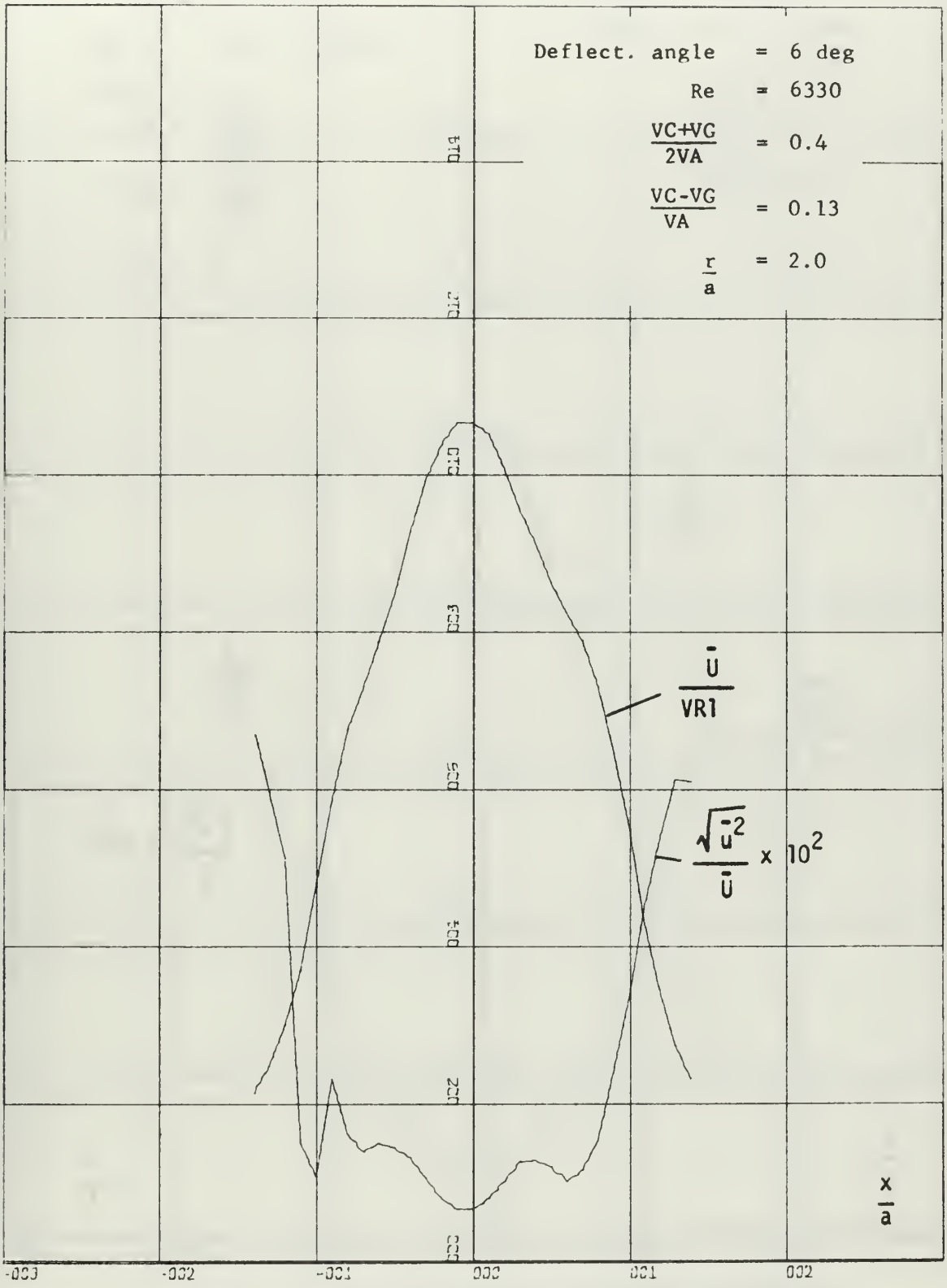

FIGURE 46 VELOCITY PROFILE AND TURBULENCE INTENSITY

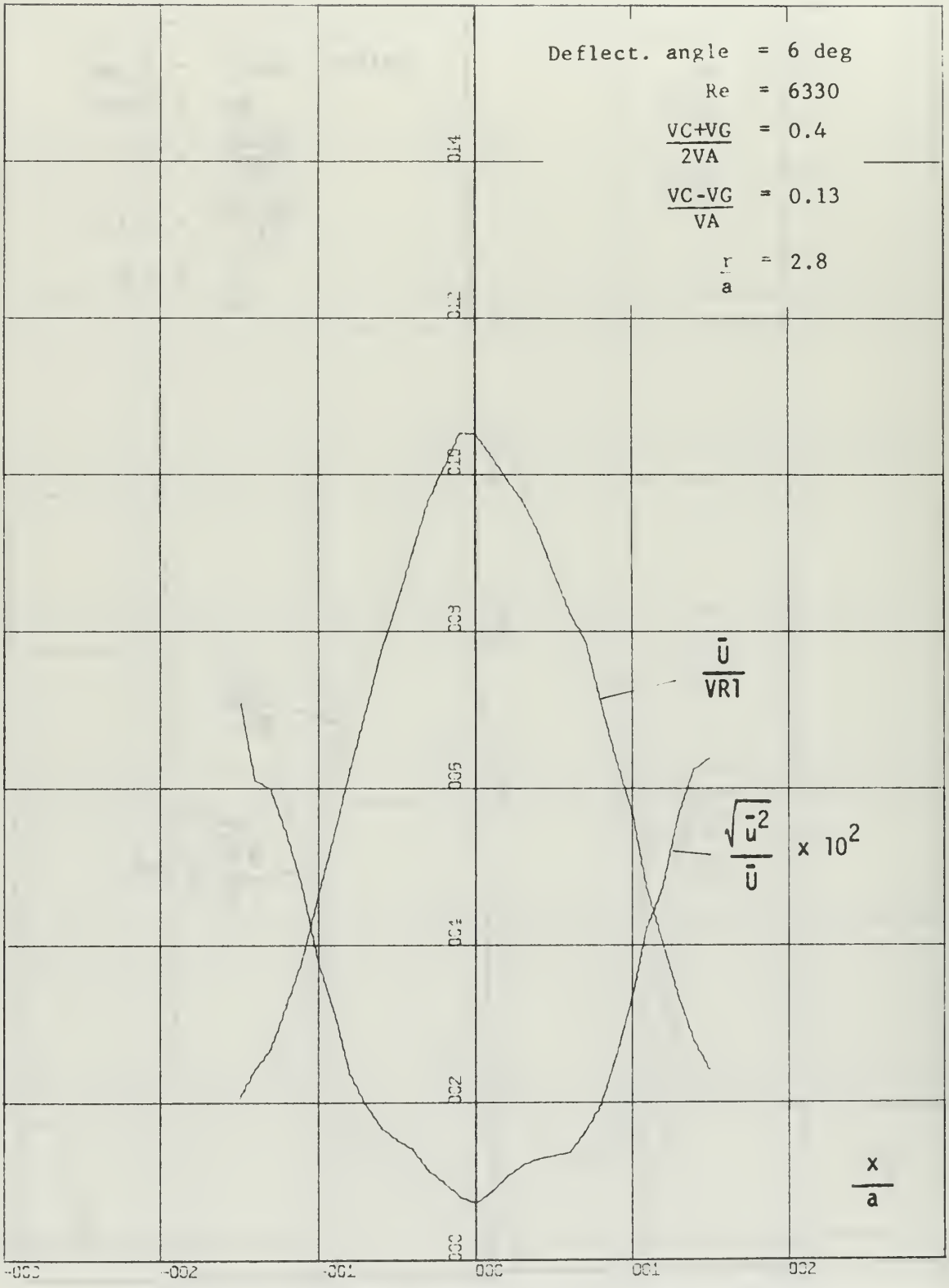

FIGURE 47 VELOCITY PROFILE AND TURBULENCE INTENSITY

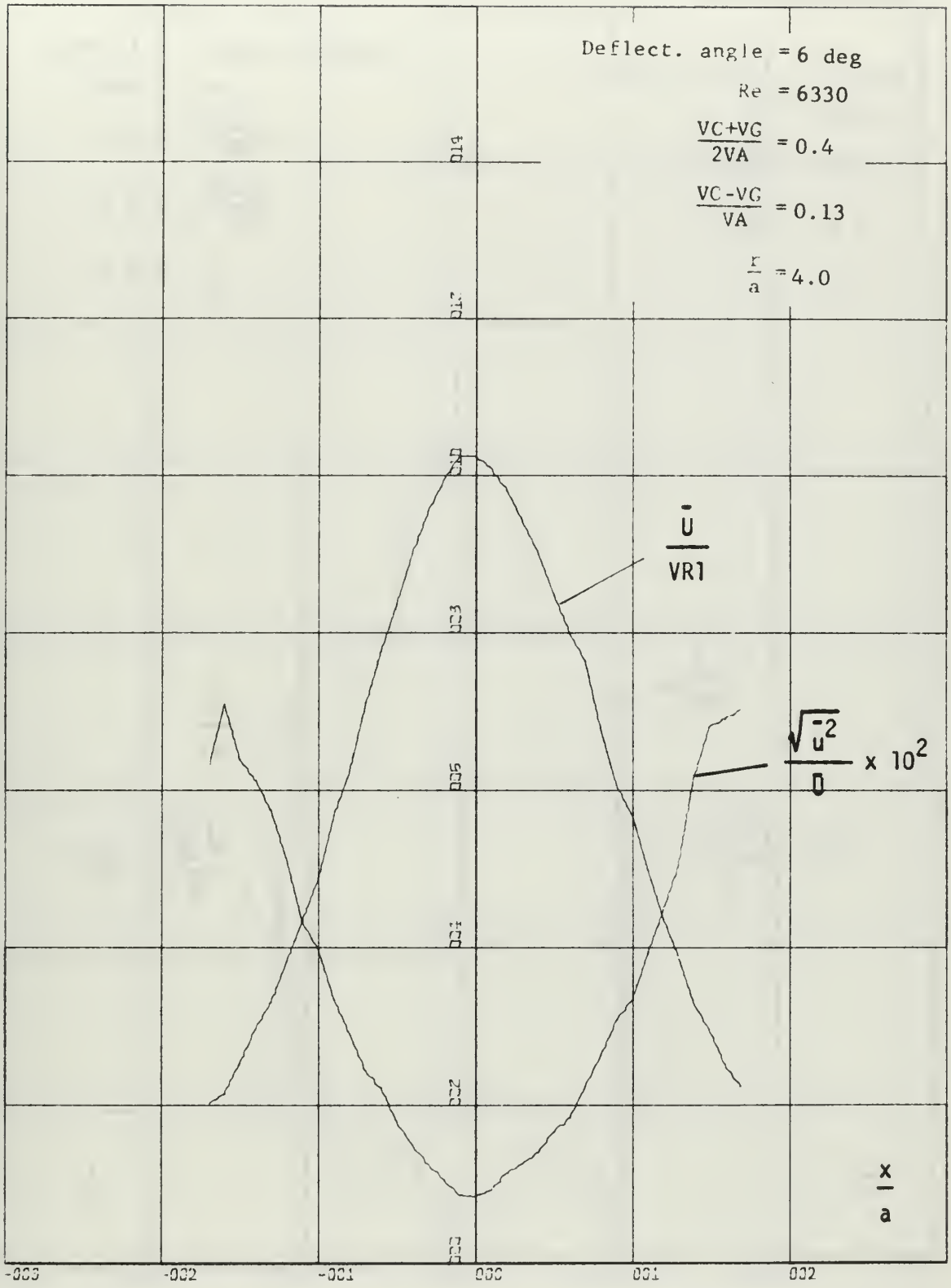

FIGURE 48 VELOCITY PROFILE AND TURBULENCE INTENSITY

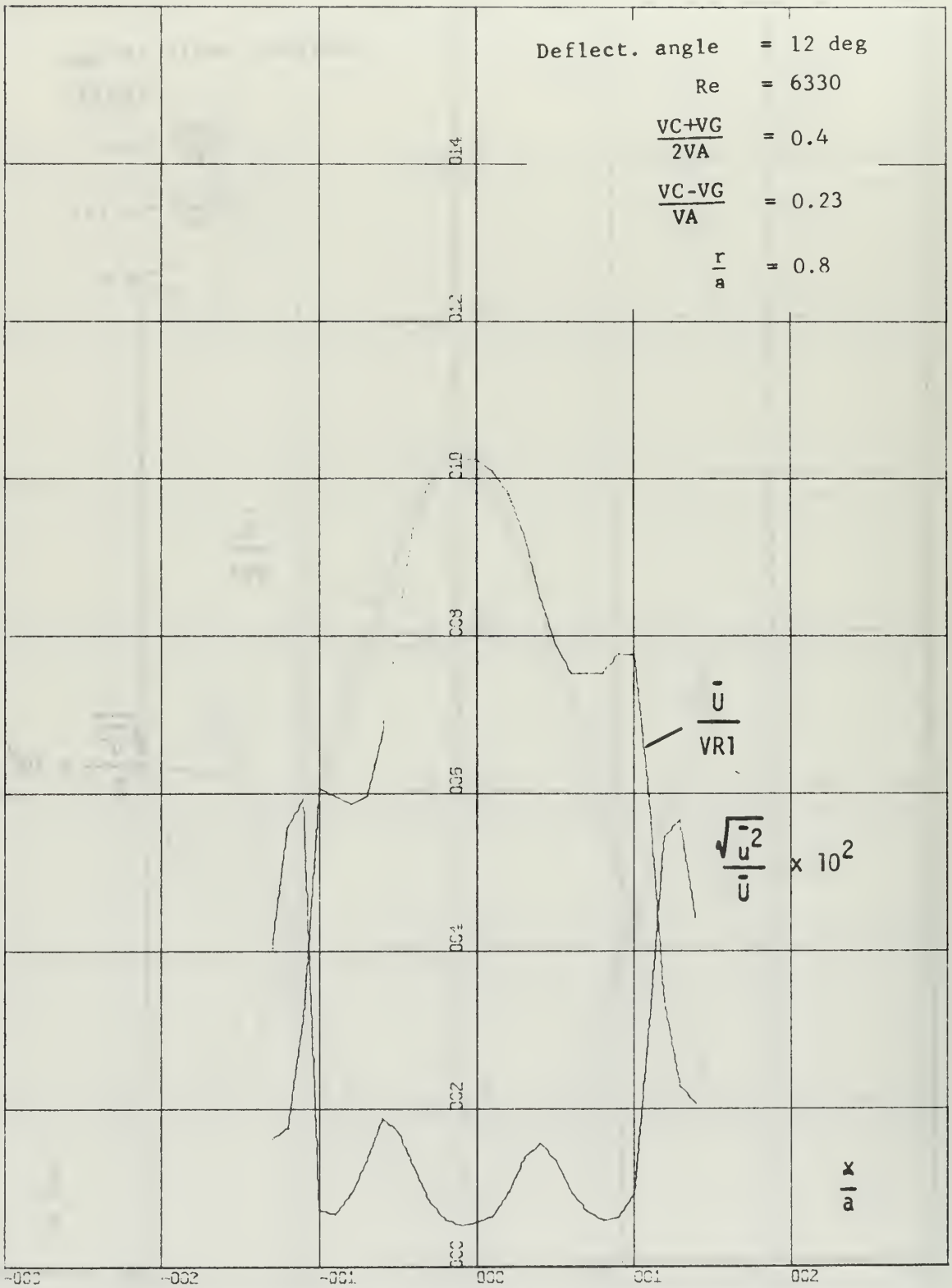

FIGURE 49 VELOCITY PROFILE AND TURBULENCE INTENSITY

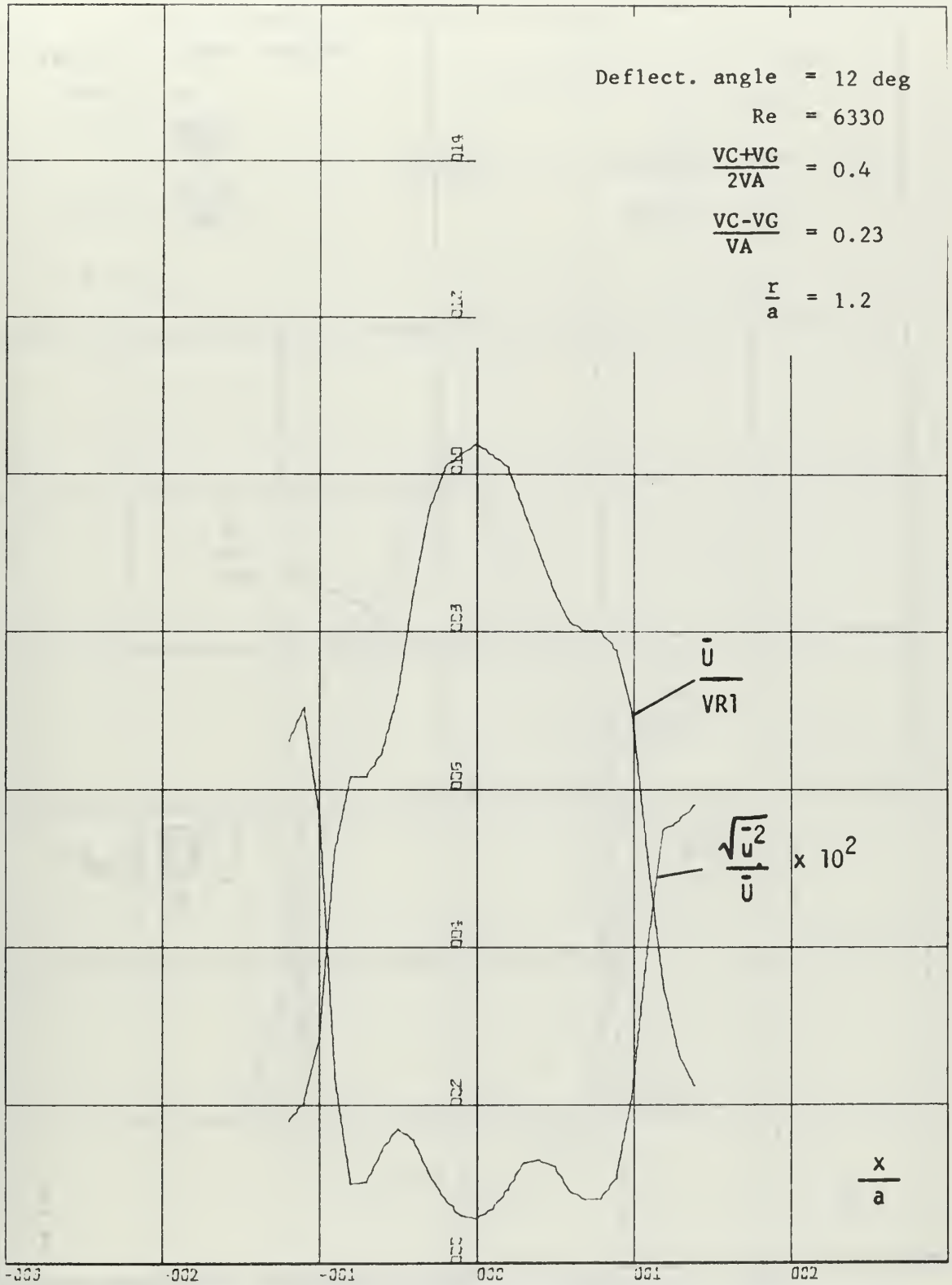

FIGURE 50 VELOCITY PROFILE AND TURBULENCE INTENSITY

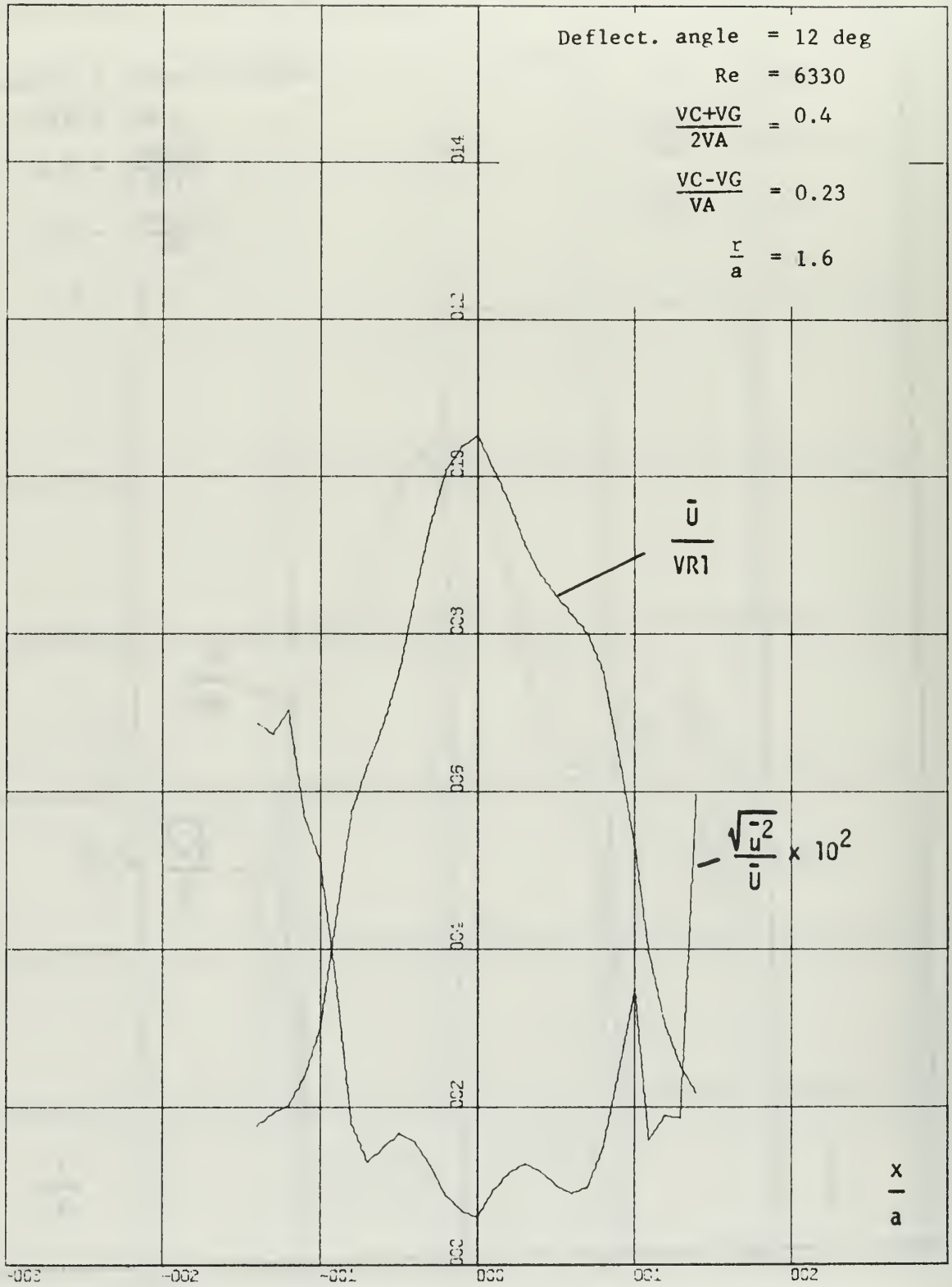

FIGURE 51 VELOCITY PROFILE AND TURBULENCE INTENSITY

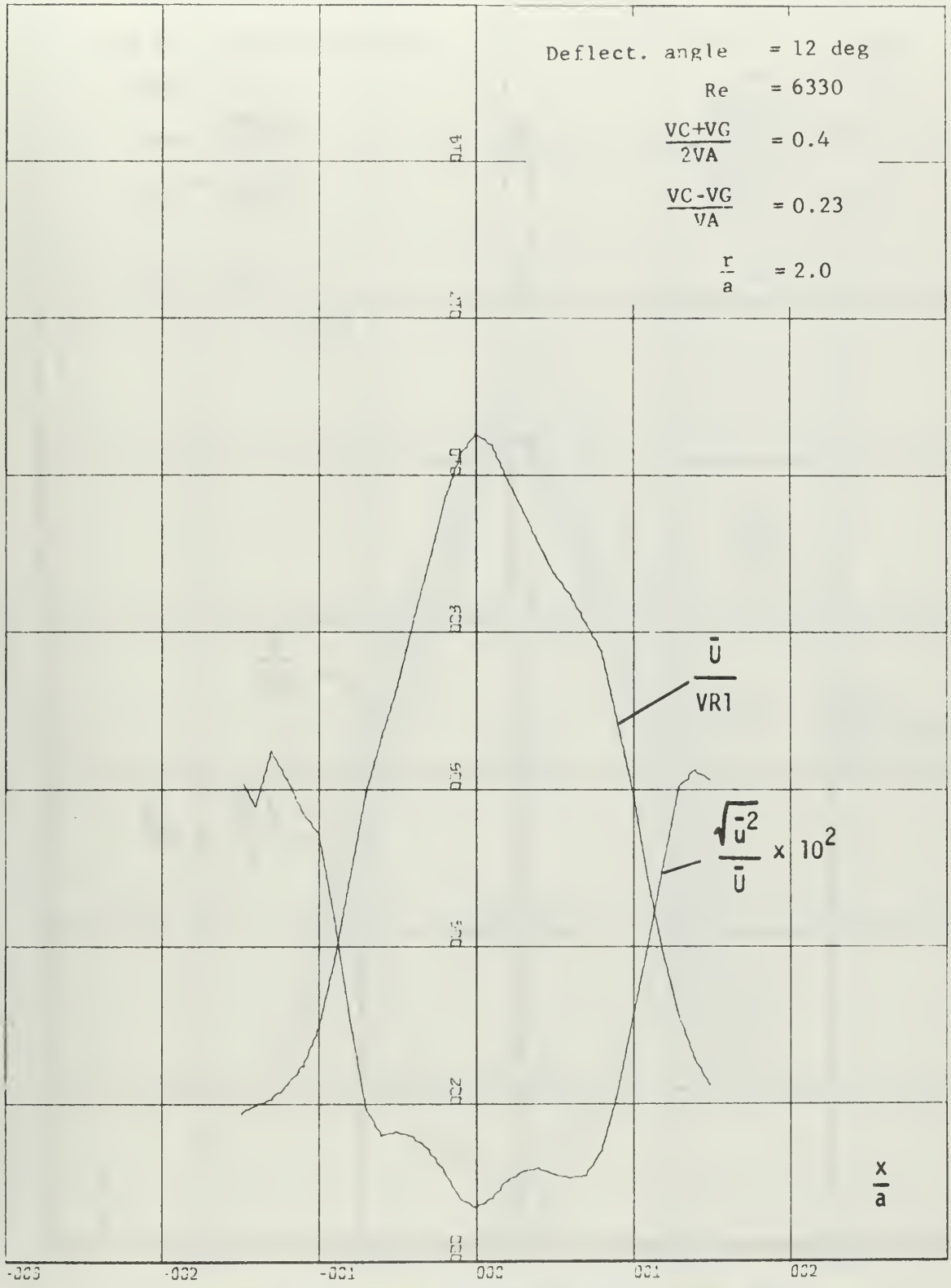

FIGURE 52 VELOCITY PROFILE AND TURBULENCE INTENSITY

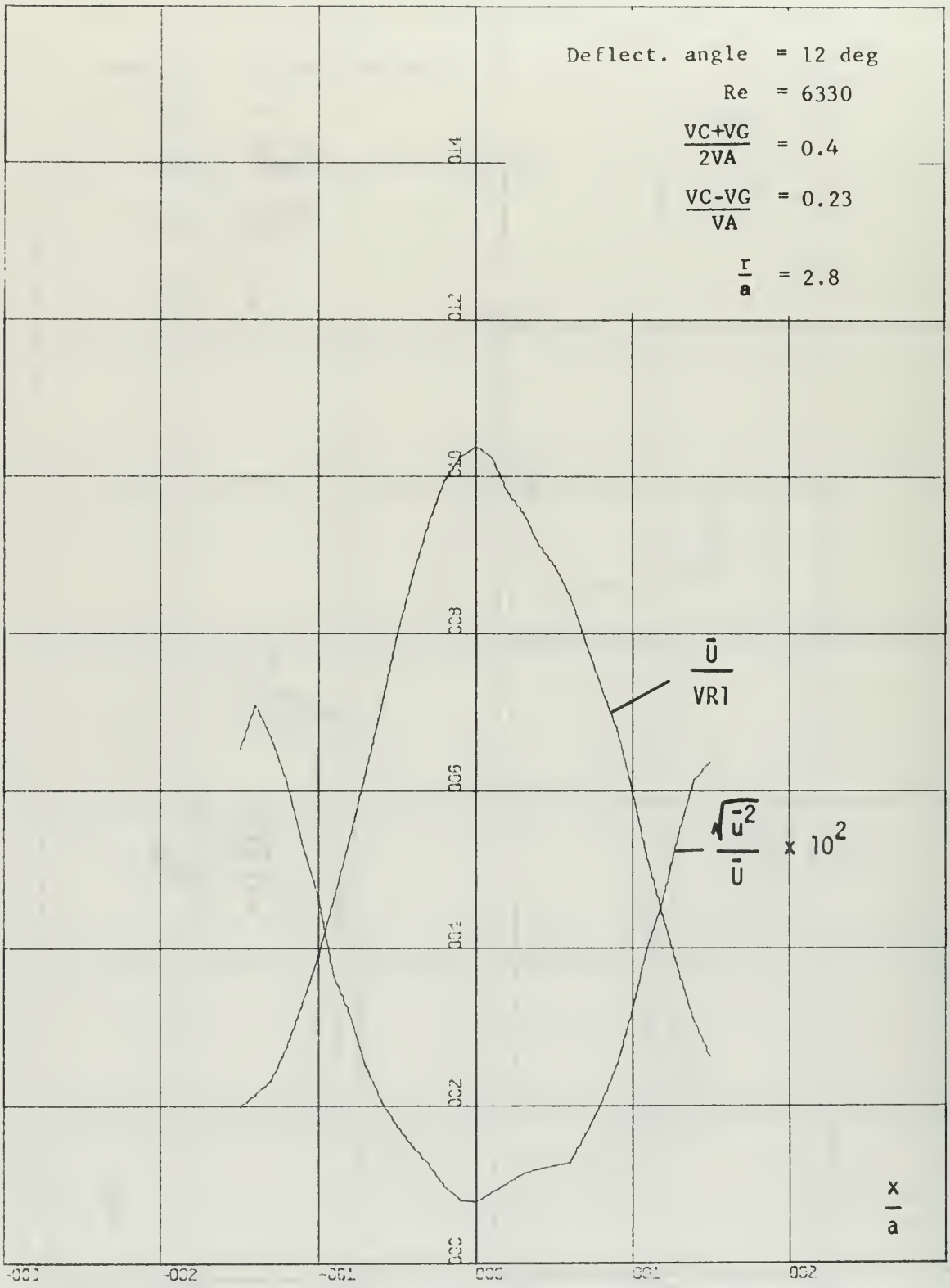

FIGURE 53 VELOCITY PROFILE AND TURBULENCE INTENSITY

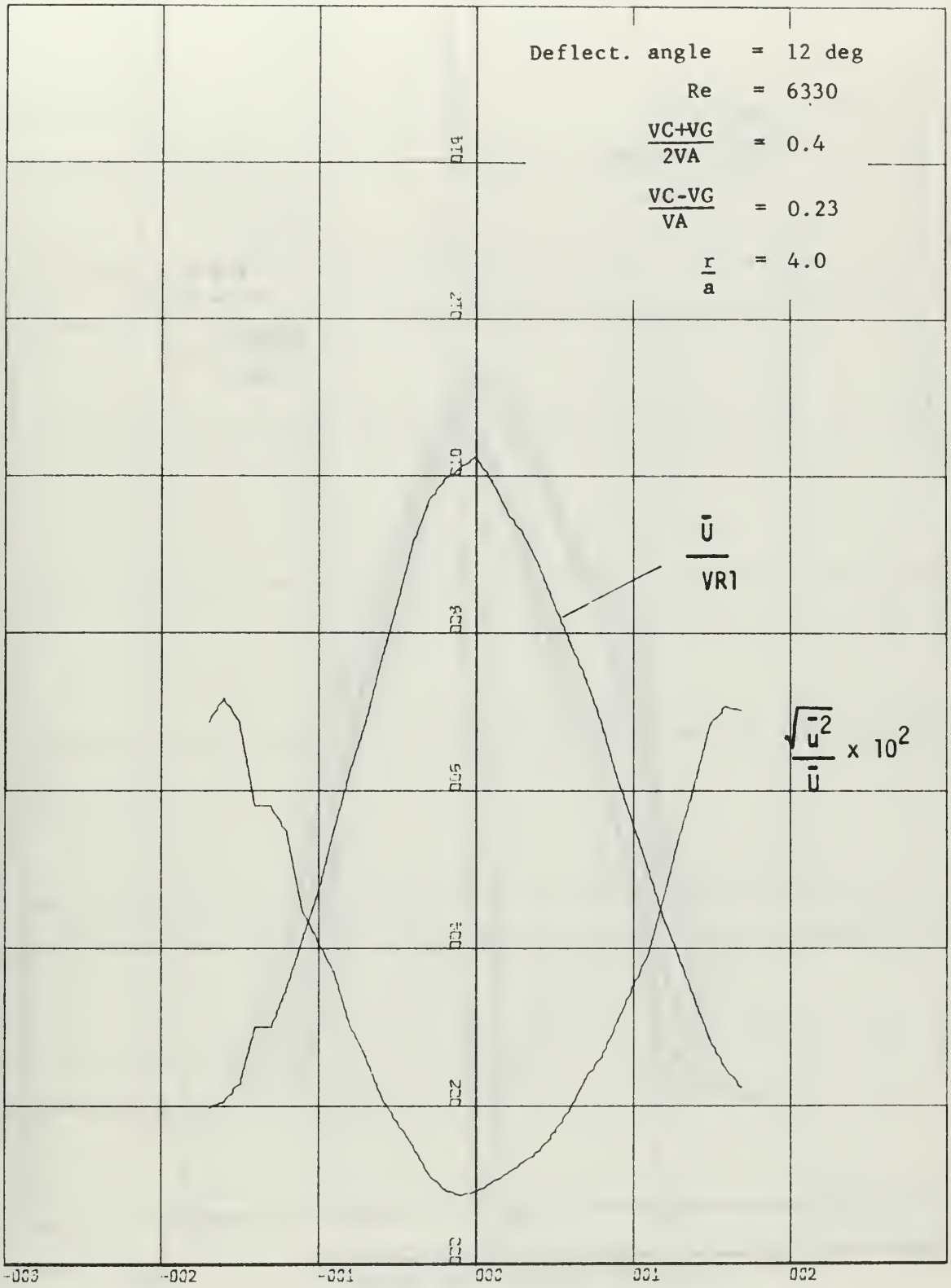

FIGURE 54 VELOCITY PROFILE AND TURBULENCE INTENSITY

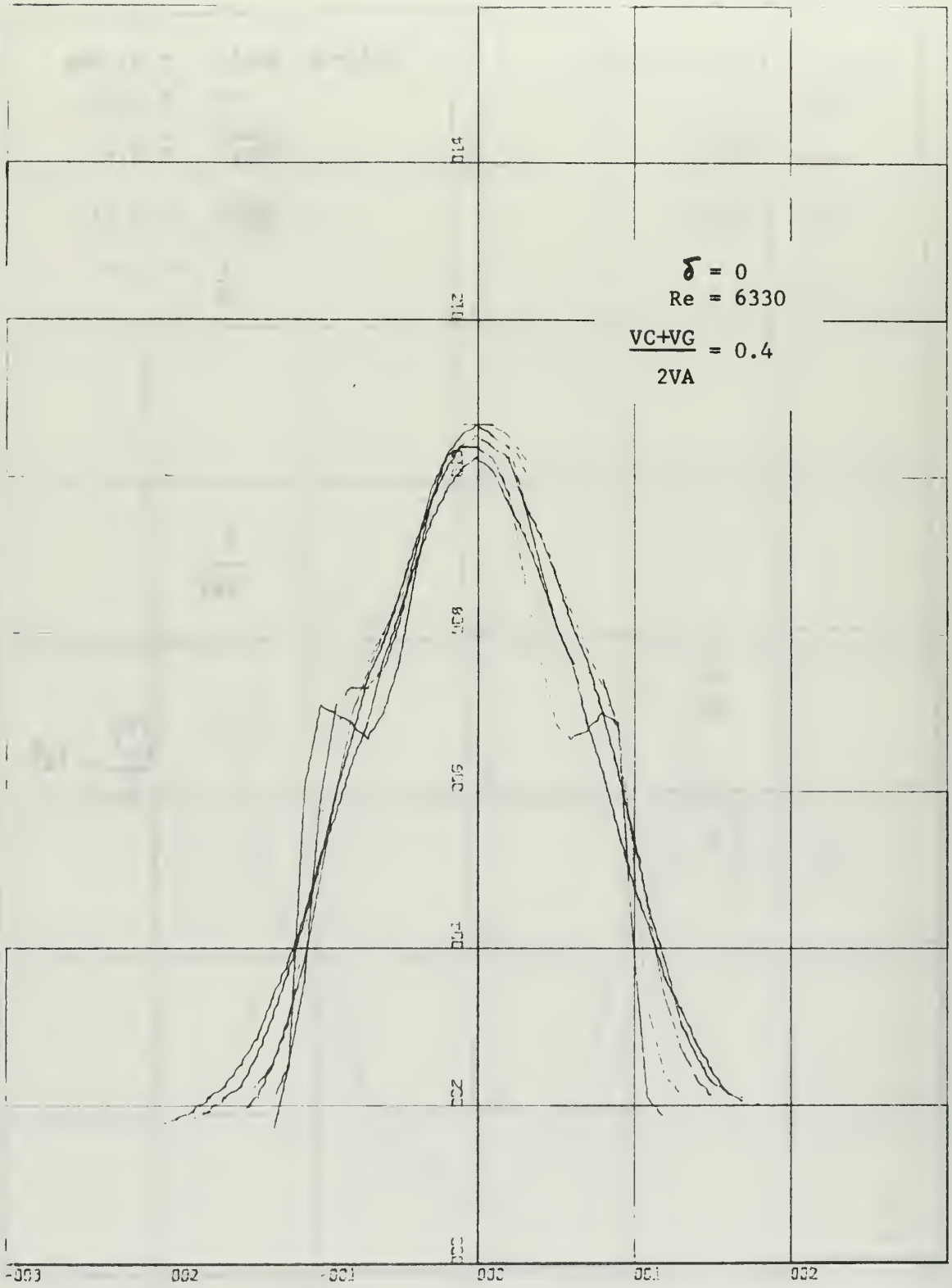

FIGURE 55 VELOCITY PROFILES

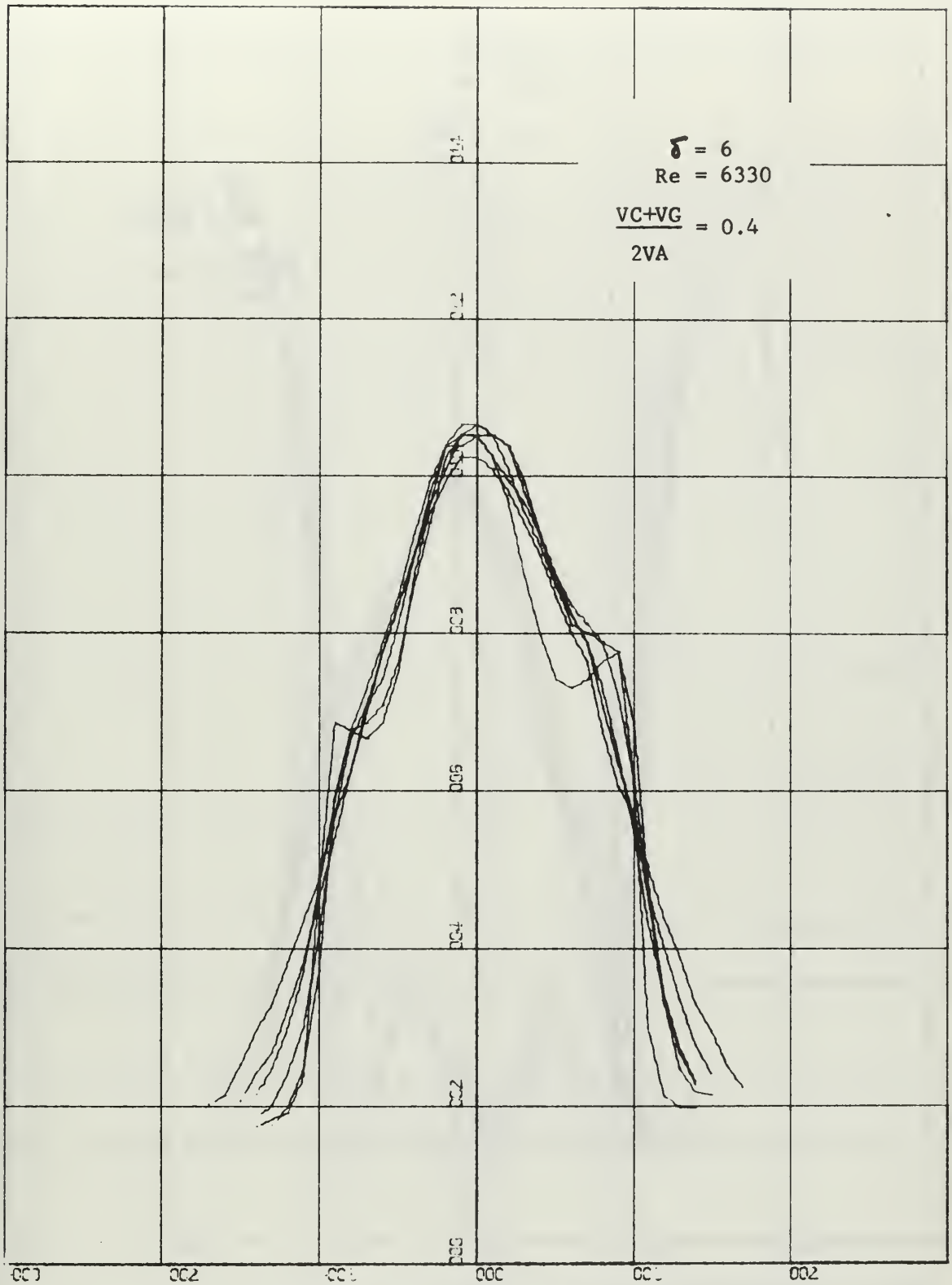

FIGURE 56 VELOCITY PROFILES

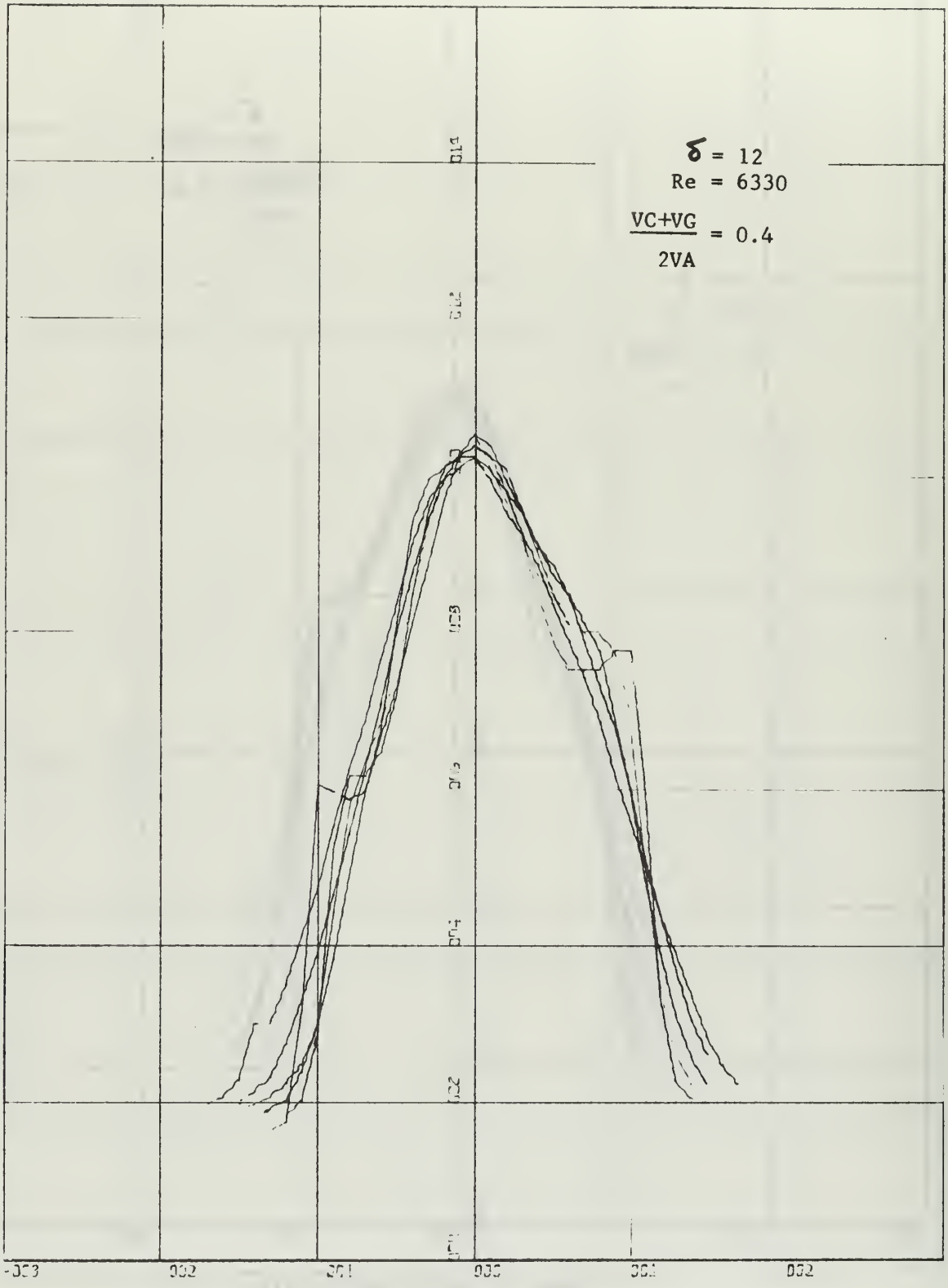

FIGURE 57 VELOCITY PROFILES

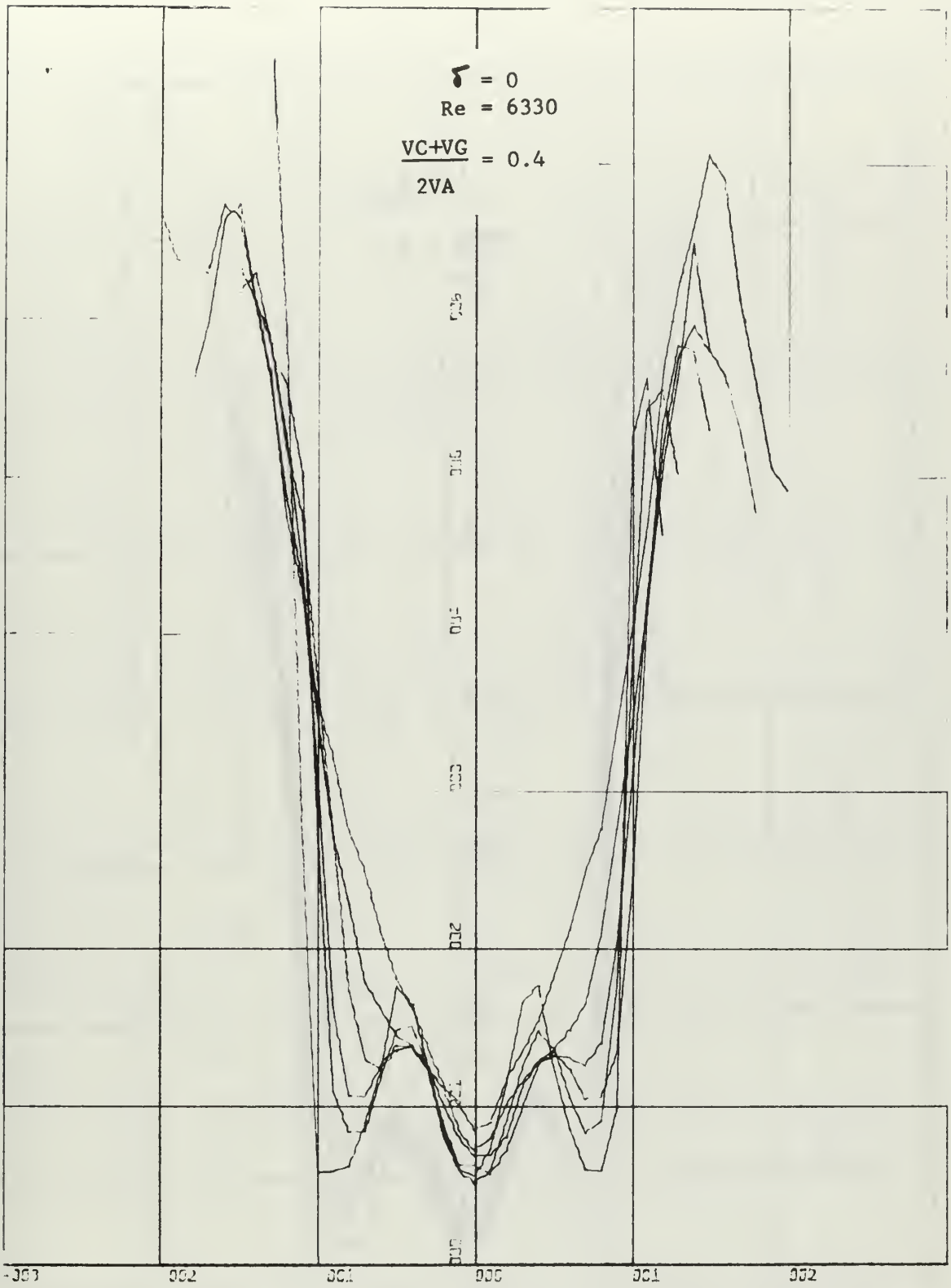

FIGURE 58 TURBULENCE INTENSITY

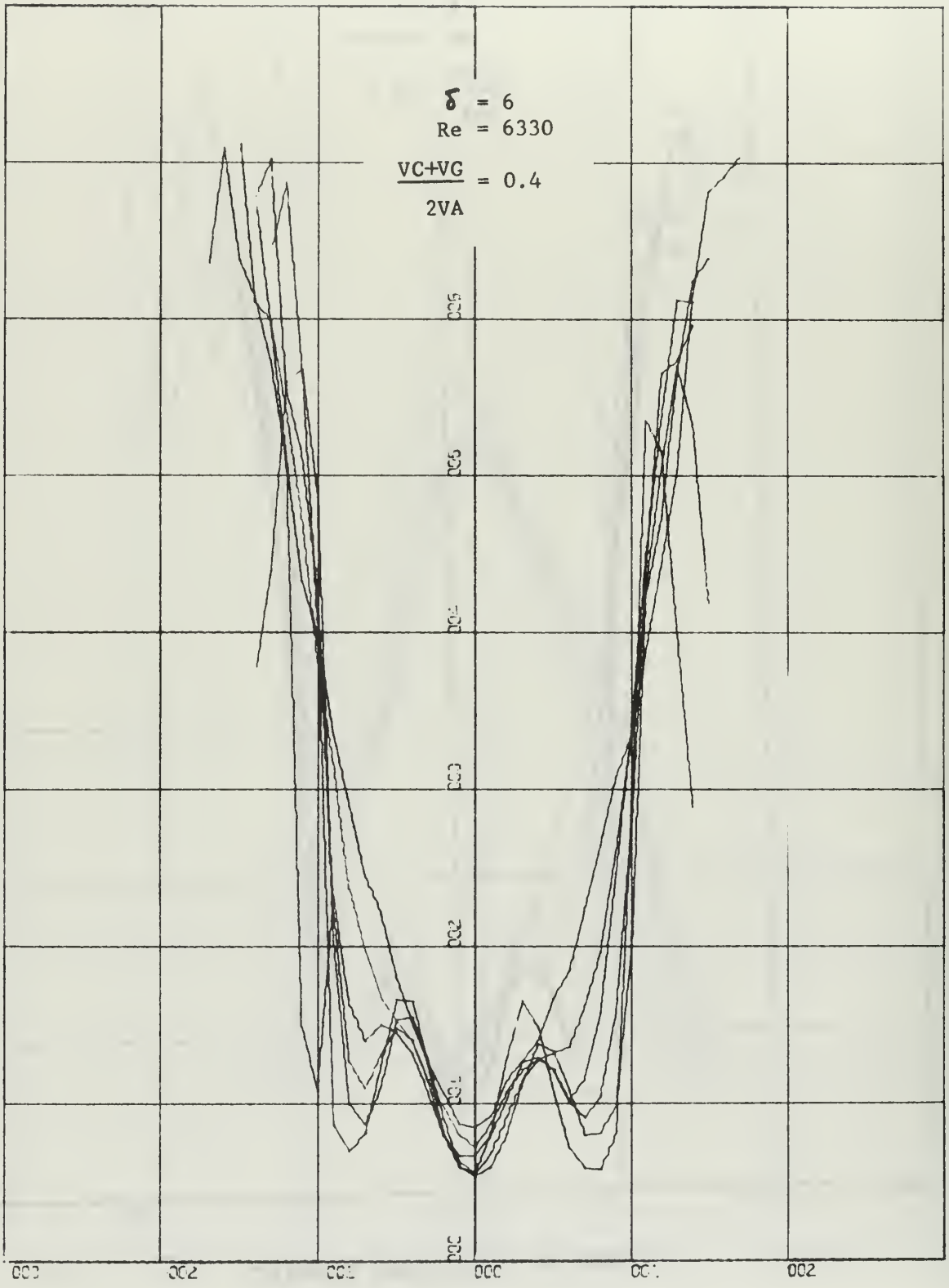

FIGURE 59 TURBULENCE INTENSITY

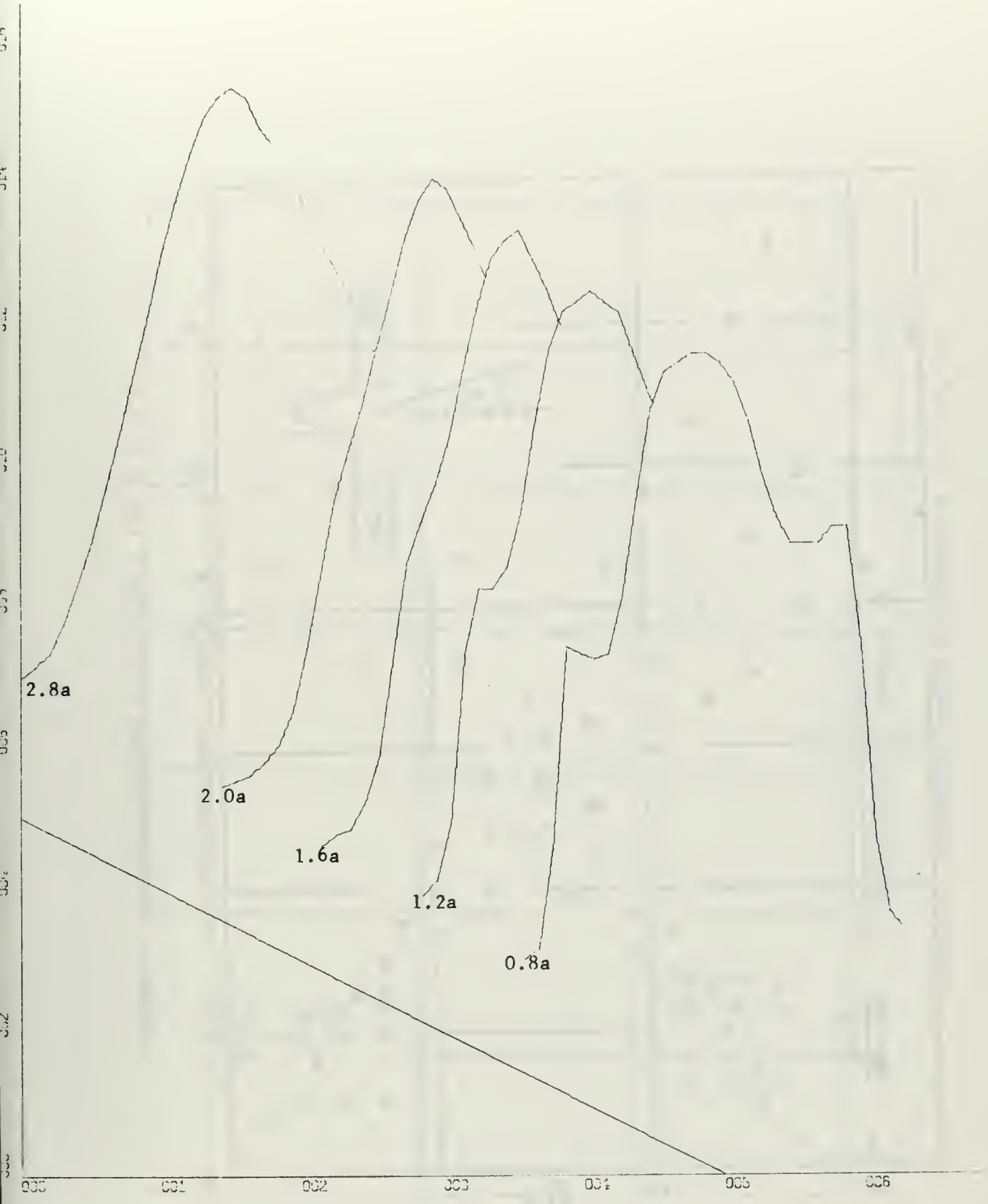

FIGURE 60 VELOCITY PROFILES AT DIFFERENT STATIONS DOWNSTREAM

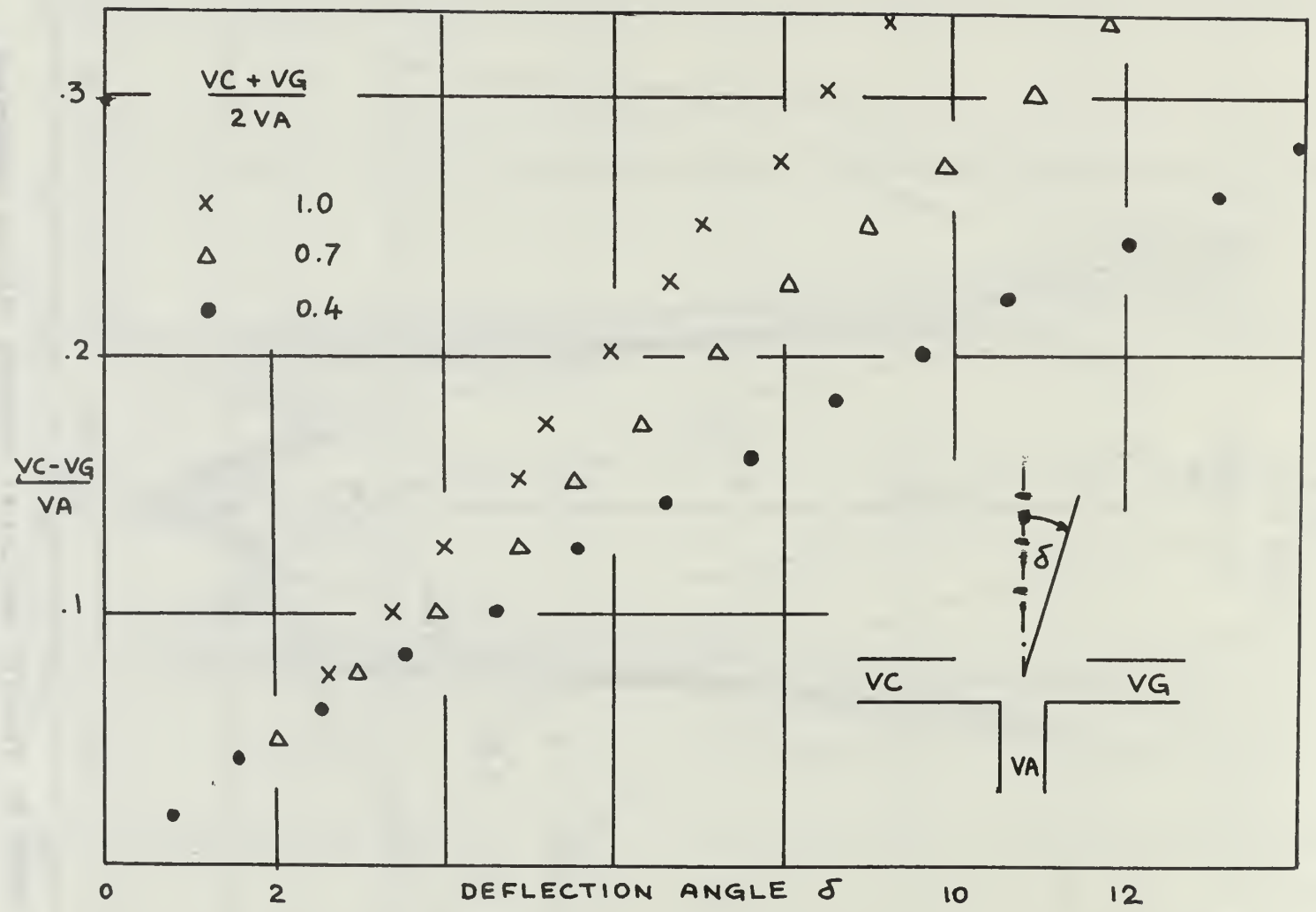

FIGURE 61 DEFLECTION ANGLES (VC+VG)/2VA = 1.0, 0.7, 0.4

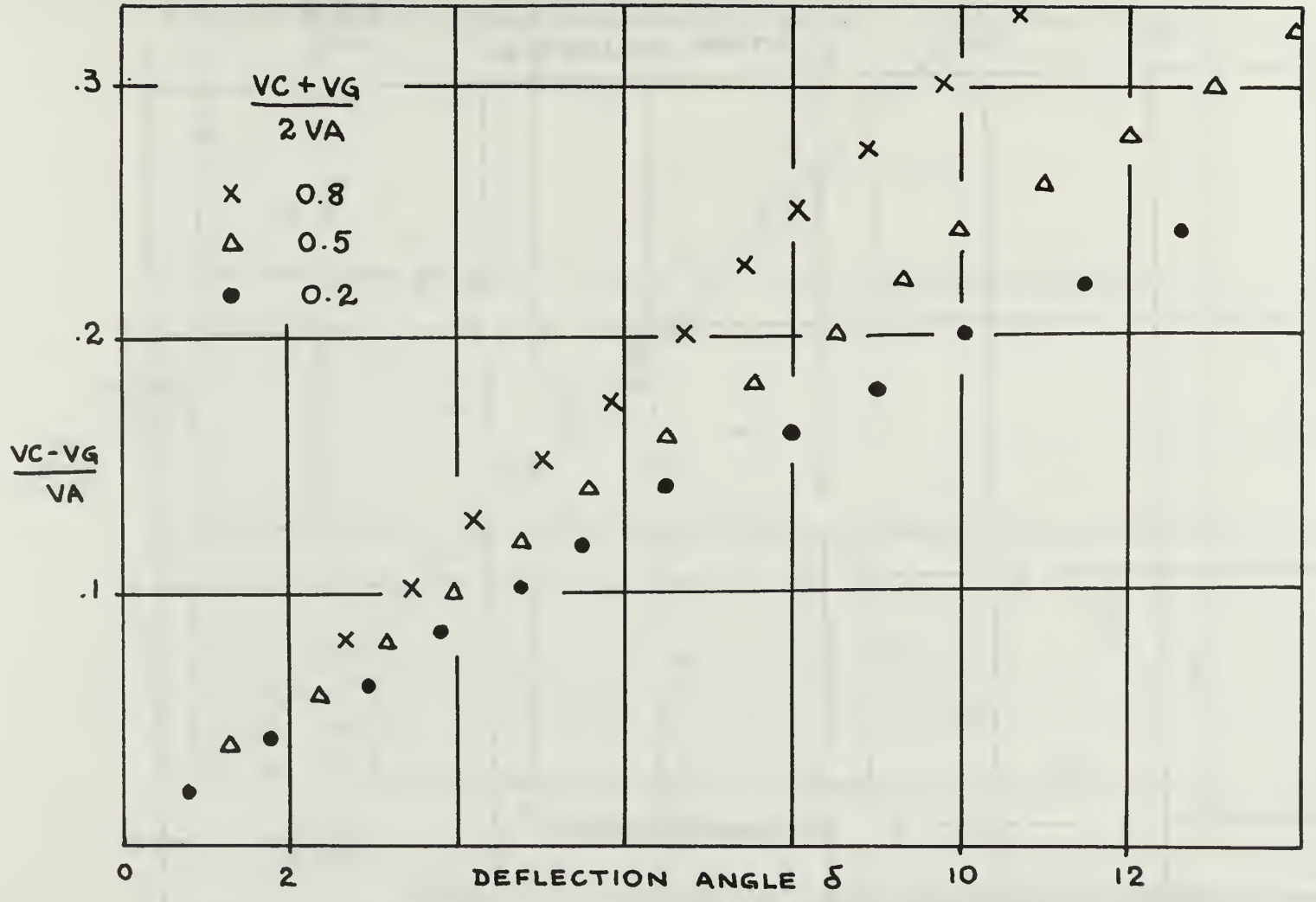

FIGURE 62 DEFLECTION ANGLES (VC+VG)/2VA = 0.9, 0.6, 0.3

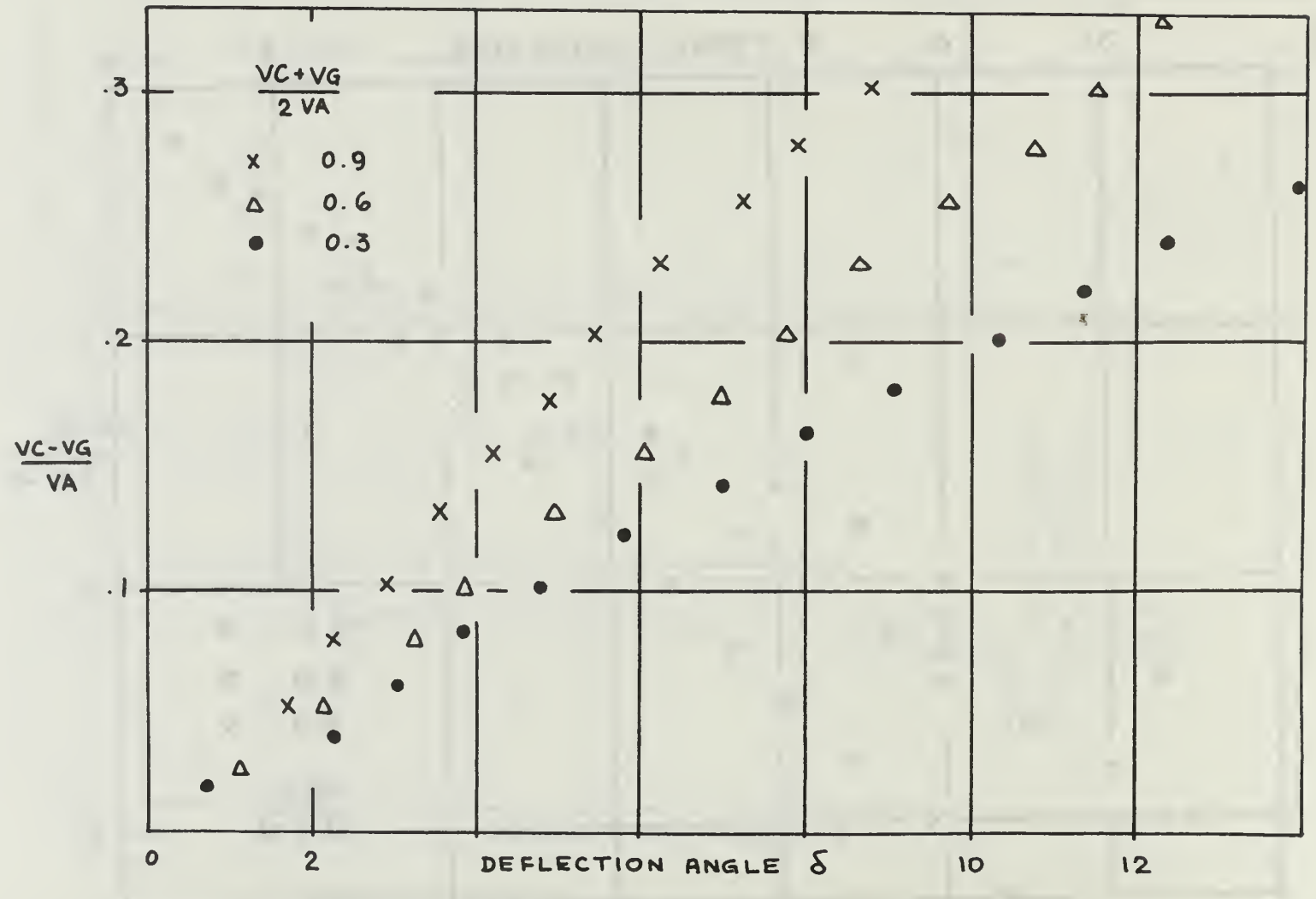

FIGURE 63 DEFLECTION ANGLES (VC+VG)/2VA = 0.8, 0.5, 0.2

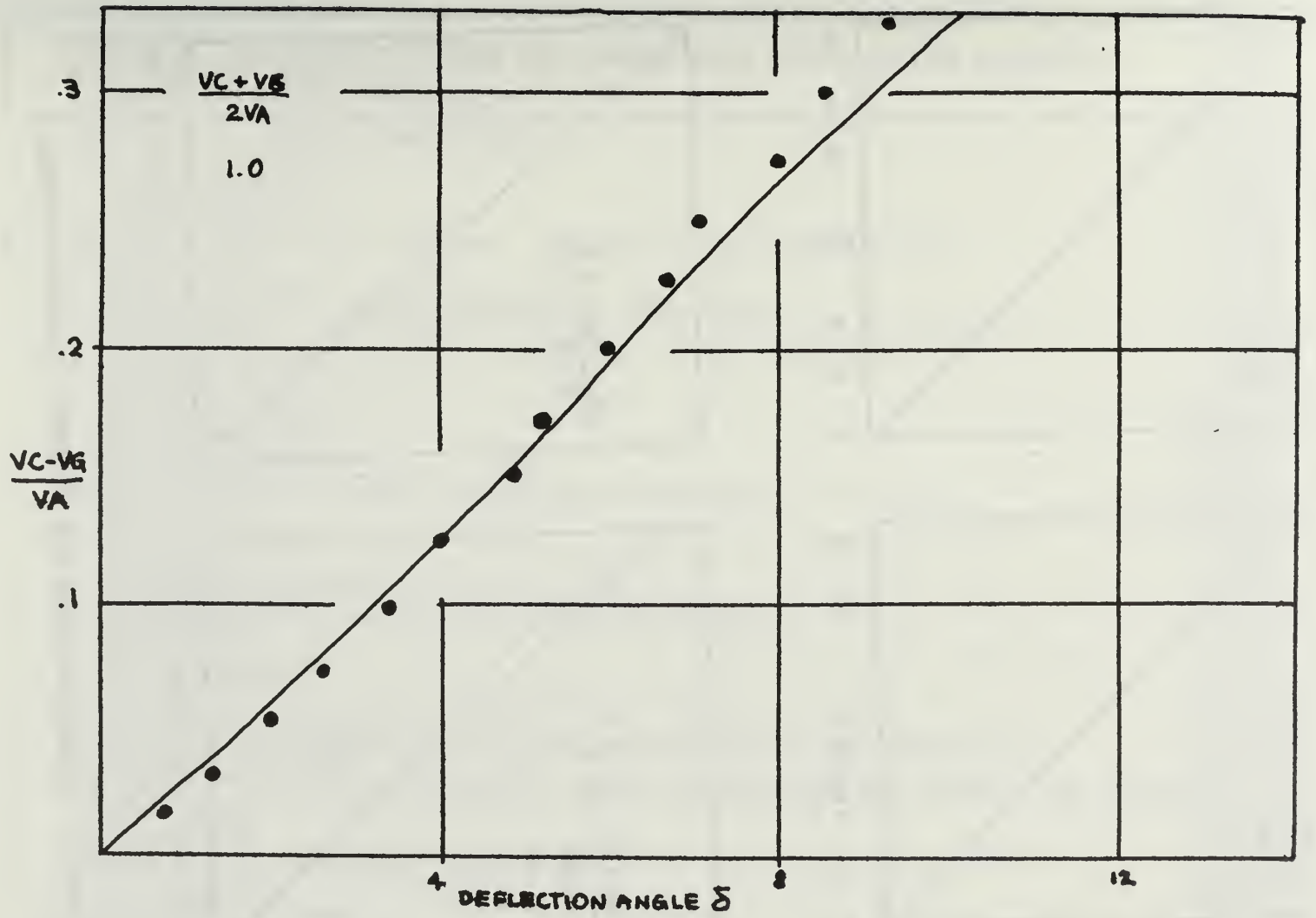

FIGURE 64 EXPERIMENTAL AND THEORETICAL DEFLECTION ANGLES

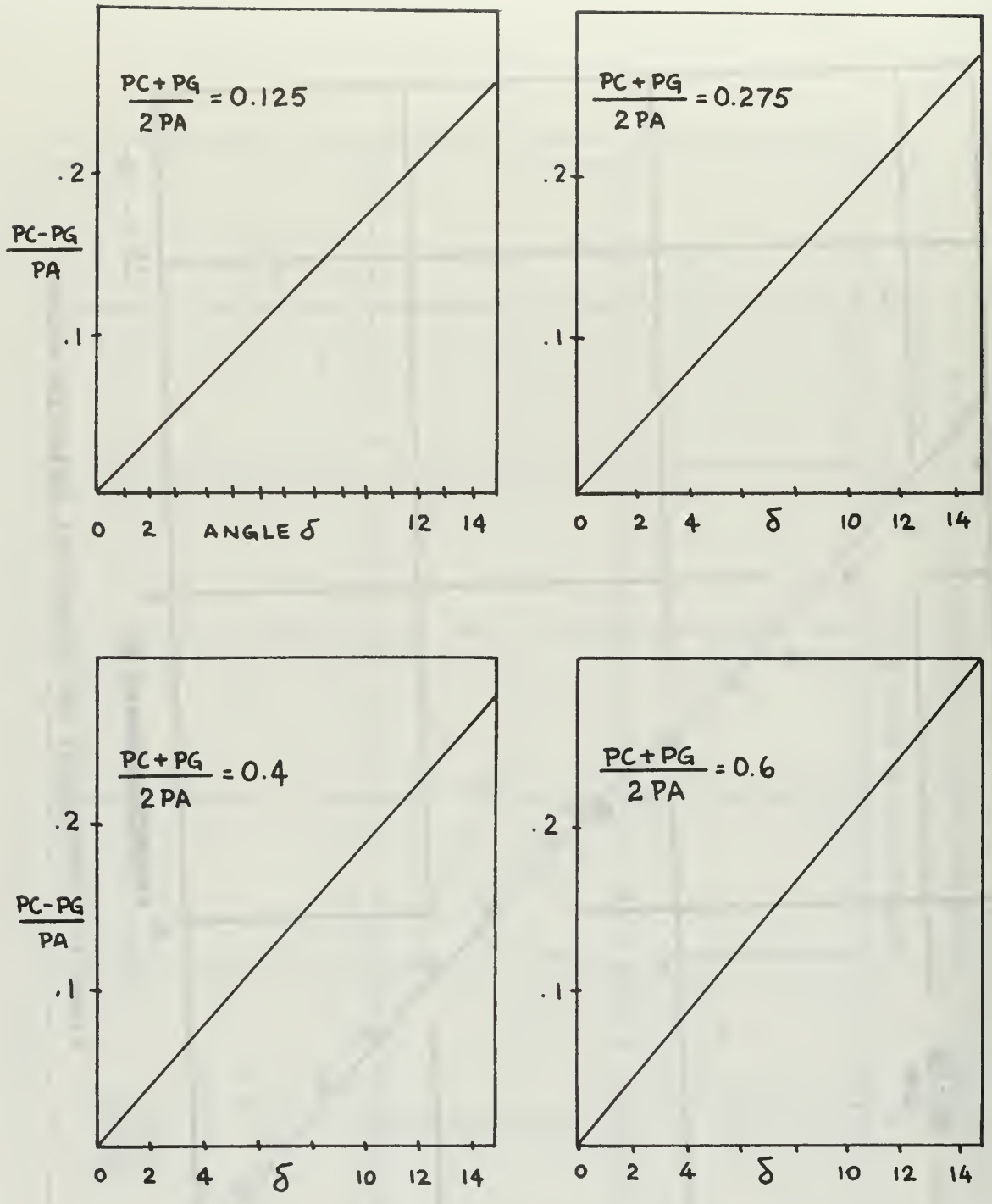

FIGURE 65 DEFLECTION ANGLE FOR DIFFERENT PRESSURES AVERAGE

```
C*************************************************************************** GER00010
C    PROGRAM A                                                              GER00020
C    ITERATION PROCESS TO SOLVE FOR ANGLE BETA FOR A GIVEN GEOMETRY         GER00030
C    AND VELOCITY RATIOS.                                                   GER00040
C    PROGRAM IN DOUBLE PRECISION                                            GER00050
C*************************************************************************** GER00060
      IMPLICIT REAL*8(A-H,K,O-Z)                                            GER00070
C    DEFINE CONSTANTS                                                       GER00080
      PI=3.1415926D0                                                        GER00090
      PI2=2.0D0/PI                                                          GER00100
      EPS=0.005D0                                                           GER00110
C    ASSIGN GEOMETRICAL VALUES    AOB=A/B , AP2SOB=(A+2S)/B                 GER00120
      AOB=1.0D0                                                             GER00130
      AP2SOB=3.0D0                                                          GER00140
C    ASSIGN VELOCITY RATIOS VCA=VC/VA ,VGA=VG/VA                            GER00150
      VCA=1.1D0                                                             GER00160
      DO 10 I=1,5                                                           GER00170
      VCA=VCA-0.1D0                                                         GER00180
      VGA=VCA                                                               GER00190
      DO 11 J=1,10                                                          GER00200
      VCA=VCA+0.02D0                                                        GER00210
      VGA=VGA-0.02D0                                                        GER00220
      DVA=VCA-VGA                                                           GER00230
C    ASSIGN VALUES TO ANGLE BETA FOR ITERATION                              GER00240
      BE=90.0D0                                                             GER00250
      DO 12 N=1,100                                                         GER00260
      BE=BE-0.1                                                             GER00270
      BETA=BE*PI/180.0D0                                                    GER00280
      S=DSIN(BETA)                                                          GER00290
C    ASSIGN VALUES TO PARAMETER K FOR ITERATION                             GER00300
      K=0.999D0                                                             GER00310
      DO 13 M=1,1000                                                        GER00320
      K=K-0.0002D0                                                          GER00330
      KK=K*K                                                                GER00340
      SK=DSQRT(1.0D0-KK)                                                    GER00350
C    CALCULATE VA (POWER JET VELOCITY)/(RESULTANT JET VELOCITY)             GER00360
      VA=K/(1.0D0+SK)                                                       GER00370
C    CALCULATE VC AND VG (VELOCITY RATIO OF CONTROL AND RESULT JET VELOC)   GER00380
      VC=VCA*VA                                                             GER00390
      VG=VGA*VA                                                             GER00400
C    CALCULATE PARAMETERS F,C AND G                                         GER00410
      FF=(1.0D0-S*S*KK)/(1.0D0-S*S)                                         GER00420
      F=DSQRT(FF)                                                           GER00430
      SF=DSQRT(FF-KK)                                                       GER00440
      SSF=DSQRT(FF-1.0D0)                                                   GER00450
      GG=1.0D0-(1.0D0-KK)*((1.0D0-VG*VG)/(1.0D0+VG*VG))**2                  GER00460
      G=DSQRT(GG)                                                           GER00470
      SG=DSQRT(GG-KK)                                                       GER00480
```

```
      SSG=DSQRT(1.0D0-GG)                                                    GER00490
      CC=1.0D0-(1.0D0-KK)*((1.0D0-VC*VC)/(1.0D0+VC*VC))**2                   GER00500
      C=DSQRT(CC)                                                            GER00510
      SC=DSQRT(CC-KK)                                                        GER00520
      SSC=DSQRT(1.0D0-CC)                                                    GER00530
C     CONTINUITY EQUATION WHERE DOB=D/B                                      GER00540
      DOB=VC+VG+VA*AOB                                                       GER00550
C     CORRECTION TO THE CONTRACCION COEFFICIENT                              GER00551
      DCB=0.4D0*DCB                                                          GER00552
C     DEFINE TERMS TO BE USED IN EQUATICN FOR HORIZONTAL COMPONENT           GER00560
      T1=DOB*S                                                               GER00570
      T2=DARSIN(K)                                                           GER00580
      T3=(VC/SC)*DLOG(SSC/(SC+SK))                                           GER00590
      T4=(VG/SG)*DLOG(SSG/(SG+SK))                                           GER00600
      T5=(DOB/SF)*DLOG(SSF/(SF+SK))                                          GER00610
      HORIZ=T1+2.0D0*(SK/PI)*(T2-T3-T4+T5)                                   GER00620
C     CHECK FOR DIFERENCE BETWEEN HORIZ AND AP2SOB                           GER00630
      IF(DABS(HORIZ-AP2SOB).GT.EPS) GO TO 13                                 GER00640
C     CALCULATIONS OF THE VERTICAL COMPONENTS WHITH ELLIPTIC FUNCTIONS       GER00650
      HH=4.0D0*K/(1.0D0+K)**2                                                GER00660
      H=DSQRT(HH)                                                            GER00670
      ACC=2.0D0*(K+C)/((K+1.0D0)*(C+1.0D0))                                  GER00680
      AGG=2.0D0*(K-G)/((1.0D0-G)*(K+1.0D0))                                  GER00690
      AFF=2.0D0*(K+F)/((K+1.0D0)*(F+1.0D0))                                  GER00700
      COEF1=PI2*(VC*(1.0D0+C*K)/(C+K)+VG*(1.0D0-G*K)/(K-G)-DOB               GER00710
     **(1.0D0+F*K)/(F+K))/(K+1.0D0)                                          GER00720
      COEF2= PI2*( 1.0D0-K)/(1.0D0+K)                                        GER00730
      ZC=VC*(C-1.0D0)/(C+K)                                                  GER00740
      ZG=VG*(G+1.0D0)/(G-K)                                                  GER00750
      ZC=DOB*(F-1.0D0)/(F+K)                                                 GER00760
      CALL DCEL1( EK,H,IK)                                                   GER00770
      CALL DCEL3(PIC,ACC,HH)                                                 GER00780
      CALL DCEL3(PIG,AGG,HH)                                                 GER00790
      CALL DCEL3(PIF,AFF,HH)                                                 GER00800
      VERTI=COEF1*EK+COEF2*(ZC*PIC+ZG*PIG-ZD*PIF)-DOB*DCOS(BETA)             GER00810
C     CHECK IF VERTICAL COMPONENT IS ZERO                                    GER00820
      IF(DABS(VERTI).GT.EPS) GO TO 13                                        GER00830
      WRITE(6,1) BE,DVA,HORIZ,VERTI                                          GER00840
      GO TO 11                                                               GER00850
   13 CONTINUE                                                               GER00860
   12 CONTINUE                                                               GER00870
   11 CONTINUE                                                               GER00880
   10 CONTINUE                                                               GER00890
    1  FORMAT(4F10.3)                                                        GER00900
      STOP                                                                   GER00910
      END                                                                    GER00920

      SUBROUTINE DCEL3(RES,AA,HH)                                            GER00930
```

```
C    SUBROUTINE TO EVALUATE ELIPTIC INTEGRALS OF THE THIRD KIND                GER00940
       IMPLICIT REAL*8(A-H,O-Z)                                                GER00950
       H=DSQRT(HH)                                                             GER00960
       HPP=1.0D0-HH                                                            GER00970
       HP=DSQRT(HPP)                                                           GER00980
       A=DSQRT(DABS(AA))                                                       GER00990
       SA=DSQRT(DABS(AA-HH))                                                   GER01000
       SSA=DSQRT(DABS(1.0D0-AA))*SA                                            GER01010
       CALL DCEL1(EK,H,IK)                                                     GER01020
       CALL DCEL2(EE,H,1.0D0,HPP,IE)                                           GER01030
       IF(AA.LT.0.0D0) GO TO 53                                                GER01040
       IF(AA.LT.1.0D0.AND.AA.GT.HH) GO TO 52                                   GER01050
       IF(AA.LT.HH) GO TO 51                                                   GER01060
       B=DARSIN(1.0D0/A)                                                       GER01070
       CALL ZETA(Z,B,HP,EK,EE)                                                 GER01080
       RES=-A*EK*Z/SSA                                                         GER01090
       RETURN                                                                  GER01100
  51   B=DARSIN(A/H)                                                           GER01110
       CALL ZETA(Z,B,HP,EK,EE)                                                 GER01120
       RES=EK+A*EK*Z/SSA                                                       GER01130
       RETURN                                                                  GER01140
  52   B=DARSIN(SA/(A*HP))                                                     GER01150
       CALL HEUMAN(HEU,B,H,EK,EE)                                              GER01160
       RES=3.1415926D0*A*HEU*0.5D0/SSA                                         GER01170
       RETURN                                                                  GER01180
  53   B=DARSIN(A/SA)                                                          GER01190
       CALL HEUMAN(HEU,B,H,EK,EE)                                              GER01200
       RES=HH*EK/(HH-AA)-3.1415926D0*0.5D0*AA*HEU/(A*SSA)                      GER01210
       RETURN                                                                  GER01220
       END                                                                     GER01230

       SUBROUTINE ZETA(Z,ZA,HP,EK,EE)                                          GER01240
C    SUBROUTINE TO EVALUATE ZETA JACOBIAN FUNCTIONS                            GER01241
       IMPLICIT REAL*8(A-H,O-Z)                                                GER01250
       HPP=HP*HP                                                               GER01260
       ZA=DTAN(ZA)                                                             GER01270
       CALL DELI2(ZE,ZA,HP,1.0D0,HPP)                                          GER01280
       CALL DELI1(ZF,ZA,HP)                                                    GER01290
       Z=ZE-EE*ZF/EK                                                           GER01300
       RETURN                                                                  GER01310
       END                                                                     GER01320

       SUBROUTINE HEUMAN(HEU,HA,H,EK,EE)                                       GER01330
C    SUBROUTINE TO EVALUATE HEUMAN'S LAMBDA FUNCTIONS                          GER01331
       IMPLICIT REAL*8(A-H,O-Z)                                                GER01340
       HH=H*H                                                                  GER01350
```

```
      HA=DTAN(HA)                                                       GER01360
      CALL DELI1(HF,HA,H)                                               GER01370
      CALL DELI2(HE,HA,H,1.0D0,HH)                                      GER01380
      HEU=2.0D0*((EE-EK)*HF+EK*HE)/3.141592600                          GER01390
      RETURN                                                            GER01400
      END                                                               GER01410

      SUBROUTINE DCEL1(RES,AK,IER)                                      GER01420
C     SUBROUTINE TO EVALUATE COMPLETE ELLIPTIC INTEGRALS OF FIRST KIND  GER01421
      IER=0                                                             GER01430
      ARI=2.                                                            GER01440
      GEO=(0.5-AK)+0.5                                                  GER01450
      GEO=GEO+GEO*AK                                                    GER01460
      RES=0.5                                                           GER01470
      IF(GEO)1,2,4                                                      GER01480
    1 IER=1                                                             GER01490
    2 RES=1.E75                                                         GER01500
      RETURN                                                            GER01510
    3 GEO=GEO*AARI                                                      GER01520
    4 GEO=SQRT(GEO)                                                     GER01530
      GEO=GEO+GEO                                                       GER01540
      AARI=ARI                                                          GER01550
      ARI=ARI+GEO                                                       GER01560
      RES=RES+RES                                                       GER01570
      IF(GEO/AARI-0.9999)3,5,5                                          GER01580
    5 RES=RES/ARI*6.283185F0                                            GER01590
      RETURN                                                            GER01600
      END                                                               GER01610

      SUBROUTINE DCEL2(RES,AK,A,B,IER)                                  GER01620
C     SUBROUTINE TO EVALUATE COMPLETE ELLIPTIC INTEGRALS OF SECOND KIND GER01621
      IER=0                                                             GER01630
      ARI=2.                                                            GER01640
      GEO=(0.5-AK)+0.5                                                  GER01650
      GEO=GEO+GEO*AK                                                    GER01660
      RES=A                                                             GER01670
      A1=A+B                                                            GER01680
      BO=B+B                                                            GER01690
      IF(GEO)1,2,6                                                      GER01700
    1 IER=1                                                             GER01710
    2 IF(B)3,8,4                                                        GER01720
    3 RES=-1.E75                                                        GER01730
      RETURN                                                            GER01740
    4 RES=1.E75                                                         GER01750
      RETURN                                                            GER01760
    5 GEO=GEO*AARI                                                      GER01770
```

```
    6 GEO=SQRT(GEO)                                                    GER01780
      GEO=GEO+GEO                                                      GER01790
      AARI=ARI                                                         GER01800
      ARI=ARI+GEO                                                      GER01810
      BO=BO+RES*GEO                                                    GER01820
      RES=A1                                                           GER01830
      BO=BO+BO                                                         GER01840
      A1=BO/ARI+A1                                                     GER01850
      IF(GEO/AARI-0.9999)5,7,7                                         GER01860
    7 RES=A1/ARI                                                       GER01870
      RES=RES+0.5707963E0*RES                                          GER01880
    8 RETURN                                                           GER01890
      END                                                              GER01900

      SUBROUTINE DELI1(RES,X,CK)                                       GER01910
C     SUBROUTINE TO EVALUATE ELLIPTIC INTEGRALS OF THE FIRST KIND      GER01920
      IF(X)2,1,2                                                       GER01930
    1 RES=0.                                                           GER01940
      RETURN                                                           GER01950
    2 IF(CK)4,3,4                                                      GER01960
    3 RES=ALOG(ABS(X)+SQRT(1.+X*X))                                    GER01970
      GOTO 13                                                          GER01980
    4 ANGLE=ABS(1./X)                                                  GER01990
      GEO=ABS(CK)                                                      GER02000
      ARI=1.                                                           GER02010
      PIM=0.                                                           GER02020
    5 SQGEO=ARI*GEO                                                    GER02030
      AARI=ARI                                                         GER02040
      ARI=GEO+ARI                                                      GER02050
      ANGLE=-SQGEO/ANGLE+ANGLE                                         GER02060
      SQGEO=SQRT(SQGEO)                                                GER02070
      IF(ANGLE)7,6,7                                                   GER02080
C       REPLACE 0 BY SMALL VALUE                                       GER02090
    6 ANGLE=SQGEO*1.E-8                                                GER02100
    7 TEST=AARI*1.E-4                                                  GER02110
      IF(ABS(AARI-GEO)-TEST)10,10,8                                    GER02120
    8 GEO=SQGEO+SQGEO                                                  GER02130
      PIM=PIM+PIM                                                      GER02140
      IF(ANGLE)9,5,5                                                   GER02150
    9 PIM=PIM+3.1415927                                                GER02160
      GOTO 5                                                           GER02170
   10 IF(ANGLE)11,12,12                                                GER02180
   11 PIM=PIM+3.1415927                                                GER02190
   12 RES=(ATAN(ARI/ANGLE)+PIM)/ARI                                    GER02200
   13 IF(X)14,15,15                                                    GER02210
   14 RES=-RES                                                         GER02220
   15 RETURN                                                           GER02230
```

```
      END                                                               GER02240

      SUBROUTINE CELI2(R,X,CK,A,B)                                      GER02250
C   SUBROUTINE TO EVALUATE ELLIPTIC INTEGRALS OF THE SECOND KIND        GER02251
C        TEST ARGUMENT                                                GER02260
      IF(X)2,1,2                                                        GER02270
    1 R=0.                                                              GER02280
      RETURN                                                            GER02290
C        TEST MODULUS                                                 GER02300
    2 C=0.                                                              GER02310
      D=0.5                                                             GER02320
      IF(CK)7,3,7                                                       GER02330
    3 R=SQRT(1.+X*X)                                                    GER02340
      R=(A-B)*ABS(X)/R+B*ALOG(ABS(X)+R)                                 GER02350
C        TEST SIGN OF ARGUMENT                                        GER02360
    4 R=R+C*(A-B)                                                       GER02370
      IF(X)5,6,6                                                        GER02380
    5 R=-R                                                              GER02390
    6 RETURN                                                            GER02400
C        INITIALIZATION                                               GER02410
    7 AN=(B+A)*0.5                                                      GER02420
      AA=A                                                              GER02430
      R=B                                                               GER02440
      ANG=ABS(1./X)                                                     GER02450
      PIM=0.                                                            GER02460
      ISI=0                                                             GER02470
      ARI=1.                                                            GER02480
      GEO=ABS(CK)                                                       GER02490
C        LANDEN TRANSFORMATION                                        GER02500
    8 R=AA*GEO+R                                                        GER02510
      SGEO=ARI*GEO                                                      GER02520
      AA=AN                                                             GER02530
      AARI=ARI                                                          GER02540
C        ARITHMETIC MEAN                                              GER02550
      ARI=GEO+ARI                                                       GER02560
C        SUM OF SINE VALUES                                           GER02570
      AN=(R/ARI+AA)*0.5                                                 GER02580
      AANG=ABS(ANG)                                                     GER02590
      ANG=-SGEO/ANG+ANG                                                 GER02600
      PIMA=PIM                                                          GER02610
      IF(ANG)10,9,11                                                    GER02620
    9 ANG=-1.E-8*AANG                                                   GER02630
   10 PIM=PIM+3.1415927                                                 GER02640
      ISI=ISI+1                                                         GER02650
   11 AANG=ARI*ARI+ANG*ANG                                              GER02660
      P=D/SQRT(AANG)                                                    GER02670
      IF(ISI-4)13,12,12                                                 GER02680
```

```
   12 ISI=ISI-4                                                          GER02690
   13 IF(ISI-2)15,14,14                                                  GER02700
   14 P=-P                                                               GER02710
   15 C=C+P                                                              GER02720
      D=D*(AARI-GEO)*0.5/ARI                                             GER02730
      IF(ABS(AARI-GEO)-1.E-4*AARI)17,17,16                               GER02740
   16 SGEO=SQRT(SGEO)                                                    GER02750
C        GEOMETRIC MEAN                                                 GER02760
      GEO=SGEO+SGEO                                                      GER02770
      PIM=PIM+PIMA                                                       GER02780
      ISI=ISI+ISI                                                        GER02790
      GOTO 8                                                             GER02800
C        ACCURACY WAS SUFFICIENT                                        GER02810
   17 R=(ATAN(ARI/ANG)+PIM)*AN/ARI                                       GER02820
      C=C+D*ANG/AANG                                                     GER02830
      GOTO 4                                                             GER02840
      END                                                                GER02850
```

```
C*************************************************************************  GHLCCC1C
C    PROGRAM B                                                              GHLCCC2C
C    MAIN DATA REDUCTION PROGRAM                                            GHLCCC3C
C    CALIBRATION CURVE,VELOCITY PROFILES AND TURBULENCE                     GHLCCC4C
C    INTENSITY ARE CALCULATED AND PLOTTED                                   GHLCCC5C
C*************************************************************************  GHLCCC6C
      DIMENSION P(100),E(100),EE(100),SQRU(100),X(100),ET(100),U(100),      GHLCCC7C
     *LT(100)                                                               GHLCCC8C
      REAL*8 IT(12)                                                         GHLCCC9C
C*************************************************************************  GHLCC10C
C    CALIBRATION CURVE  SQUARE ROOT OF VELOCITY AGAINST VOLTAGE SQUARE      GHLCC11C
C*************************************************************************  GHLCC12C
C    INTRODUCE PRESSURE AND VOLTAGE READINGS                                GHLCC13C
      READ(5,1)(P(I),I=1,21)                                                GHLCC14C
      READ(5,1)(E(I),I=1,21)                                                GHLCC15C
C    DENSITY OF WATER IN SLUG/CUF                                           GHLCC16C
      RWATER=1.9325                                                         GHLCC17C
C    DENSITY OF AIR IN SLUG/CUF AT 74 DEG F                                 GHLCC18C
      RAIR =0.002368                                                        GHLCC19C
C    ACCELERATION OF GRAVITY IN FT/SEC**2                                   GHLCC20C
      G  =32.1719                                                           GHLCC21C
      FACT=SQRT(RWATER*G/RAIR)                                              GHLCC22C
C    REDUCING DATA (P AND E)  INTO SQRT OF VELOCITY (SQRU)                  GHLCC23C
C    AND VOLTAGE SQUARE (EE)                                                GHLCC24C
      DO 2C I=1,21                                                          GHLCC25C
      SQRU(I)=SQRT(FACT*SQRT(P(I)/12.0))                                    GHLCC26C
   2C EE(I)=E(I)*E(I)                                                       GHLCC27C
      WRITE(6,71)                                                           GHLCC28C
   71  FORMAT(1H1,T40,'CALIBARTION POINTS',///)                             GHLCC29C
      WRITE(6,72)                                                           GHLCC30C
   72  FORMAT(T3,'I',T10,'P(IN.WATER)',T30,'E(VOLTS)',T50,'SQRT VELOC',     GHLCC31C
     * T70,'VOLTAGE SQUARE',//)                                            GHLCC32C
      WRITE(6,9)(I,P(I),E(I),SQRU(I),EE(I),I=1,21)                          GHLCC33C
    9 FORMAT(1X,I2,T15,F4.2,T35,F5.3,T55,F8.3,T75,F10.3,/)                  GHLCC34C
C    FIND THE SLOPE OF THE CALIBRATION CURVE                                GHLCC35C
      SL=0.0                                                                GHLCC36C
      DO 74 K=1,20                                                          GHLCC37C
      A = (EE(K)-EE(K+1))/(SQRU(K)-SQRU(K+1))                               GHLCC38C
   74 SL=SL+A                                                               GHLCC39C
      SLOPE=SL/20.0                                                         GHLCC40C
      WRITE(6,8) SLOPE                                                      GHLCC41C
    8 FORMAT(T10,'SLOPE=',F9.3)                                             GHLCC42C
C*************************************************************************  GHLCC43C
C    VELOCITY PROFILES AND TURBULENCE INTENSITY                             GHLCC44C
C*************************************************************************  GHLCC45C
      EC=1.55                                                               GHLCC46C
C    INTRODUCE TITLE FOR GRAPH,REYNOLDS NUMBER, R/W ,(VC-VG)/VA             GHLCC47C
C    (VC+VG)/2VA,ANGLE BETA,DISTANCE X OF THE FIRST POINT AND               GHLCC48C
```

```
C    NUMBER OF POINTS                                                          GHLCC49C
       DO 22 M=1,49                                                            GHLCC5CC
       READ(5,2) (IT(I),I=1,12)                                                GHLCC51C
       READ(5,2) RE,RW,DLP,PUP,BETA,X1,N                                       GHLCC52C
C    INTRODUCE VOLTAGE AND TURBULENCE READINGS                                 GHLCC53C
       READ(5,1) (E(I),I=1,N)                                                  GHLCC54C
       READ(5,1) (ET(I),I=1,N)                                                 GHLCC55C
C    CALCULATE MEAN VELOCITY AND TURBULENCE INTENSITY                          GHLCC56C
       X(1)=X1                                                                 GHLCC57C
       DO 21 K=1,N                                                             GHLCC58C
       U(K)=E(K)**4/SLOPE**2                                                   GHLCC59C
       X(K+1)=X(K)+0.1                                                         GHLCC6CC
    21 UT(K)=4.0*E(K)/(E(K)*E(K)-E0*E0)*ET(K) *100.0                           GHLCC61C
       CALL DRAW(N,X,U ,1,0,4H     ,IT,1.0,20.0,0,3,2,2,6,8,1,LAST)            GHLCC62C
       CALL DRAW(N,X,UT,3,0,4H     ,IT,1.0,20.0,0,3,2,2,6,8,1,LAST)            GHLCC63C
    29 WRITE(6,4)                                                              GHLCC64C
       WRITE(6,41) BETA,DLP,PLP,RW,RE                                          GHLCC65C
       WRITE(6,6)                                                              GHLCC66C
       WRITE(6,7)(L,X(L),U(L),UT(L),E(L),ET(L),L=1,N)                          GHLCC67C
    22 CONTINUE                                                                GHLCC68C
    41 FORMAT(T1C,'BETA=',F5.1,'DEG',T38,'(UR-UL)/UP=',F4.2,T58,'(UR+UL)/GHLCC69C
      *2UP=',F4.2,T80,'R/W=',F3.1,T98,'RE=',F8.1,///)                          GHLOC7CC
      3 FORMAT(6A8)                                                            GHLCC71C
      2 FORMAT(6F6.C,I4)                                                       GHLCC72C
      4 FORMAT(1H1,T30,'VELOCITY PROFILE AND TURBULENCE INTENSITY',/)          GHLCC73C
      6 FORMAT(T3,'L',T13,'X/W',T30,'   VELOCITY U',T50,'TURB.INTENS'          GHLCC74C
       *,T75,'E',T92,'ET',/)                                                   GHLCC75C
      7 FORMAT(1X,I2,T10,F7.2,T30,F12.3,T50,F8.3,T70,F8.3,T80,F8.3)            GHLCC76C
      1 FORMAT(12F6.C)                                                         GHLCC77C
        STOP                                                                   GHLCC78C
        END                                                                    GHLCC79C
```

REFERENCES

1. Dexter, E. M., "An Analog Pure Fluid Amplifier," ASME Fluid Jet Control Devices, Symposium Proceedings, (November 1962).

2. Moynihan, F. A., and Reilly, R. J., "Deflection and Relative Flow of Three Interacting Jets," Proceedings of the Second Fluid Amplification Symposium, 1, pp: 123-146, (October 1964).

3. Douglas, J. F., and Neve, R. S., "Investigation into the Behaviour of a Jet Interaction Proportional Amplifier," Proceedings of the Second Cranfield Fluidics Conference, Paper C3, pp: 29-38, (January 1967).

4. Byrd, P. F., and Friedeman, M. D., Handbook of Elliptic Integrals for Engineers and Physicists, Springer-Verlag, 1954.

5. Heuman, C., "Table of Complete Elliptic Integrals" Journal of Math. Phys., Vol. 19-20, (1940-1941).

6. Gröbner, W., und Hofreiter, N., Integraletafel, Springer-Verlag, 1965.

INITIAL DISTRIBUTION LIST

		No. Copies
1.	Defense Documentation Center Cameron Station Alexandria, Virginia 22314	20
2.	Library, Code 0212 Naval Postgraduate School Monterey, California 93940	2
3.	Mechanical Engineering Department Naval Postgraduate School Monterey, California 93940	2
4.	Professor T. Sarpkaya Chairman, Department of Mechanical Engineering Naval Postgraduate School Monterey, California 93940	5
5.	Escuela de Ingenieria Naval Correo Naval Valparaiso, Chile	3
6.	Teniente Gerardo Hiriart Direccion de Ingenieria Correo Naval Valparaiso, Chile	7

DOCUMENT CONTROL DATA - R & D

(Security classification of title, body of abstract and indexing annotation must be entered when the overall report is classified)

1 ORIGINATING ACTIVITY (Corporate author)	2a. REPORT SECURITY CLASSIFICATION
Naval Postgraduate School Monterey, California 93940	Unclassified
	2b. GROUP

3 REPORT TITLE

A Theoretical and Experimental Study of the Three Jet Interaction

4 DESCRIPTIVE NOTES *(Type of report and inclusive dates)*

Master's Thesis; April 1970

5. AUTHOR(S) *(First name, middle initial, last name)*

Gerardo Hiriart Le-Bert

6. REPORT DATE	7a. TOTAL NO. OF PAGES	7b. NO. OF REFS
April 1970	127	6

8a. CONTRACT OR GRANT NO.	9a. ORIGINATOR'S REPORT NUMBER(S)
b. PROJECT NO.	
c.	9b. OTHER REPORT NO(S) *(Any other numbers that may be assigned this report)*
d.	

10. DISTRIBUTION STATEMENT

This document has been approved for public release and sale, its distribution is unlimited.

11. SUPPLEMENTARY NOTES	12. SPONSORING MILITARY ACTIVITY
	Naval Postgraduate School Monterey, California 93940

13. ABSTRACT

The interaction of three jets is studied both theoretically and experimentally. The angle of deflection and the velocity and turbulence distributions were determined through the use of a hot-wire anemometer. The free-streamline theory has been applied to the determination of the jet deflection and the results so obtained were found to be in good agreement with those obtained experimentally. The study is a convincing evidence of the fact that a proper combination of inviscid flow analysis together with experimental results can provide the necessary guidance for the design of proportional amplifiers.

14 KEY WORDS	LINK A		LINK B		LINK C	
	ROLE	WT	ROLE	WT	ROLE	WT
Jet interaction						
Fluid amplifiers						
Proportional amplifiers						
Beam-deflection						
Theoretical & experimental analysis of jet deflection						

Thesis
H5776
c.1

Hiriart Le-Bert
A theoretical and
experimantal study of
three jet interaction.

128157